OUKA
Osaka University Knowledge Archive

Title	COMPLEMENTARY STUDIES OF NEET IN ^<189>Os AND THE OBSERVATION OF NEET IN ^<237>Np
Author(s)	Saito, Tadashi
Citation	大阪大学, 1980, 博士論文
Version Type	VoR
URL	https://hdl.handle.net/11094/24336
rights	
Note	

Osaka University Knowledge Archive : OUKA

https://ir.library.osaka-u.ac.jp/

Osaka University

COMPLEMENTARY STUDIES OF NEET IN ^{189}Os AND THE OBSERVATION OF NEET IN ^{237}Np

BY

Tadashi SAITO

A THESIS

SUBMITTED TO

FACULTY OF SCIENCE

OSAKA UNIVERSITY

1980

Acknowledgments

The works described in this thesis have been carried out under the direction of Professor Kiyoteru Otozai. I would like to express my sincere thanks to Professor K. Otozai, who has led me to these works, for his many valuable suggestions, helpful advices, interesting discussions and kind encouragement. I am greatly indebted to Dr. Hiroshi Baba of the Tokai Research Establishment of JAERI for his offering the ^{103}Rh target and making the BOB75 γ-spectra analyzing code available. I wish to express my gratitude to Dr. Motoyoshi Hatada and Dr. Keiji Matsuda of Osaka Laboratory of JAERI for their kind operation of the transformer-type electron accelerator. I appreciate the helpful discussions of Dr. Tatsuo Tabata of the Radiation Center of Osaka Prefecture. I am deeply indebted to Dr. Shigeru Okabe of the Radiation Center of Osaka Prefecture for making the accelerator available, and to Dr. Michiharu Kitagawa, Dr. Yoshihiko Shono and Dr. Takashi Oka of the same Center for their kind operation of the Cockcroft-Walton electron accelerator. I am grateful to Professor Takashi Nakamura of Institute for Nuclear Studies, Tokyo University, and Dr. Kazuo Shin of Department of Nuclear Engineering, Kyoto University, for offering the DIBRE code. I wish to appreciate the helpful suggestions by Professor Masato Morita of

Department of Physics, Osaka University. The interest of Mr. Shigeki Hayashi of the Reactor Institute of Kyoto University is appreciated. I would like to acknowledge heartily the helpful advice and contribution of Professor Ichiro Fujiwara of Atomic Energy Institute, Kyoto University, to the ^{237}Np target preparation. I am deeply indebted to Professor Nobuhiko Kunitomi and Professor Yutaka Nakai of Department of Physics, Osaka University, for their making the ^{57}Co source available. The support of Professor Tomota Nishi of Atomic Energy Institute, Kyoto University, and Dr. Hirotake Moriyama of Department of Nuclear Engineering, Kyoto University, in the purification of ^{237}Np is gratefully appreciated. I am pleased to thank my fellow students, Atsushi Shinohara and Taichi Miura who is now at Tokyo Metropolitan University, for their helps in the variuos stages of this study. I express my gratitude to Yoshitaka Ohkubo, now at Purdue University, to Dr. Ryuichi Arakawa, now at College of General Education, and to Satoshi Morimoto, now at Figaro Giken Co.. I thank my parents, Naoko and Sadao Saito, for their kind and patient support.

Synopsis

Two complementary studies of NEET in ^{189}Os and the first observation of NEET in ^{237}Np are described.

Chapter I is devoted to the Coulomb excitation experiment on ^{103}Rh by low-energetic electrons, the purpose of which is to check that the de Forest-Walecka formula, used for estimating the interfering contribution of Coulomb excitation by electrons in the NEET observation in ^{189}Os, is valid in such a lowest energy region well below 1 MeV. The excitation function for Coulomb excitation of the 357-keV level in ^{103}Rh by electrons was measured below 800 keV by the radioactivity measurement of the induced isomer ^{103m}Rh. The experimental results agree well with those calculated by the de Forest-Walecka formula. This fact can verify the estimate of Coulomb excitation in ^{189}Os as an interfering mode competing with NEET, and hence give an additional support for NEET in ^{189}Os.

In Chapter II, NEET in ^{189}Os following K-shell photoionization is described. Bremsstrahlung is used to ionize the K shells of ^{189}Os atoms, instead of electron projectiles, to exclude the interference of Coulomb excitation and to obtain further evidence for NEET. The isomer ^{189m}Os could be activated by NEET following photoionization, although only a qualitative agreement could be obtained with the

electron experiment. Some NEET parameters were reevaluated by taking various electronic transitions participating in NEET in ^{189}Os into account.

In Chapter III, the first observation of NEET in ^{237}Np is reported. The deexcitation γ-rays with energy of 60 keV could be detected, when the ^{237}Np target was irradiated with γ-radiations from ^{57}Co. This is explained as a result of the nuclear excitation of the 103-keV level in ^{237}Np induced by the KL_3 electronic radiationless transition following K-shell photoionization. The NEET probability could be deduced to be 2.1×10^{-4} for ^{237}Np, subsequent to ^{189}Os.

Contents

INTRODUCTION

1. NUCLEAR EXCITATION BY ELECTRON TRANSITION

Immediately after ionization of an atomic inner shell, an electron makes transition from an outer shell to the vacated one, being accompanied with the emission of a characteristic X-ray or an Auger electron. Morita[1] proposed an additional deexcitation mode in which the nucleus is excited to a higher energy level instead of X-ray or Auger-electron emission. He discussed this mechanism by the perturbation theory, and called it nuclear excitation by electron transition, abbreviated to NEET. As a quite similar problem, an analogue of NEET has already been observed in the muonic atoms.[2] In the muonic atoms of rather heavy elements, it is well established that the orbital muons cascade to the inner shells by excitation of

the nucleus as well as by ordinary radiative and radiationless (Auger-electron emission) transitions. This situation is also valid for the usual electronic atoms, if a corresponding nuclear transition exists favorably when the atomic transtion energies are scaled down to those in the normal electron system.

The nuclear and extranuclear electron transitions in an atom must fulfill two favorable conditions (NEET conditions) to realize NEET between them. First, both transitions must have nearly equal transition energies. The exact equality of those energies is not neccessarily required. The other condition is that both transitions should have the common multipolarity, obeying the conservation laws of angular momentum and parity.

2. MORITA'S THEORY FOR NEET

The Morita theory for NEET[1] is briefly reviewed and the practical formulas,[3-5] derived from it, are presented below.

In the NEET theory, the nucleus and the orbital electrons are treated as the resultant system of the atom, and the electromagnetic transition between different states of that system is studied.

The wave function ϕ_i denotes the i-th electron-hole state with an energy of E_i ($E_i > E_{i+1}$). An electron hole created in ϕ_1 moves to $\phi_2, \phi_3, \cdots$, spontaneously. The wave functions ψ_1 and ψ_2 represent respectively the initial and final states of a nuclear transition with energy E_N. Since the initial nuclear state can be restricted to the ground state of the nucleus, the final one is fixed to the state with an excitation energy of E_N. The wave function Ψ of the resultant system of the nucleus and electrons is assumed to be the product of individual wave functions

$$\Psi = \psi_1\phi_1, \psi_1\phi_2, \cdots, \psi_2\phi_1, \psi_2\phi_2, \cdots. \qquad (1)$$

In the usual cases, the electromagnetic transitions between Ψ, represented by $\psi_1\phi_i \rightarrow \psi_1\phi_j$, are accompanied with the emission of X-rays and Auger electrons. (For the latter case, ϕ_j includes the j'-th hole state in addition to the j-th state.)

In the case where NEET is expected to occur, the nuclear excitation energy is nearly equal to that of the electron transition $\phi_1 \rightarrow \phi_2$, that is,

$$E_N \approx E_1 - E_2 \equiv E_A. \qquad (2)$$

Figure 1 shows the NEET diagram for a general case. The

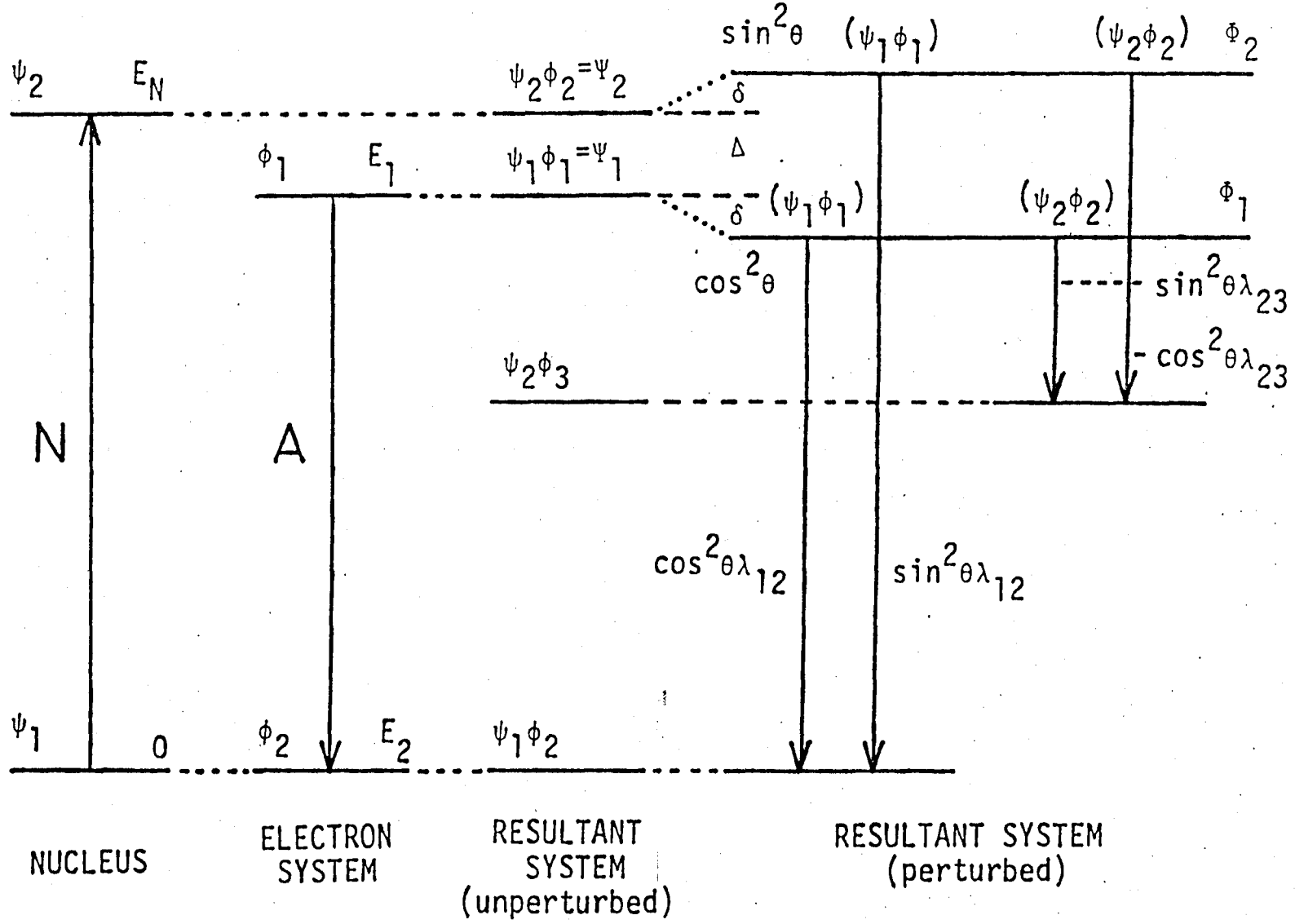

Fig. 1. Principle of NEET. The electron transition A and the nuclear transition N satisfy the NEET conditions.

states Ψ_1 (= $\psi_1\phi_1$) and Ψ_2 (= $\psi_2\phi_2$) have the unperturbed energies of E_1 and $E_2 + E_N$, respectively. In this case the energies of Ψ_1 and Ψ_2 are nearly degenerated; therefore, these two states are no longer the eigenstates of the energy. The true eigenstates Φ_1 and Φ_2 are obtained by taking the interaction between Ψ_1 and Ψ_2 into account as follows.

$$\begin{aligned} \Phi_1 &= \Psi_1\cos\theta + \Psi_2\sin\theta, \\ \Phi_2 &= -\Psi_1\sin\theta + \Psi_2\cos\theta. \end{aligned} \tag{3}$$

These perturbed states are the linear combinations of the unperturbed wave functions Ψ_1 and Ψ_2, and repulse each other resulting an energy shift δ. The mixing ratio is determined by angle θ as

$$\cos\theta\sin\theta = (\Psi_2|H'|\Psi_1)/[E(\Phi_1) - E(\Phi_2)], \tag{4}$$

wgere $E(\Phi_1)$ and $E(\Phi_2)$ are the energies for the states Φ_1 and Φ_2, respectively. Eq. (3) indicates that, when the state Ψ_1 is produced, the states Φ_1 and Φ_2 are produced with the probabilities of $\cos^2\theta$ and $\sin^2\theta$, respectively. These states can decay to both the states $\psi_1\phi_i$ (i = 2, 3, ...) and $\psi_2\phi_j$ (j = 3, 4, ...) with the respective transition rates as shown in Fig. 1. The former leads to the production of the nuclear ground state, whereas the latter to that of the

nuclear excited state.

The NEET probability, P, is expressed, for small θ, by

$$P = (1 + \Lambda_2/\Lambda_1)\tan^2\theta, \tag{5}$$

where Λ_1 and Λ_2 are the total decay constants of Ψ_1 and Ψ_2, and θ, defined in eq. (4), is approximated by

$$\tan\theta = E'/\Delta. \tag{6}$$

Here E' is the Coulomb interaction energy between the nucleus and electrons, namely, the eigenvalue of the Coulomb perturbation H', and Δ is the energy difference between the nuclear and electronic transitions,

$$\Delta = E_A - E_N = E_1 - E_2 - E_N. \tag{7}$$

The energy shift δ can be expressed from the energy balance as

$$\delta = \Delta\tan^2\theta = E'^2/\Delta. \tag{8}$$

For the Eℓ multipole, E' is given by

$$E' = -\frac{4\pi}{2\ell + 1}\alpha Z < r_N^{\ell} > < r_e^{-(\ell+1)} > m_e c^2, \tag{9}$$

where α is the fine structure constant, Z is the atomic number, $< >$ indicates the off-diagonal matrix element, r_N and r_e are the nuclear and electronic coordinates, and $m_e c^2$ is the rest mass energy of the electron. By a crude approximation, E' is obtained numerically as

$$E'(\mathrm{eV}) = -3.41\times10^{2}\times(2.27\times10^{-5})^{\ell}A^{\ell/3}Z^{\ell+2}f/[(2\ell+1)\bar{n}^{2(\ell+1)}], \tag{10}$$

where A is the mass number of the nucleus, f the correction factor due to the collective character of the nuclear transition, and $\bar{n}$ the mean of the principal quantum numbers of the initial and final electron states.

3. NEET IN ^{189}Os

Among several nuclides which satisfy the NEET conditions and besides are expected to have the appreciable NEET probability, ^{189}Os is the best choice to obtain some evidence for the existence of NEET, because this nuclide has an isomer suitable for residual radioactivity measurement. An experimental technique which employs the decay analysis of the activity can achieve an extremely high sensitivity because of being free from the background due to the

ionizing beam, and identify the activity by its half-life. As Figure 2 shows, the K-hole state which has produced by some favorable beam generate perturbation, and hence the 70-keV nuclear state is produced with the probability P. This excited state decays to the ground state in an extremely short time, but has a small probability of feeding to the isomeric level. The latter branch can be readily detected with the residual activity of the isomer. Otozai et al.[6] detected the 6-h isomer ^{189m}Os after bombardment of Os by electrons with energies below 100 keV. The amounts of the isomer produced were measured as a function of the energy of incident electrons. The excitation function shows that the isomer production is due to NEET of the 70-keV level.

In the improved experiment,[5] numerical vlues for some quantities relating to NEET were determined more precisely. The NEET probability is obtained as $P = (1.7 \pm 0.2) \times 10^{-7}$, and the mixing angle is given, through eq. (5), as $\tan\theta = -3.9 \times 10^{-4}$. The interaction energy is $E' = -0.89$ eV from eq. (6) with $\Delta = +2.25$ keV, and hence the energy shift is $\delta = 3.5 \times 10^{-4}$ eV from eq. (8). The correction factor f in eq. (10) is determined to be 1.5 for this E2 transition.

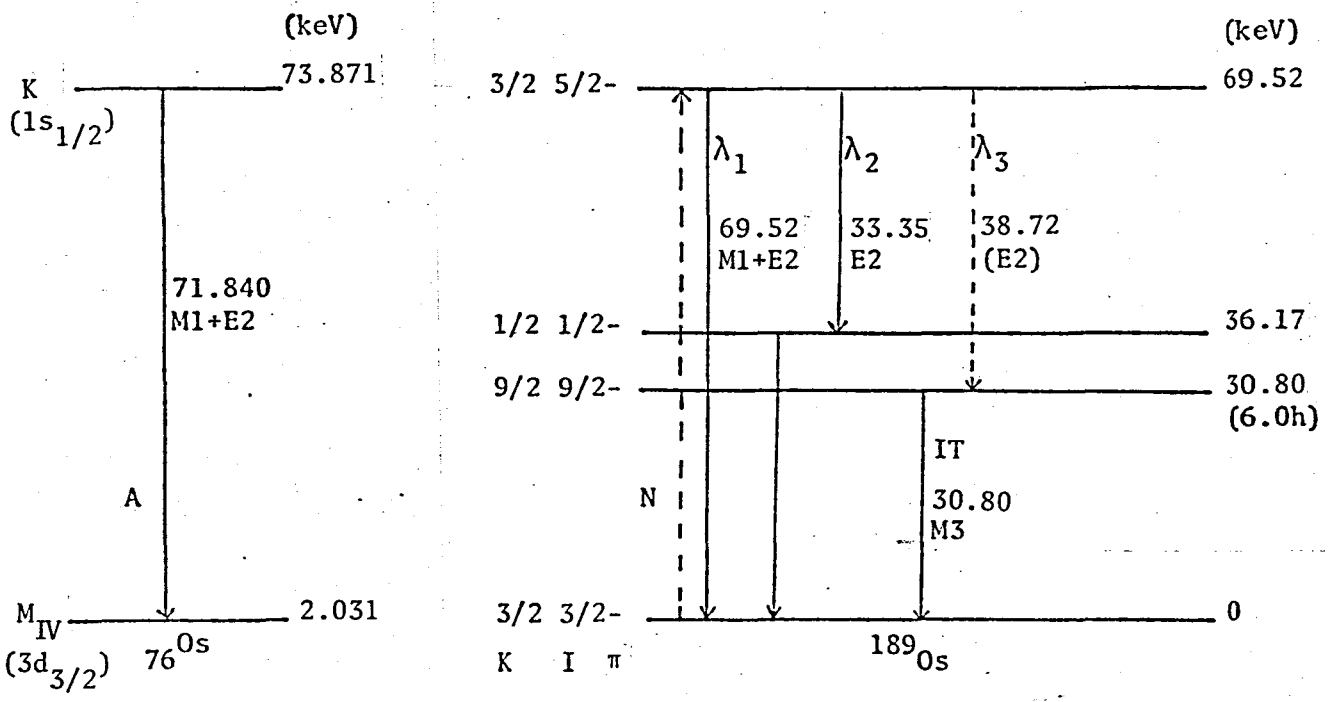

Fig. 2. NEET diagram for ^{189}Os. The electron-hole transition A and the nuclear transition N fulfill the NEET conditions. The 30.80-keV level is the isomer ^{189m}Os which is detected after electron bombardment.

4. COULOMB EXCITATION BY MEANS OF ELECTRONS

In the electron-bombarding experiments on ^{189}Os [ref. 5,6], Coulomb excitation by means of electrons had to be taken into consideration as an inevitable mechanism competing with NEET for isomer production. The experimental excitation function for producing the isomer ^{189m}Os has the threshold at approximately 74 keV, as shown in Fig. 3 [ref. 5]. It agrees with the fact that the threshold of NEET of the 70-keV level in ^{189}Os is not the energy of that nuclear level but the K-edge energy of an Os atom, 73.9 keV. If Coulomb excitation was responsible for isomer production, the threshold would be at 69.5 keV. It is evident that the isomer production in ^{189}Os by electrons, in the region studied, is incapable of being attributed fully to Coulomb excitation. The isomer production cross sections via Coulomb excitation of the 70-keV level by impinging electrons were calculated as a function of electron energy by using an approximate formula of de Forest and Walecka[7] based on the oscillating liquid drop model, and it was shown that this theoretical excitation function, as shown by the dashed line in Fig. 3, was about twenty times smaller than the experimental one. In the lowest energy region, however, it is of significance to test the applicability of this formula further by experiments, because there are almost no

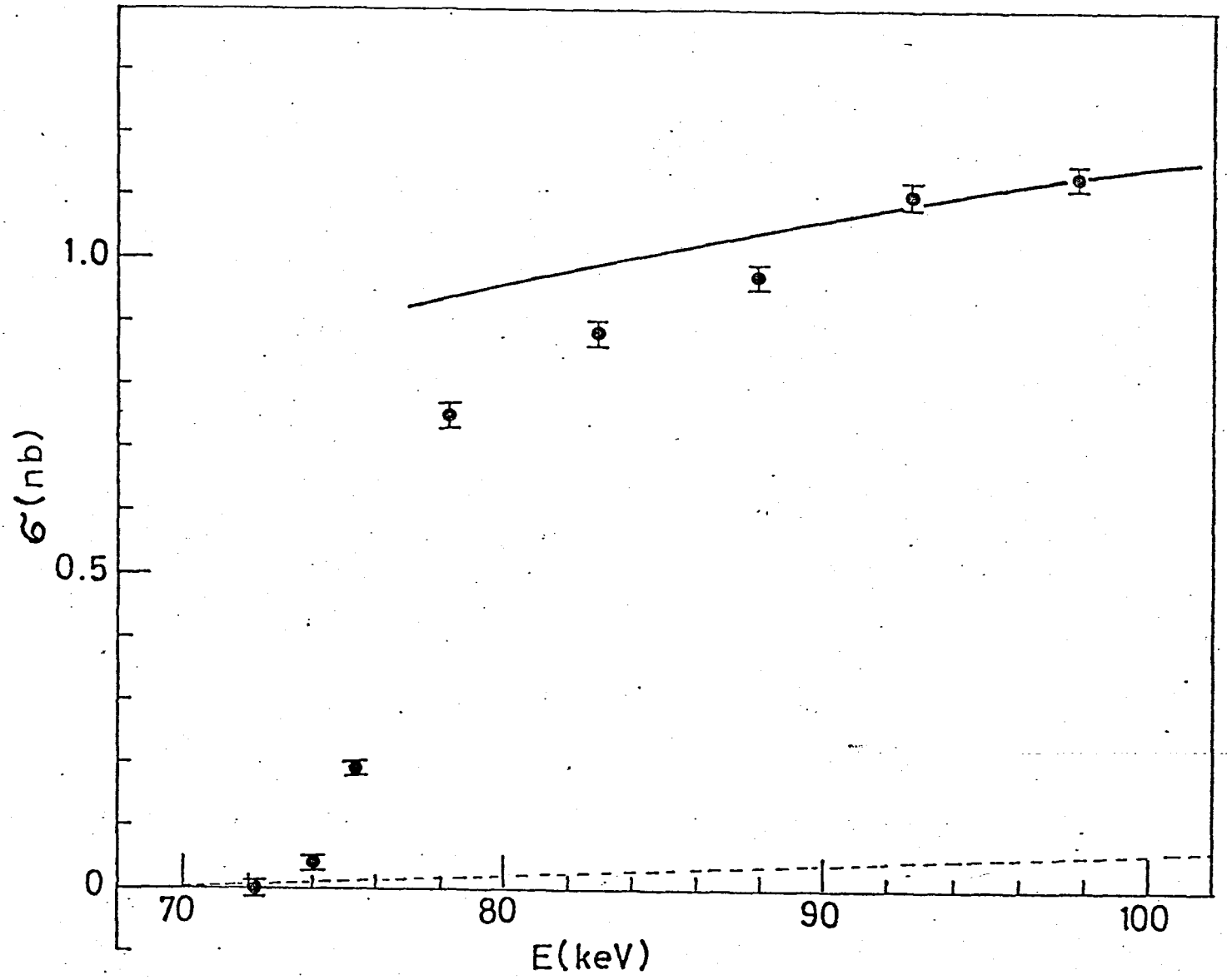

Fig. 3. Isomer production cross sections in ^{189}Os in a function of incident electron energy. Points show the expermimental cross sections. The solid line indicates the theoretical curve for NEET, and the dashed line indicates that through Coulomb excitation by means of electrons.

experimental studies of Coulomb excitation by electrons performed especially in the region well below 1 MeV.

The purpose of the study described in Chapter I is to check the formula of de Forest and Walecka in the energy region of some tenths MeV, and to give a supplementary verification of NEET in ^{189}Os.

5. NEET IN ^{189}Os FOLLOWING PHOTOIONIZATION

The first stage of NEET in ^{189}Os is the creation of K-hole in the ^{189}Os atom. This was done by electrons in the experiments reported in ref. 5,6. As mentioned above, Coulomb excitation by electron projectiles had to be taken into account as an inevitably competing mechanism for isomer production in those experiments. The K-vacancy in atoms can also be created by photons as well as by electrons. Therefore, NEET can be observed without the interference of Coulomb excitation in those experiments in which photons are used for K-shell ionization.

In Chapter II, the experimental study on NEET in ^{189}Os following K-shell photoionization is described. As a photon source, bremsstrahlung produced in a converter bombarded with electrons was used for its ready availability of high intensity beam.

6. NEET IN ^{237}Np

The nuclide ^{237}Np is another candidate which satisfys the NEET conditions. The nuclear excitation of the 102.95-keV level in ^{237}Np proceeds by E1 as does the electronic transition between the K and L_3 shells with an energy of 101.072 keV. Therefore, NEET is attainable by the exchange of virtual photons between these transitions. Since ^{237}Np has no isomeric level suitable for residual radioactivity measurement, the technique employed in the ^{189}Os experiment is not applicable to this nuclide.

Since ^{237}Pu has a large branch of decaying to the ground state of ^{237}Np by K-electron capture, the stage is set automatically for NEET in such circumstances, as shown in Fig. 4. Some attempts to detect NEET in ^{237}Np have been made by Otozai et al.[3,4,8,9] with an ingenious method of examining the perturbed X-ray spectrum in the EC decay of ^{237}Pu. The satellite X-ray peaks will appear according to the level repulsion as shown in Fig. 1. The satellite lines corresponding to the transitions $\Phi_1 \rightarrow \psi_1\phi_{2,3,\ldots}$ and $\Phi_2 \rightarrow \psi_2\phi_{3,4,\ldots}$ have energies different by δ from that unperturbed, whereas the complementary satellites from the transitions $\Phi_1 \rightarrow \psi_2\phi_{3,4,\ldots}$ and $\Phi_2 \rightarrow \psi_1\phi_{2,3,\ldots}$ have energies different by $\Delta + \delta$ from the unperturbed ones. The latter satellite peaks may be detectable, although γ-rays following NEET

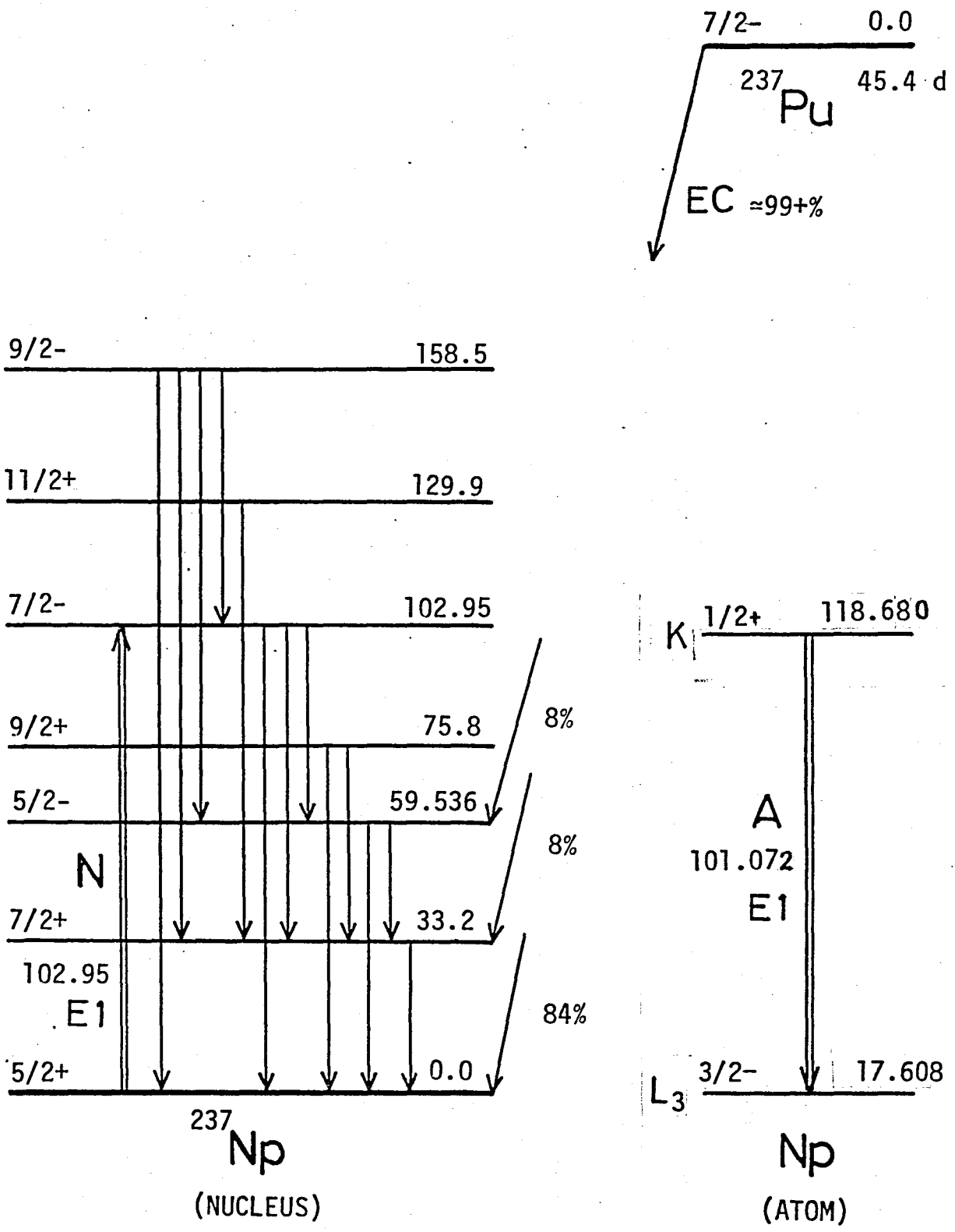

Fig. 4. Decay scheme of ^{237}Pu. The nuclear transition N and the atomic transition A in ^{237}Np fulfill the NEET conditions. The K-hole state is produced in the K-electron capure decay of ^{237}Pu

are not distinguishable from those emitted in the normal decay of ^{237}Pu. Otozai et al.[3,4,8] focussed their efforts on the $L\alpha_1$ satellite. Nevertheless, the U L X-rays from ^{236}Pu and ^{238}Pu interfered with that satellite peak. Shinohara et al.[9] examined the $K\alpha_1$ satellite, as shown in Fig. 5m and obtained an upper limit of 2×10^{-3} for the NEET probability *P*.

In Chapter III another attempt to observe NEET in ^{237}Np is described. Deexcitation γ-rays from the NEET-excited level at 103 keV may be detectable during irradiation of a ^{237}Np target with ionizing particles. The 69-keV γ-ray was searched by a photon spectrometer in a course of irradiation with γ-radiations from a ^{57}Co source.

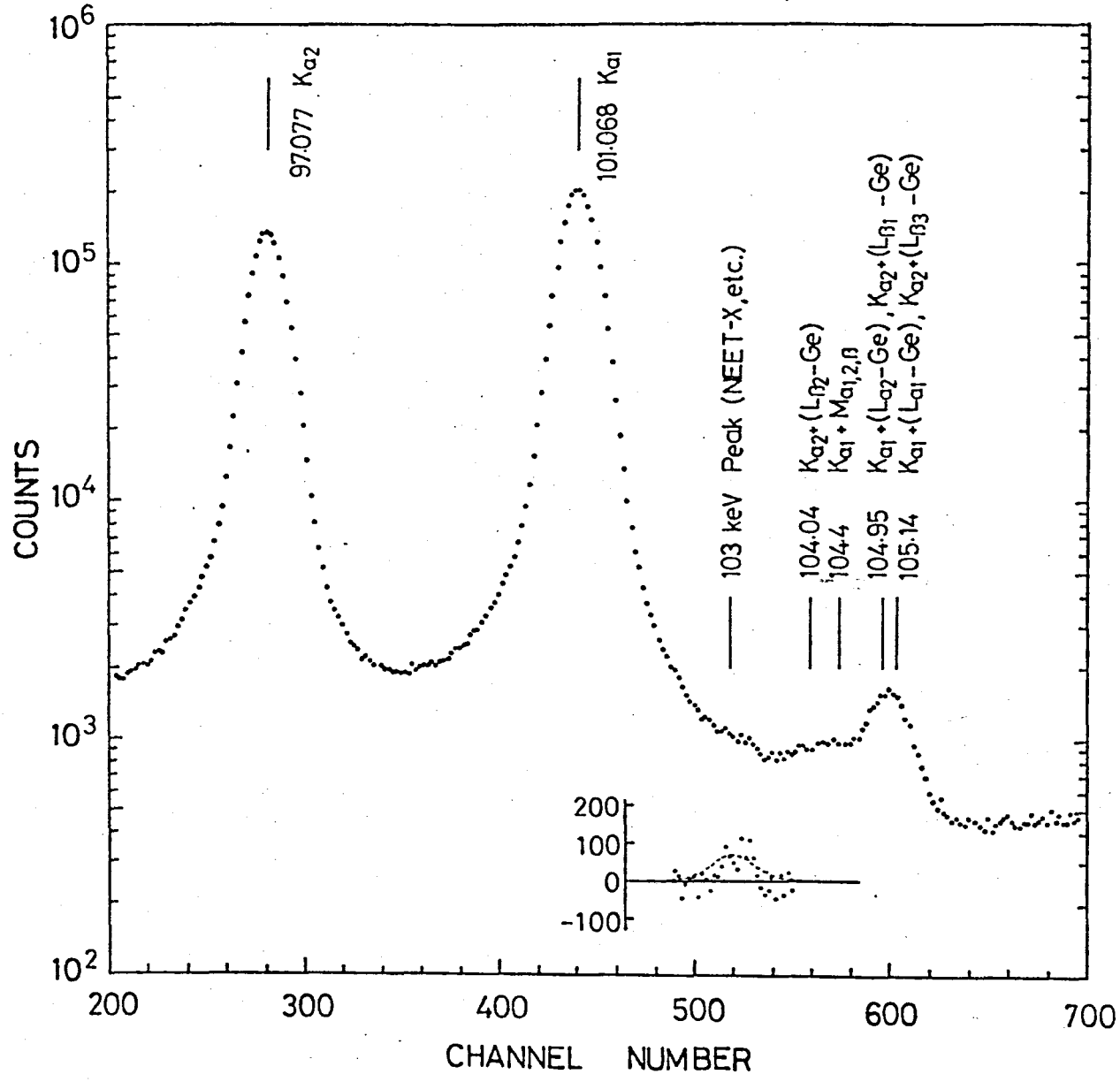

Fig. 5. $K\alpha_{1,2}$ X-ray peaks from ^{237}Pu. The satellite peak of the $K\alpha_1$ X ray is located at 103 keV.

References

1) M. Morita, *Prog. Theor. Phys.* 49, 1574 (1973).

2) See, e.g., S. Devons and I. Duerdoth, *Adv. Nucl. Phys.* 2, 295 (1969); J. Hüfner, F. Scheck and C. S. Wu, in "*Muon physics*", ed. V. M. Hughes and C. S. Wu, vol. 1 (Academic press, New York, 1977) p. 202.

3) K. Otozai, *Butsuri* 30, 273 (1975).

4) K. Otozai, Osaka University Laboratory of Nuclear Studies report OULNS 77-5 (1977).

5) K. Otozai, R. Arakawa and T. Saito, *Nucl. Phys.* A297, 97 (1978).

6) K. Otozai, R. Arakawa and M. Morita, *Prog. Theor. Phys.* 50, 1771 (1973).

7) T. de Forest, Jr. and J. D. Walecka, *Adv. Phys.* 15, 1 (1966).

8) K. Otozai, R. Arakawa, M. Morita, H. Baba, K. Hata and T. Suzuki, unpublished work.

9) A. Shinohara, T. Saito, R. Arakawa, K. Otozai, H. Baba, K. Hata and T. Suzuki, to be published.

CHAPTER I

COULOMB EXCITATION BY ELECTRON PROJECTILES IN ^{103}Rh

1. Introductory Remarks

When charged particles such as the nuclear particles and the electron collide with nuclei, the nucleus can be raised to an excited state and at the same time the projectile is inelastically scattered as a result of the electromagnetic interaction between them. This process is commonly referred to as Coulomb excitation. In the case of nuclear projectiles, their energy is normally kept below the Coulomb barrier to avoid the effect of nuclear forces. Since the Coulomb barrier height V_B is approximately expressed by $V_B \approx Z_{proj} Z/(A^{1/3})$ MeV, Z_{proj} and Z being the atomic numbers of the projectile

and the target, respectively, and A the mass number of the target, the projectiles with energies less than about $10Z_{proj}$ MeV are favored. On the other hand, the most favorable energies for electron projectiles are around 100 MeV or more, since nuclear excitation by electrons results only from the electromagnetic interaction. For that reason, Coulomb excitation by electrons (or inelastic electron scattering) has been widely used as a powerful tool for studying nuclear structure. This is extensively discussed for the various types of interaction by de Forest and Walecka in their review article.[1] The theoretical treatments are compared to the experimental results obtained in the favorable regions of electron energy and target Z numbers.

In the NEET experiments on ^{189}Os [ref. 2,3], electrons were used to ionize the K-shell of an ^{189}Os atom, and hence Coulomb excitation of the ^{189}Os nucleus by incident electrons may have been occur in such circumstances. This process had to be taken into account as an inevitable mechanism competing with NEET for isomer production. The contribution of this process to the production of isomer was calculated by using a formula of de Forest and Walecka,[1] and found to be much smaller than the experimental results. The applicability of this formula to the lowest energy region, however, should be checked further by experiments, because that formula is discussed in the framework of first Born

approximation, which is expected to be a good approximation for small $Z\alpha/\beta$, α being the fine structure constant ($\simeq 1/137$) and β ($= v/c$) the velocity of incident electron divided by that of light, and is modified to a simpler form by arguments permissible in the limiting conditions.

The lowest energy, at which Coulomb excitation by electrons was investigated, was probably atout 1 MeV on ^{115}In by Booth and Brownson.[4] Their experiment is the activation of a low-lying, long-lived isomeric state in the stable nuclues ^{115}In by excitation of higher, short-lived states which have finite branching ratios to the isomeric state. This method is incapable of obtaining the differential cross section and limited to the measurement of the total cross section. There exists another nucleus which, having an isomer, is a likely candidate for excitation and hence for the study in the lower energy region. Coulomb excitation by electrons was studied on ^{103}Rh in the energy region of some tenths MeV.

The 295-keV and 357-keV levels in ^{103}Rh are strongly excited by Coulomb excitation; moreover, only the latter level has a detectable branch decaying the the isomeric state which has an appropriate half-life for the residual radioactivity measurement. In addition, the occurence of NEET need not be taken into consideration in ^{103}Rh, since ^{103}Rh does not fulfill the NEET conditions at all. (Even

the lowest nuclear excited level at 40 keV is much higher in energy than the highest electronic states at 23 keV.) The total cross section for Coulomb excitation of the 357-keV level in ^{103}Rh is readily obtained from that for isomer production. The experimental excitation function was compared with that calculated by the formula of de Forest and Walecka. The applicability of this formula was thus checked in that lowest energy region, though the energy region below 100 keV, as for ^{189}Os, could not be attained by the lack of a suitable nucleus. This result will give a supplementary verification of NEET in ^{189}Os.

2. Experimental

2.1. BOMBARDMENT

A metallic Rh foil 25 μm (31 mg/cm^2) thick and 30 mm in diameter, supplied by A. D. Mackay Inc., NY, was used as a target. Rhodium is a monoisotopic element which consists of one stable nuclide with the mass number 103. Although presumably 0.1% impurities are contained in the target, no interfering activities can be produced in this experiment.

The target was bombarded in air with 350–800-keV electrons from a rectified transformer type electron accelerator in the Osaka Laboratory of the Japan Atomic Energy Research Institute (JAERI). A target assembly is shown in Fig. 1.1. The bombarded area of the target was 5.3 cm^2 (circle with the diameter of 2.6 cm). The bombarding energy of the electron beam was calibrated with an accuracy of about 10 keV by comparing the energy dissipation distribution in cellulose triacetate (CTA) films with that obtained from a Van de Graaff electron accelerator.[5] The Van de Graaff accelerator was calibrated by measuring the range of electrons in Al at 1.000 MeV and by extrapolating the threshold energy of the ^{9}Be(γ,n)^{8}Be reaction with an activation method.[6] That calibration of the former accelerator includes the energy degradation of bombarding

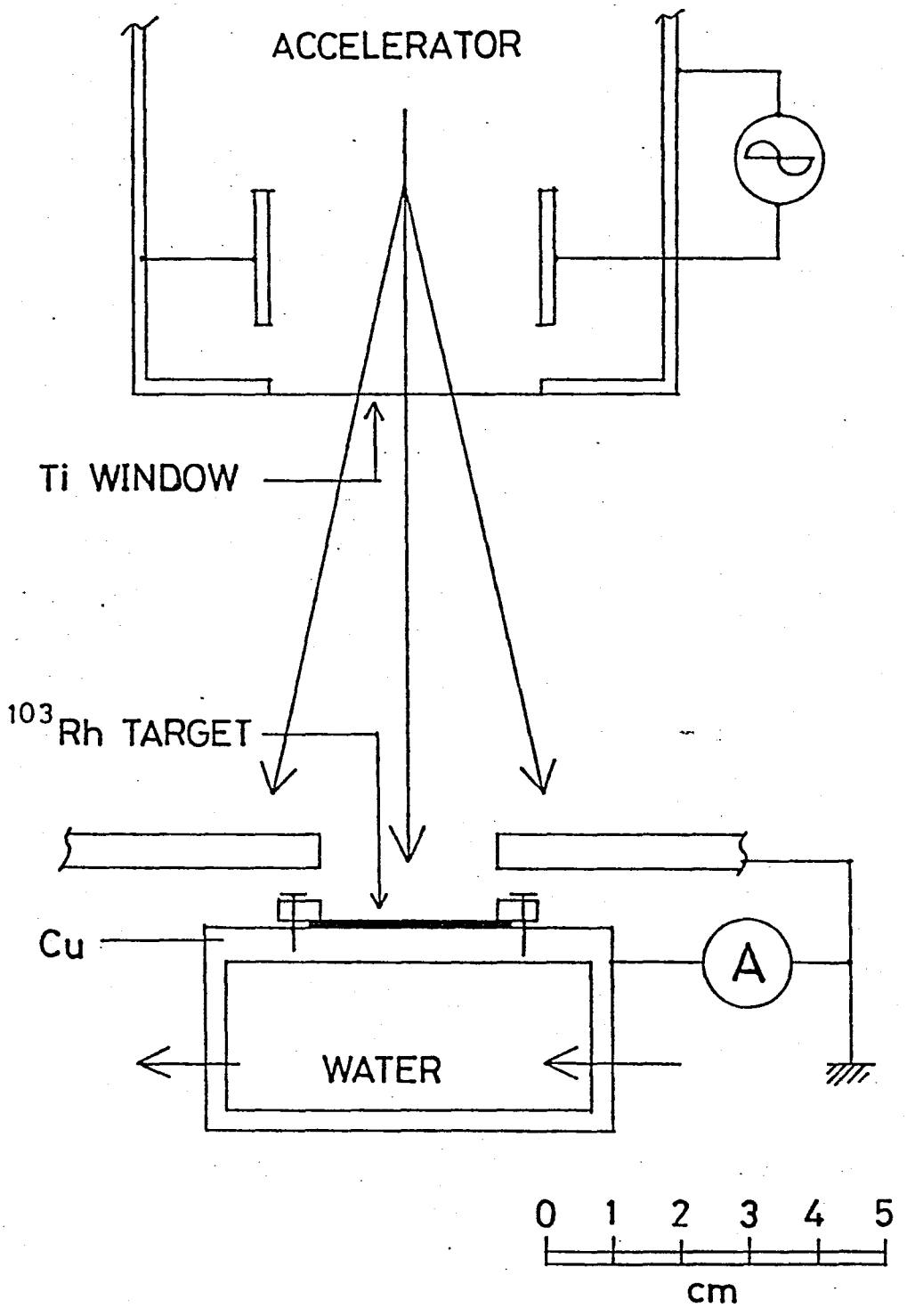

Fig. 1.1. Target assembly for irradiation with electrons. The electron accelerator is drawn down to scale.

electrons in the 0.03-mm thick Ti exist window of the accelerator, and in air with a distance of 8 cm, through which the electron beam traversed to the target. The bombarding current was monitored by an ampermeter connected to the target assembly which is cooled with circulating water. The bombarding energy and current are tabulated (Table 1.1).

2.2. CORRECTION OF BOMBARDING CURRENT

In the bombarding current measurement, reduction in currents due to electrons scattered out in the backward direction were corrected by estimating the coefficients for backscattering of incident electrons and emission of secondary electrons. The bombarding current, I, was obtained from the measured current, I_{meas}, by the relation

$$I = I_{meas} / (1 - \eta_S - \eta_B - \eta_T \eta_B' \eta_T'), \qquad (1.1)$$

where η_S is the secondary emission coefficient, η_B is the backscattering coefficient of electrons for the Rh target, η_T and η_T' are the transmission coefficients of electrons through the target in their forward and backward movements, respectively, and η_B' is the saturation backscattering

Table 1.1. Bombarding energy and current.

Energy/keV	Current/μA	
	Measured	Corrected
800	296	393
720	307	413
650	255	348
575	216	300
500	189	268
425	151	219
350	145	218

coefficient for the target mount consisting of a thick (5 mm) Cu plate (see Fig. 1.2). For all incident energies, η_S was set to be 0.005, the value that Frederickson[7] placed as an upper limit from his careful measurement, although currently adopted values which were obtained at much lower energies are larger than this value. On the other hand, the coefficients for backscattering and transmission were determined for each incident energy, E_0. In estimating these coefficients, the assumption was made that electrons traversed the interface of the Rh target and the Cu mount perpendicularly, and that the electrons actually distributed in energy were delegated by monoenergetic electrons with the most probable energy. Since the Rh target used was not so thick as to give the saturation backscattering, η_B was determined relative to the saturation value $\eta_B(\mathrm{sat})$ according to an empirical expression of Koral and Cohen.[8] The $\eta_B(\mathrm{sat})$ values were obtained from an empirical equation for the backscattering coefficient at saturation by Tabata et al.[9] and by the same equation η_B' was estimated for electrons with an energy of $E_m = E_0 - \Delta E_m$, where ΔE_m is the most probable energy loss of transmitted electrons through the target in their forward movement and was calculated after Landau's theory.[10] The transmission coefficients η_T and η_T' were estimated by an empirical equation of Tabata and Ito.[11] Here η_T' is for electrons of energy $E_m' = E_m - \Delta E_m'$,

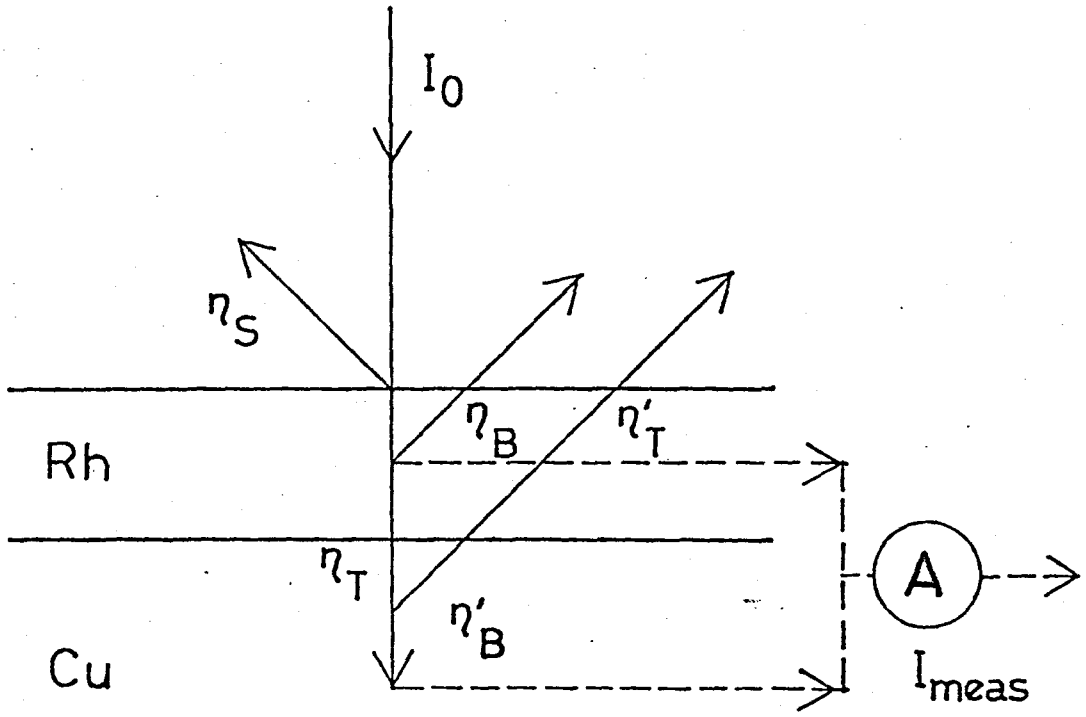

Fig. 1.2. Correction for bombarding current. η_S is set to be 0.005 for all incident energies, whereas other coefficients are evaluated as a function of energy.

where $\Delta E_m'$ is the most probable energy loss of backscattered electrons from Cu.[12] Details for these procedures will be given in Appendix 1.1. The values obtained for η_B, η_T, η_B' and η_T' are given in Table 1.2. The sums of η_B and $\eta_T\eta_B'\eta_T'$ are smaller than η_B(sat). Therefore, these estimate for η's may be considered to be reasonable. The overall correction factor F is given in Table 1.2, and the corrected bombarding currents are listed in Table 1.1.

The bombarding currents were also estimated from the total output currents of the accelerator and the relative current density at the target site which was obtained by measuring the spatial dose distribution with CTA dosimeters.[13] These values are in agreement with the corrected ones given above.

2.3. MEASUREMENT OF RADIOACTIVITY

After 2-h bombardment the radioactivity induced in the target was measured with a 2π windowless Q-gas flow GM counter, surrounded by peripheral anticounters, with a background below 0.02 counts/s at this Faculty. The obtained decay curve of target activity were analyzed by the least-squares fit of the ^{103m}Rh component ($t_{1/2}$ = 56.12 min [ref. 14]) and a constant background component with the aid of the

Table 1.2. Numerical values for η_S, η_B, η_T, η_B' and η_T' in Eq. (1.1), and the obtained correction factor for bombarding current, F.[a)]

E_0/keV	η_S	η_B	η_T	η_B'	η_T'	F
800	0.005	0.069	0.889	0.237	0.821	1.329
720	0.005	0.089	0.869	0.242	0.778	1.346
650	0.005	0.112	0.846	0.246	0.724	1.365
575	0.005	0.145	0.812	0.251	0.638	1.390
500	0.005	0.192	0.764	0.255	0.505	1.419
425	0.005	0.252	0.692	0.260	0.307	1.453
350	0.005	0.317	0.578	0.264	0.086	1.504

a) $F = 1/(1 - \eta_S - \eta_B - \eta_T\eta_B'\eta_T')$.

CLSQ code[15] using an ACOS computer at Osaka University, since this experiment was free from radioactivities other than ^{103m}Rh. As an example, Fig. 1.3 shows the decay curve obtained at an electron energy of 800 keV.

Since the target was thicker than the ranges of conversion electrons from ^{103m}Rh, typically 2.1 mg/cm^2 for the intensest L_3-conversion electrons (extrapolated range estimated by a semiempirical equation of Tabata et al.[16] for their energy E = 36.75 keV), inevitable ambiguity was introduced in determining the detection coefficient of the GM counter for the electrons. In order to obtain the absolute cross sections, X-ray counting was carried out with a photon detector in the case of 720 and 800 keV. The targets simultaneously bombarded were assayed separately to electron and photon countings. The detector was an ORTEC hyperpure Ge low-energy photon spectrometer (LEPS) with resolution of 290 eV at 20 keV. As Fig. 1.4 shows, the output pulses of the spectrometer were fed to a Hewlett-Packard multi-channel analyzer (MCA) through standard electronics. The gain of an analog-to-digital converter was set to be 256 channels and the memory of the MCA was divided into four sections. With this setting, the decay of ^{103m}Rh was followed for over 10 half-life period of the isomer. The typical photon spectrum of ^{103m}Rh is shown in Fig. 1.5. The Rh $K\alpha_{1,2}$ (20.22 and 20.07 keV) and $K\beta_{1,2}$

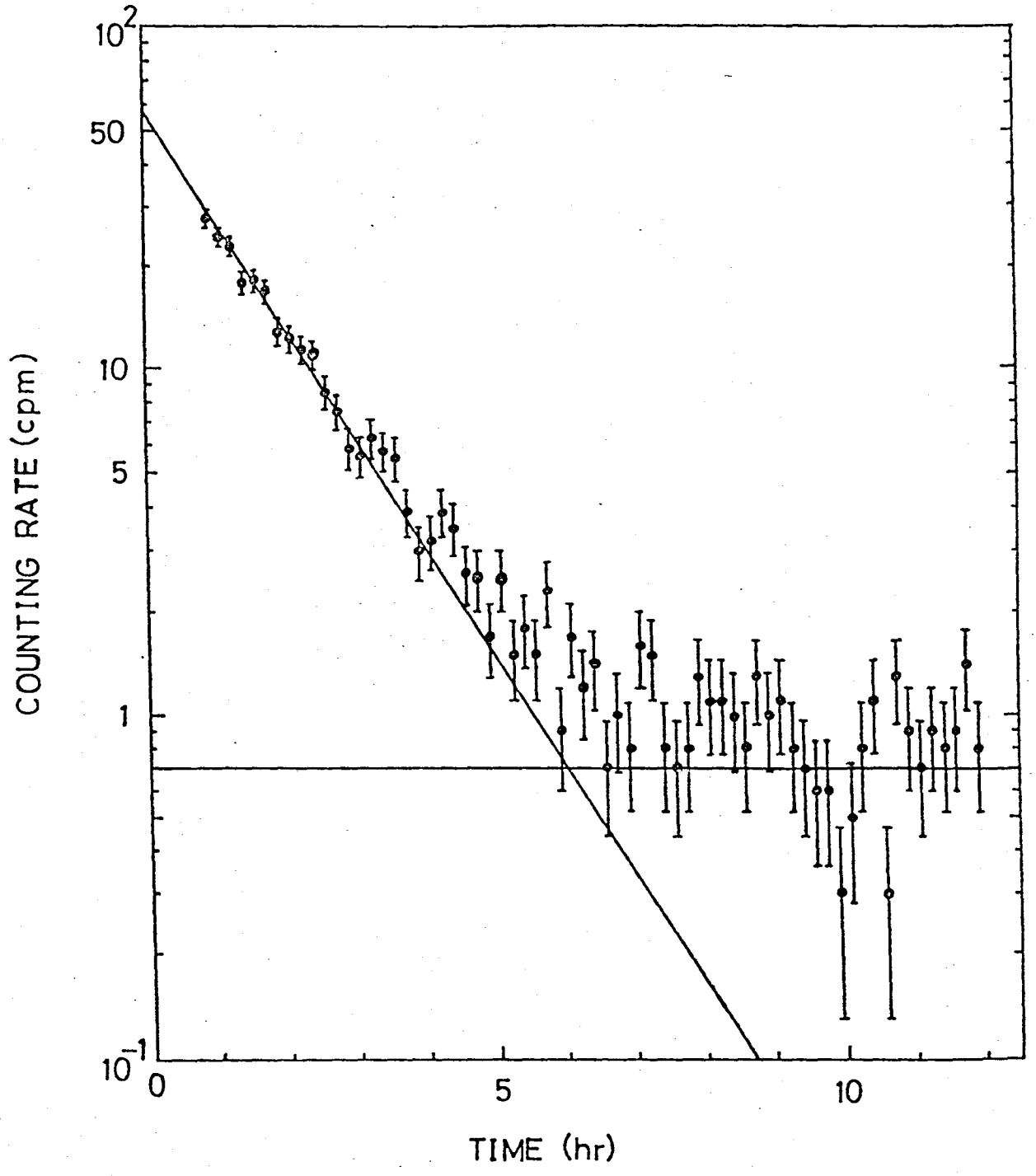

Fig. 1.3. Typical decay curve of ^{103m}Rh obtained with 800 keV electrons. The solid line indicate the result of a least-squares fit.

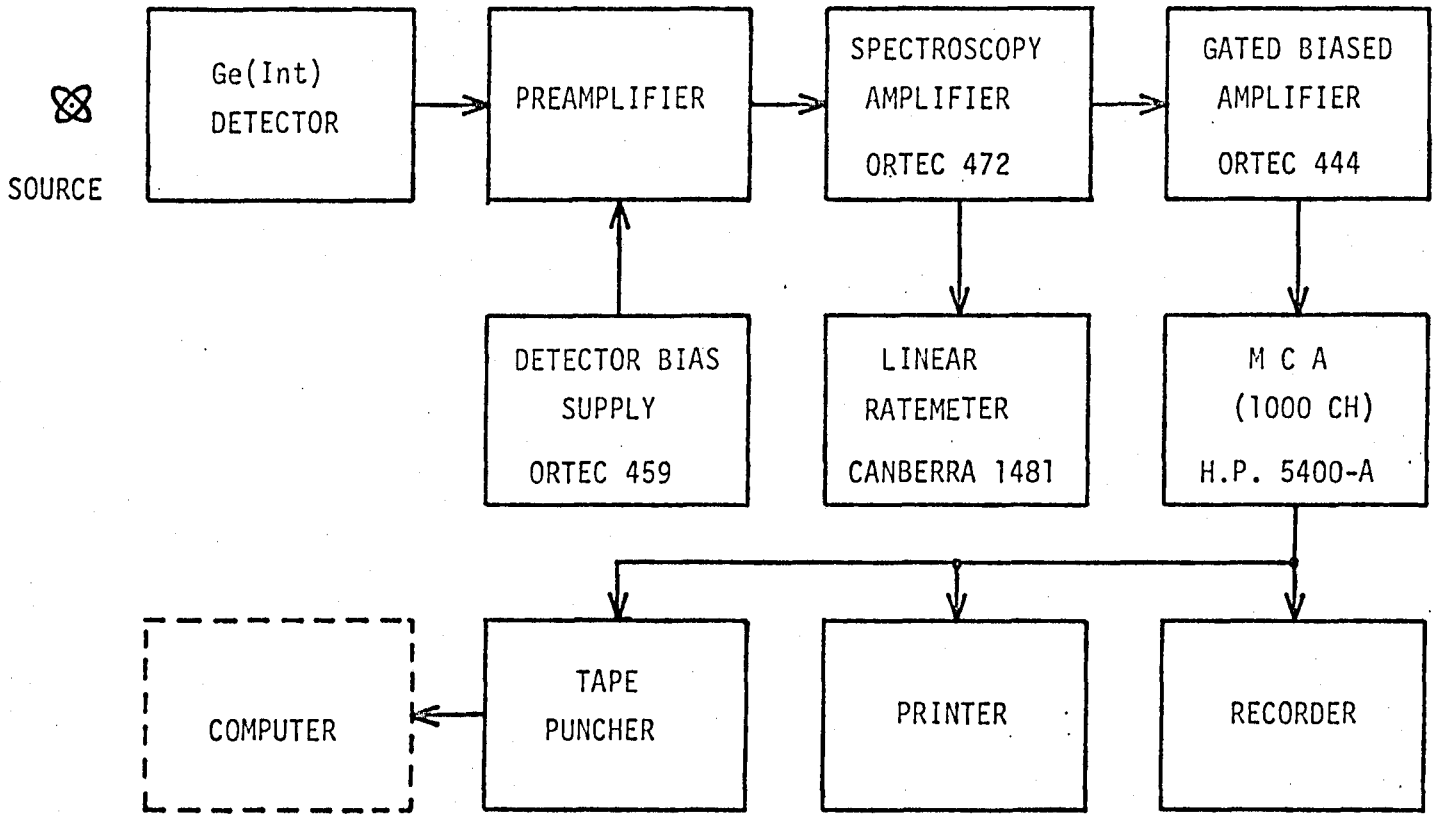

Fig. 1.4. Block diagram of a photon counting system. The ADC gain was set to be 256 channels and the memory was divided into four sections in order to follow the decay of ^{103m}Rh.

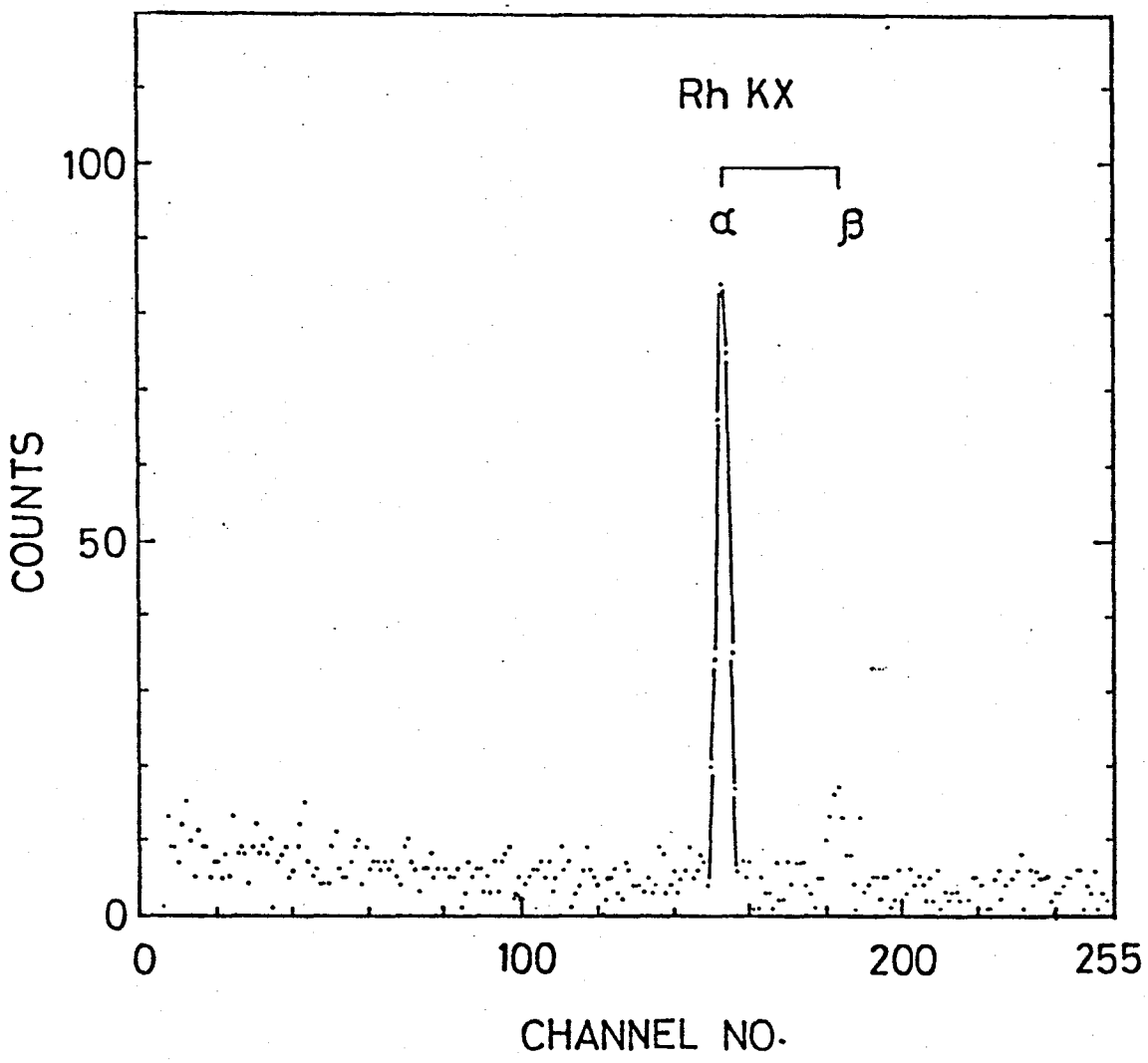

Fig. 1.5. Typical photon spectrum of ^{103m}Rh induced by 720-keV electrons. The accumulation time was 200 min. from 50 min. after EOB. The Rh $K\alpha_{1,2}$ (20.22 and 20.07 keV) and $K\beta_{1,2}$ (22.72 and 23.17 keV) lines are clearly observed.

(22.72 and 23.17 keV) lines are clearly observed in the spectrum. The area of the Kα peak was calculated by using the BOB73 γ-spectrum analyzing code.[17–20] The decay of the peak counts was analyzed with the aid of the CLSQ code.[15] The absolute efficiency of the photon detector for the Rh Kα X-ray was calibrated by using reference sources and by estimating the geometric factor.

The absolute efficiency for photons of energy E can be written as

$$\varepsilon_{ph}(E) = \varepsilon_R(E) \cdot G(E), \qquad (1.2)$$

where ε_R is the relative efficiency of photopeaks and G is the geometric factor. The ε_R curve was constructed by referring to the point-like sources of ^{241}Am, ^{57}Co and ^{133}Ba which were calibrated and supplied by The Radiochemical Center, Amersham, England. The obtained curve is shown by the solid line in Fig. 1.6. For comparison, the theoretical curve calculated according to the stepwise procedure given by Hansen et al.[21] is shown by the dashed line in the same figure. The agreement is good on the whole. The $\varepsilon_R(E = 20$ keV) value was then determined to be 0.88 ± 0.06. The geometric factor, namely, the solid angle of the target subtended by the photon detector was calculated by a Monte Carlo method,[22] including the correction factor for attenuation

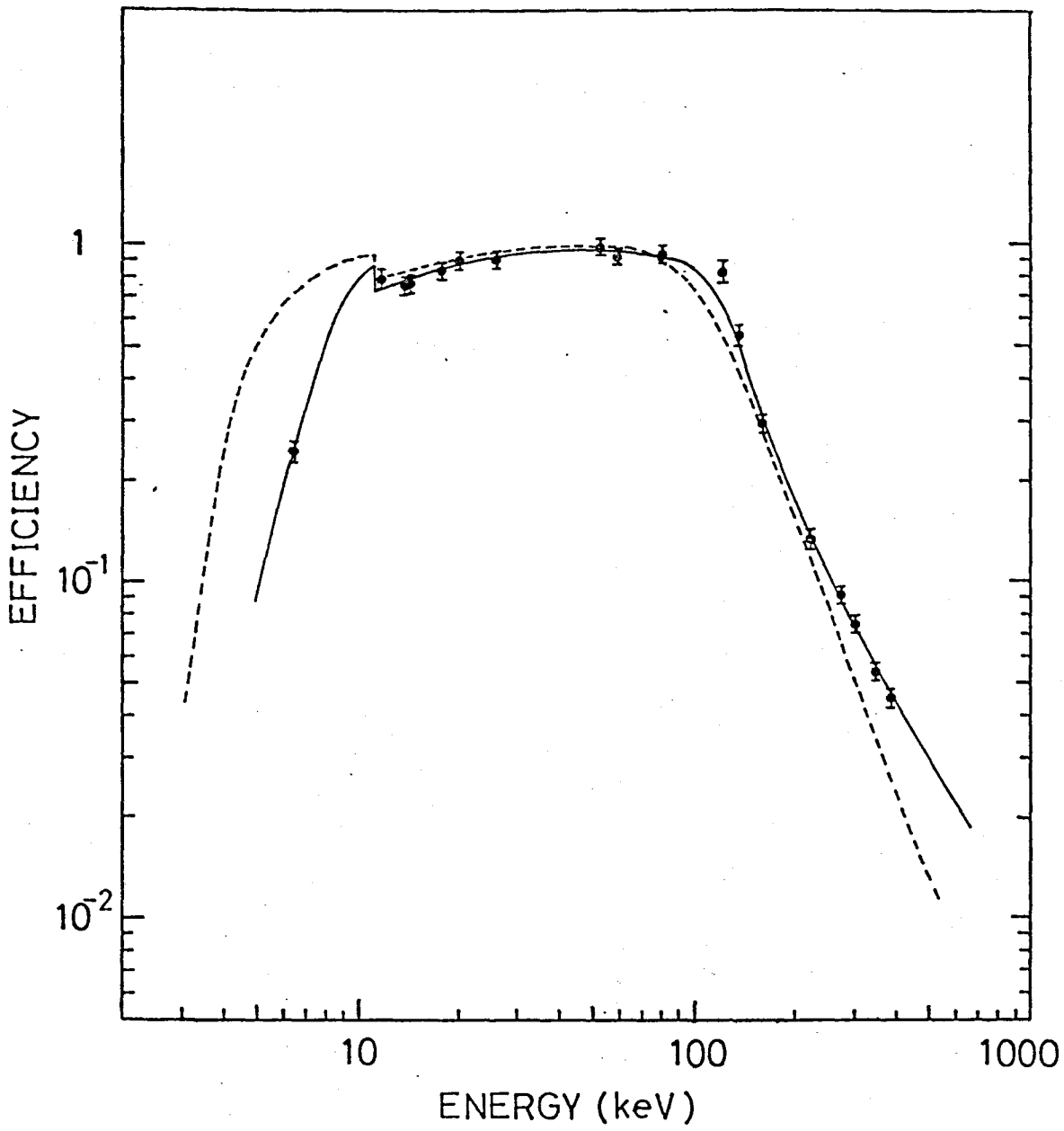

Fig. 1.6. Relative efficiency of the LEPS as a function of photon energy. The solid curve is fitted to the experimental points. For comparison, the theoretical curve is shown by the dashed line.

of photons in the target. The calculated $G(E = 20\ \text{keV})$ value for the Rh target was $(4.76 \pm 0.10) \times 10^{-2}$. From eq. (1.2) with these values, ε_{ph} was obtained as $\varepsilon_{ph} = (4.19 \pm 0.30) \times 10^{-2}$.

The number of $K\alpha$ X-rays emitted per disintegration of ^{103m}Rh is expressed by

$$\kappa_{ph} = [\alpha_K/(1 + \alpha_T)]\,[\Gamma(KL)/\Gamma(K)]\,\omega_K \ , \qquad (1.3)$$

where α_K and α_T are the K-shell and total conversion coefficients for ^{103m}Rh, respectively, $\Gamma(KL)/\Gamma(K)$ is the branching ratio of the KL transition in the decay of the K-hole state, and ω_K is the K-shell-fluorescence yield. From conversion-electron data by Grunditz et al.,[23] the values for α_K and α_T were evaluated to be $\alpha_K = 147 \pm 14$ and $\alpha_T = 1470 \pm 65$. The ratio $\Gamma(KL)/\Gamma(K) = 0.840$ was taken from the relativistic Hartree-Slater values for emission rates by Scofield,[24] and the value of $\omega_K = 0.807 \pm 0.031$ from the compiled data by Bambynek et al..[25] Substituting these values into eq. (1.3), κ_{ph} was determined as $\kappa_{ph} = (6.77 \pm 0.76) \times 10^{-2}$.

The detection coefficient of the photon detector for ^{103m}Rh, $\varepsilon_{ph}\kappa_{ph}$, was then determined to be $(2.84 \pm 0.38) \times 10^{-3}$.

2.4. CORRECTION OF RADIOACTIVITY INDUCED BY BACKSCATTERED ELECTRONS

Backscattered electrons can also excite a target nucleus in their backward traverse if they still have sufficient energies (> 0.35 MeV). This contribution has to be corrected in the present experiment, since the backscattering of incident electrons is not insignificant because of their lower energy and a thicker target. Bothe[26] has measured the relative distributions in energy of the backscattered electrons at 370-keV and 680-keV incident energy on Cu, Sn, and others. The energy distributions of electrons backscattered from the Rh target and the Cu mount respectively at incident energies of E_0 = 350–800 keV and $E_m = E_0 - \Delta E_m$ = 320–775 keV were evaluated by interpolating and extrapolating Bothe's results linearly in incident electron energy and target atomic number (see Fig. 1.7). In this procedure, it was assumed that the energy distribution was not angularly dependent and, in the case of Cu, incident energy was that of the representative electrons with the most probable energy E_m, as given in Section 2.2. The backscattering coefficients used here were those estimated in Section 2.2. By using the obtained energy distribution which was divided into ten intervals to make calculations easier, together with η_B and η_B', the radioactivity of ^{103m}Rh induced by

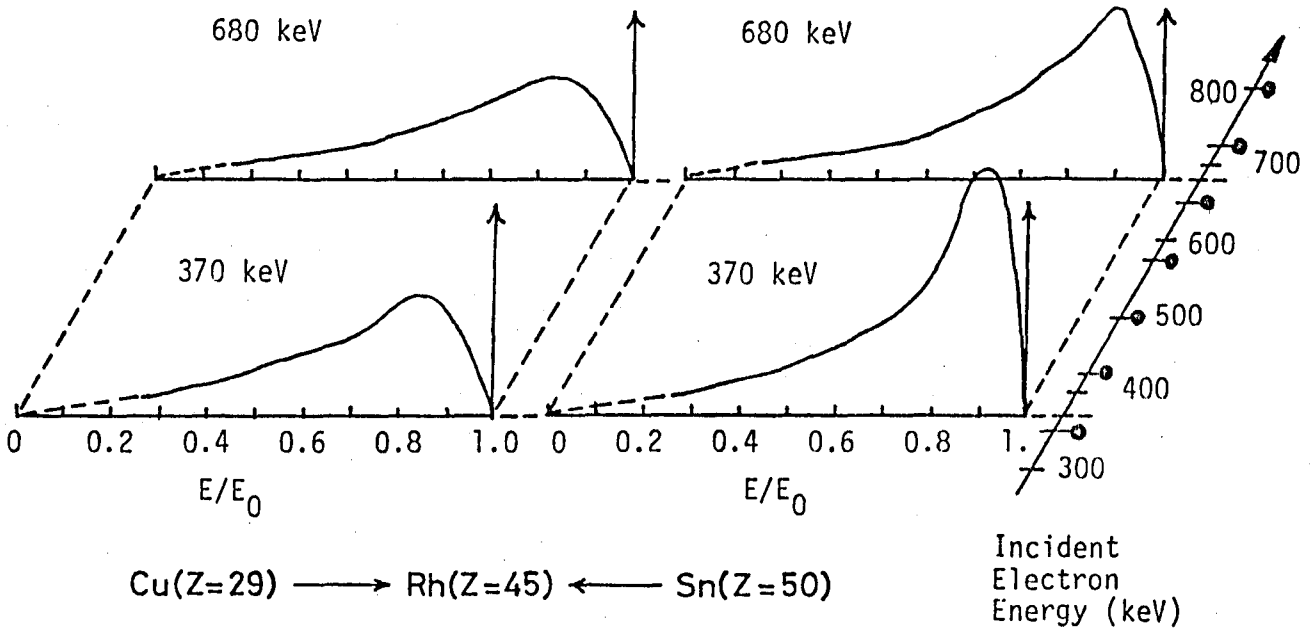

Fig. 1.7. Energy distribution of backscattered electrons. From the results of Bothe,[26] indicated by the solid curves, the distribution were interpolated or extrapolated for the Rh target at incident energies indicated by solid circles and for the Cu mount at energies corrected for energy degradation in the target.

backscattered electrons was estimated. Provided that the measured yield (the count rate of the GM counter) curve as a function of incident energy was the first preliminary one, the true yield curve for the isomer ^{103m}Rh was extracted by successive approximation. The details of this procedure will be given in Appendix 1.2. The largest correction was a reduction of the isomer yield by 4.4 cpm/mA at 800 keV.

3. Results

Results obtained by the GM counter (LBC) is summarized in Table 1.3. Counts rates for ^{103m}Rh were exprapolated to those at the end of bombardment and corrected for the contribution of backscattered electrons. The results of photon (X-ray) counting with LEPS is compared with those of electron counting with the GM counter (LBC) in Table 1.4. The ratios of LBC/LEPS obtained at two different energies agree excellently.

The cross section for isomer production in ^{103}Rh by electrons is given by

$$\sigma_{iso} = C_0/\{\kappa\varepsilon nxQ[1 - \exp(-\lambda t)]\}, \qquad (1.4)$$

where C_0 is the count rate of the GM counter for ^{103m}Rh at the end of bombardment, κ the emission probability for conversion electrons per disintegration of ^{103m}Rh, ε the counting efficiency of the GM counter for conversion electrons from ^{103m}Rh, n the atomic density of target nuclide, x the thickness of the Rh target, Q the incident rate of bombarding electrons, λ the decay constant of ^{103m}Rh and t the bombarding duration. In this experiment, $nx[1 - \exp(-\lambda t)]$ was kept contant as $7.26 \times 10^{22} \times 2.5 \times 10^{-3} \times [1 - \exp(-\ell n2 \times 120/56.12)] = 1.40 \times 10^{20}$ (cm^{-2}), and Q was

Table 1.3. Results of the measurement of ^{103m}Rh by the GM counter. The count rate, C_0, is extrapolated to that at the end of bombardment.

E_0/keV	I_0/mA	C_0/cpm	$(C_0/I_0)/(cpm/mA)$ [a]
800	0.393	46.0 ± 1.8	117.0 ± 4.5
720	0.413	35.1 ± 1.6	85.0 ± 3.8
650	0.348	19.0 ± 0.8	54.7 ± 2.3
575	0.300	12.3 ± 1.2	40.9 ± 3.9
500	0.268	9.5 ± 0.6	35.4 ± 2.2
425	0.219	6.2 ± 0.6	28.2 ± 2.9
350	0.218	0.1 ± 0.2	0.6 ± 1.1

a) Errors include only those in the radioactivity measurement.

Table 1.4. Comparison of photon counting with LEPS and electron counting with LBC (a low-background counter of the GM type).

E_0/keV	C_0(LEPS)/cpm [a]	C_0(LBC)/cpm [a]	LBC/LEPS
800	9.82 ± 0.50	50.4 ± 1.8	5.13 ± 0.32
720	7.70 ± 0.44	39.0 ± 1.6	5.06 ± 0.36
Average			5.10 ± 0.24

a) Both these values include the contribution of backscattered electrons.

measured as $Q = 60 \times 10^{-3} I_0/(1.602 \times 10^{-19}) = 3.7449 \times 10^{17} I_0$, where Q is in min^{-1} and I_0 is in mA. The product of κ and ε was experimentally determined by comparing it with that obtained by photon counting as

$$\kappa\varepsilon = (C_0/C_0')\kappa_{ph}\varepsilon_{ph} , \qquad (1.5)$$

where κ_{ph} and ε_{ph} are the same as those stated in Section 2.3 and C_0' is the count rate of photon counter for the Rh Kα X-rays at the end of bombardment. The numerical value for $\kappa_{ph}\varepsilon_{ph}$ is determined to be $(2.84 \pm 0.38) \times 10^{-3}$, as described in Section 2.3. The ratio C_0/C_0' is given in Table 1.4 as $C_0/C_0' = 5.10 \pm 0.24$, which was obtained experimentally. With these values, $\kappa\varepsilon$ is determined to be $\kappa\varepsilon = (1.45 \pm 0.11) \times 10^{-2}$. Since $\kappa \simeq 1$, one has $\varepsilon = 0.015$. This is quite reasonable from the fact that the conversion electrons from ^{103m}Rh emitted in the range, which is about one fifteenth of the total thickness of the target, are detected by an efficiency of 0.22. Finally, eq. (1.4) can be rewritten numerically as

$$\sigma_{iso} = (C_0/I_0) \times (1.32 \pm 0.19) \times 10^{-36}, \qquad (1.6)$$

where C_0/I_0 is in cpm/mA and σ_{iso} is in cm^2. The error in eq. (1.6) includes only that in the measurement of radio-

activity and the uncertainty in the correction applied to bombarding currents is believed to be less than 20% of the results.

The absolute cross sections for isomer production σ_{iso} were calculated by eq. (1.6) from the results of radioactivity measurement given in Table 1.3. The results obtained for σ_{iso} are summarized in Table 1.5 and depicted in Fig. 1.8. The cross sections for Coulomb excitation of higher excited levels by electrons will be discussed later.

Table 1.5. Summary of the experimental cross sections for isomer production in ^{103}Rh by electron projectiles.

E_0/keV	$\sigma_{iso}/10^{-36}cm^2$
800	154 ± 23[a)]
720	112 ± 17
650	72 ± 11
575	54.0 ± 9.3
500	46.7 ± 7.3
425	37.2 ± 6.6
350	0.8 ± 1.5

a) The uncertainty does not include one arising from bombarding current measurement.

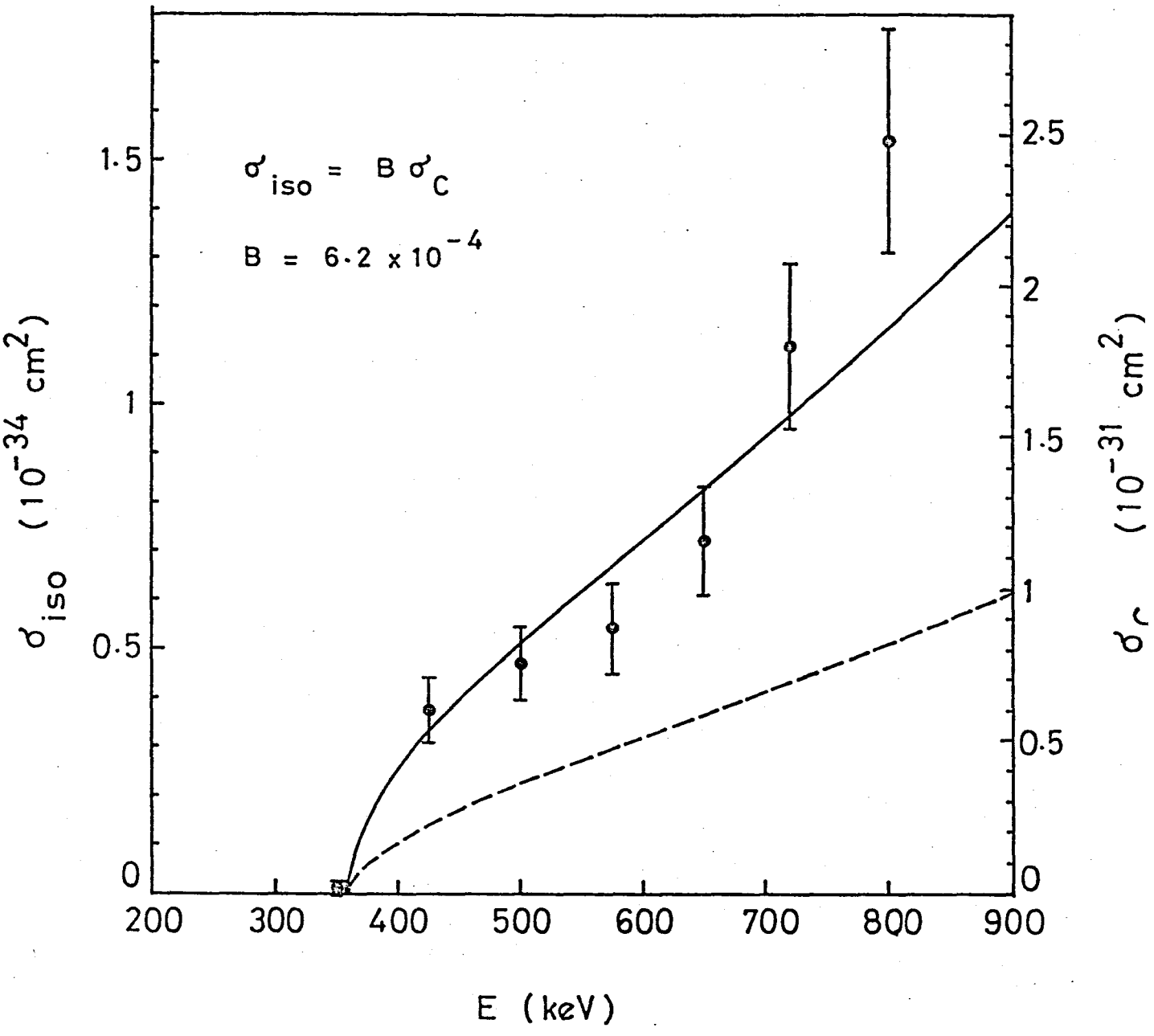

Fig. 1.8. Cross sections for isomer production in ^{103}Rh, σ_{iso}, as a function of incident electron energy E. Those for the 357-keV level excitation, σ_C, are also shown by the right ordinate. The solid line shows a theoretical excitation function calculated by a formula of de Forest and Walecka with semiempirical parameters and the dashed line indicates that obtained with the experimental B(E2)↑ value.

4. Discussion

4.1. CROSS SECTIONS FOR THE 357-keV-LEVEL EXCITATION

The level scheme of ^{103}Rh is shown in Fig. 1.9 for those levels below 800 keV.[27,28] The excited levels in ^{103}Rh are interpreted in terms of the coupling of the collective core excitation and an unpaired proton. The 3/2- level lying at 295 keV and the 5/2- level lying at 357 keV are a one-phonon doublet in the oscillating liquid drop model. Since B(E2)↑ values for those two levels are substantially equal, 0.22 and 0.37 in units of 10^{-48} e^2 cm^2, which have been measured in the Coulomb excitation experiment with nuclear projectiles,[27] the cross sections for Coulomb excitation of those levels by electrons may also be considered to be about the same in magnitude to each other. From the results of γ-ray measurement of ^{103}Pd, which decays to ^{103}Rh by electron capture, by Macias et al.[28] with the α_{tot} values for the relevant γ-transitions compiled by Kocher,[27] one can readily evaluate the value of 6.2×10^{-4} for the branching ratio of the 357-keV level to the isomeric level at 40 keV, B, and an upper limit of 2.8×10^{-5} for that of the 295-keV level, B', namely, $B/B' > 22$. This implies that, although the 295-keV level in ^{103}Rh may be raised by Coulomb excitation as much as the 357-keV level, isomers produced can be attributed

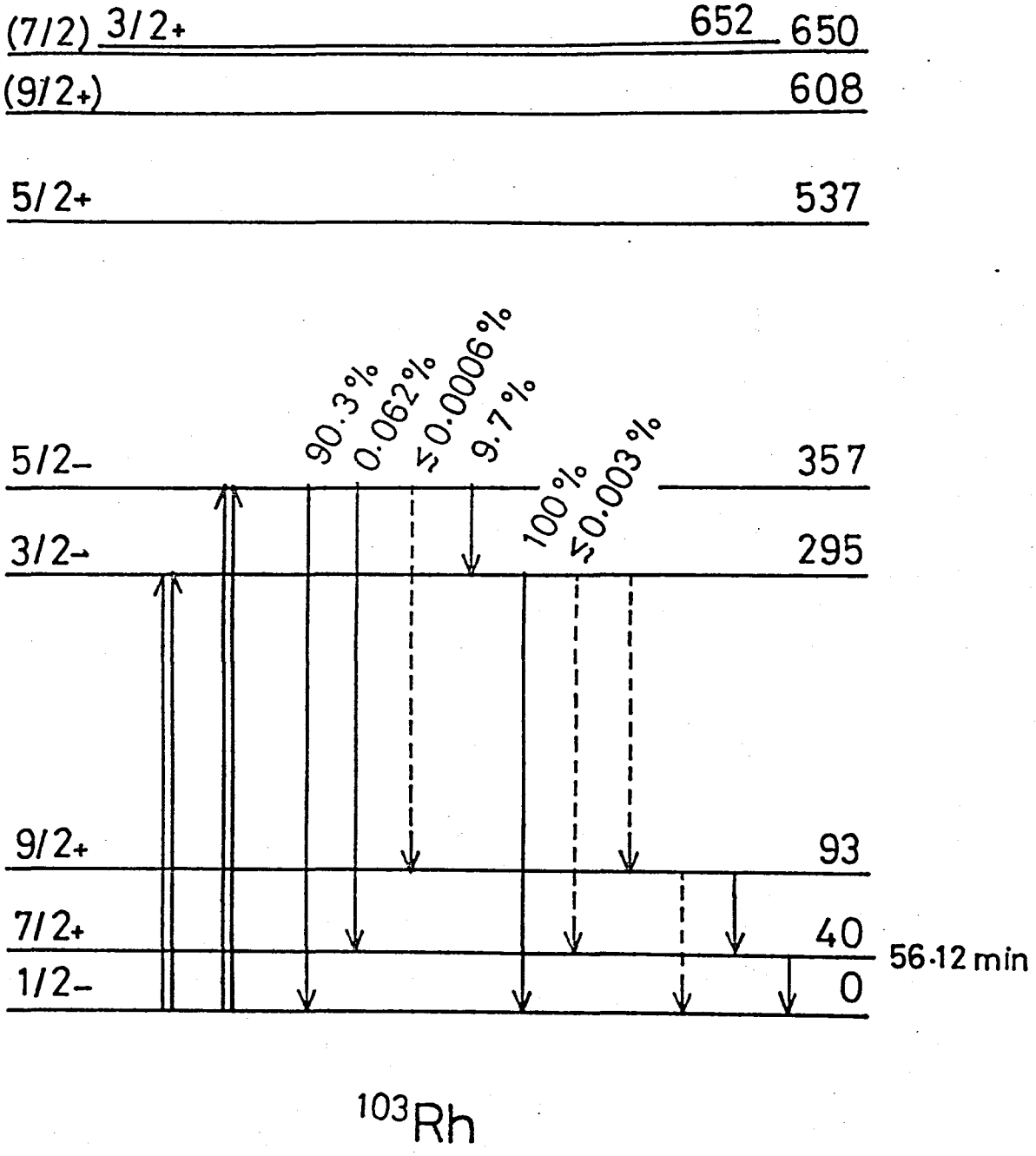

Fig. 1.9. Level scheme of ^{103}Rh below 800 keV. The double arrows indicate Coulomb excitation, and the arrows with solid lines and with dashed lines indicate seen and unseen transitions in radioactive decay studies, respectively. Transitions from the positive-parity quadruplets at 537–652 keV are omitted.

almost fully to the 357-keV-level excitation. Therefore, the isomer production through the 295-keV level can be neglected. This is confirmed in this experiment by the fact that the activity of the isomer obtained at 350 keV is negligible as shown in Fig. 1.8. In addition, the direct excitation of the isomeric state and the indirect one via the 93-keV level which decays to the isomeric state with a 100% branching can also be neglected from a theoretical consideration. The positive-parity quadruplets at 537–652 keV cannot be excited by Coulomb excitation for the reasons same as above. This is established experimentally by the use of heavy projectiles.

From the reasons presented above, the excitation function for isomer production can be regarded to be proportional only to that for Coulomb excitation of the 357-keV level, σ_C; that is ,

$$\sigma_{iso} = B\sigma_C. \tag{1.7}$$

The values of σ_C are summarized in Table 1.6. In Fig. 1.8, the value of σ_C is given at the right ordinate by multiplying σ_{iso} by $B = 6.2 \times 10^{-4}$.

Table 1.6. Summary of the experimental cross sections for Coulomb excitation of the 357-keV level in ^{103}Rh by electron projectiles.

E_0/keV	$\sigma_C/10^{-33}cm^2$ a)
800	248 ± 37
720	181 ± 27
650	116 ± 18
575	87 ± 15
500	75 ± 12
425	60 ± 11
350	1 ± 2

a) The uncertainty does not include those in the current measurement and in B.

4.2. THE DE FOREST-WALECKA FORMULA

The inelastic scattering of electron and nuclear structure was reviewed by de Forest and Walecka by confining themselves almost completely to scattering experiments where one observes only the final electron.[1] The discussion was carried out in the framework of first Born approximation or one photon exchange with the nucleus, which is expected to be a good approximation for small $Z\alpha/\beta$. The cross section for an electron with incident wave number k_1 to scatter through an angle θ to a final state with wave number k_2 with the nucleus making a transition from the state $|i\rangle$ to the state $|f\rangle$ is derived in the lowest order of α as

$$\frac{d\sigma}{d\Omega} = \frac{8\pi\alpha^2}{q_\mu^4}\left(\frac{k_2}{k_1}\right)\{V_L(\theta)\sum_{J=0}^{\infty}\frac{|\langle J_f||\hat{M}_J^{coul}(q)||J_i\rangle|^2}{2J_i+1}$$

$$+ V_T(\theta)\sum_{J=0}^{\infty}\left[\frac{|\langle J_f||\hat{T}_J^{el}(q)||J_i\rangle|^2}{2J_i+1} + \frac{|\langle J_f||\hat{T}_J^{mag}(q)||J_i\rangle|^2}{2J_i+1}\right]\}$$

$$\times \frac{1}{(1 + (k_2 - k_1\cos\theta)/E'} , \qquad (1.8)$$

where

$$V_L(\theta) = \frac{1}{2}\frac{q_\mu^4}{\underset{\sim}{q}^4}\left[(\varepsilon_1 + \varepsilon_2)^2 - \underset{\sim}{q}^2\right], \qquad (1.9)$$

$$V_T(\theta) = \underset{\sim}{Q}^2 - (\underset{\sim}{Q}\cdot\frac{\underset{\sim}{q}}{q})^2 + \frac{1}{2}q_\mu{}^2. \qquad (1.10)$$

Eqs. (1.8), (1.9) and (1.10) are given in rationalized natural units $\hbar = c = 1$. In those equations, $\hat{M}_J{}^{coul}(q)$, $\hat{T}_J{}^{el}(q)$ and $\hat{T}_J{}^{mag}(q)$ are irreducible tensor operators of rank J in the nuclear Hilbert space, and $|\langle f||\ ||i\rangle|^2/(2J_i+1)$ denotes the reduced nuclear transition probability. Moreover, $\underset{\sim}{q}$ and q_μ are the three- and four-momentum transfers, respectively, $\underset{\sim}{Q}$ is given as $\underset{\sim}{Q} = (\underset{\sim}{k}_1 + \underset{\sim}{k}_2)/2$, E' is the final total energy of the nucleus, and, ε_1 and ε_2 are the initial and final energies of electron, respectively. The energy loss of scattered electron $\omega = \varepsilon_1 - \varepsilon_2$ is related to the momentum transfer as $q_\mu{}^2 = \underset{\sim}{q}^2 - \omega^2$.

In the long wavelength limit, the transverse electric multipole matrix elements can be reduced with the aid of continuity equation to

$$\langle J_f||\hat{T}_J{}^{el}(q)||J_i\rangle \xrightarrow[q\to 0]{} \frac{E - E'}{q}\left(\frac{J+1}{J}\right)^{1/2}\langle J_f||\hat{M}_J{}^{coul}(q)||J_i\rangle \qquad (1.11)$$

where $k = E - E'$.

The oscillating liquid drop model is then introduced as a very simple model of the nucleus which turns out to be very useful in correlating and understanding some of the

systematics of electron scattering to discrete collective levels in nuclei. For the allowed single surfon (quantum of surface oscillation) transitions, which correspond to Coulomb excitation of the drop to one of the basic shape oscillations characterized by ℓ, one finds

$$|<(\ell)^1,\ell^\pi||\hat{M}_\ell(q)||0>|^2 = \frac{9Z^2}{16\pi^2}(2\ell+1)\frac{1}{2(B_\ell C_\ell)^{1/2}}|j_\ell(qa)|^2. \tag{1.12}$$

The form factor is given exactly by $|j_\ell(qa)|^2$, where $j_\ell(qa)$ is the spherical Bessel function and a is the mean radius of the liquid-drop nucleus. The nuclear transition probability goes as $Z^2/(2B_\ell C_\ell)^{1/2}$, where B_ℓ and C_ℓ are the mass parameter and the restoring parameter, respectively. When resticted to one-surfon transitions, the nuclear magnetic transitions must be forbidden from parity considerations of the nuclear medel used. Therefore, the differential cross section for these allowed one-surfon transitions is given by

$$\frac{d\sigma}{d\Omega}(\ell\leftarrow 0) = \frac{8\pi\alpha^2}{q_\mu^4}\frac{k_2}{k_1}\left\{\left[\frac{9Z^2}{16\pi^2}(2\ell+1)\frac{1}{2\sqrt{(B_\ell C_\ell)}}|j_\ell(qa)|^2\right]\right.$$
$$\left.\times\left[V_L(\theta)+V_T(\theta)\left(\frac{\omega}{q}\right)^2\frac{\ell+1}{\ell}\right]\right\}\frac{1}{1+(k_2-k_1\cos\theta)/E'}, \tag{1.13}$$

where $V_L(\theta)$ and $V_T(\theta)$ are given by eqs. (1.9) and (1.10), respectively.

In this experiment, the case of $\ell = 2$ is concerned, which is the most basic mode and is encountered frequently in almost all nuclei. The asymptotic form of the spherical Bessel function is $j_\ell(qa) \xrightarrow[q\to 0]{} (qa)^\ell/[(2\ell+1)!!]$, so one has the form factor as $|j_2(qa)|^2 = (qa)^4/(5!!)$. The transition probability is also given by de Forest and Walecka[1] as $Z^2/(2\sqrt{B_2C_2}) = Z^2 \times 3.24A^{-7/6}$ from the semiempirical mass formula.

By substitution of these relations in eq. (1.13), the cross sections for Coulomb excitation of the 357-keV level in ^{103}Rh were calculated as a function of incident electron energy. Eq. (1.13) is given in rationalized natural units as are eqs. (1.8)–(1.12). In the calculation, following relations are substituted in eq. (1.13) to convert the units into the conventional ones:

$$k_1 = (E_1^2 + 2mc^2E_1)^{1/2}/\hbar c,$$

$$k_2 = [(E_1 - \hbar\omega)^2 + 2mc^2(E_1 - \hbar\omega)]/\hbar c,$$

$$\underset{\sim}{q}^2 = k_1^2 + k_2^2 - 2k_1k_2\cos\theta,$$

$$q_\mu^2 = \underset{\sim}{q}^2 - (\omega/c)^2,$$

$$\underset{\sim}{Q}^2 = (k_1^2 + k_2^2 + 2k_1k_2\cos\theta)/4,$$

$$\underset{\sim}{Q}\cdot\underset{\sim}{q} = (k_1^2 - k_2^2)/2,$$

$$V_L(\theta) = (q_\mu^2/\underset{\sim}{q}^2)^2[(2E_1 + 2mc^2 - \hbar\omega)^2/(\hbar c)^2 - \underset{\sim}{q}^2]/2,$$

$$V_T(\theta) = \underset{\sim}{Q}^2 - (\underset{\sim}{Q}\cdot\underset{\sim}{q})^2/\underset{\sim}{q}^2 + q_\mu^2/2,$$

$$\varepsilon_1 = (E_1 + mc^2)/\hbar c,$$

and

$$\varepsilon_2 = (E_1 + mc^2 - \hbar\omega)/\hbar c. \qquad (1.14)$$

Here E_1 is incident electron energy and given in keV.

The last term in eq. (1.13), also in eq. (1.8), corresponds to a recoil correction. This factor can be readily evaluated for the conditions of this experiment. The largest recoil correction is obtained at maximum incident energy E_1 = 800 keV and at largest deflection angle $\theta = 2\pi$. This yields 2.1×10^{-5}, which is negligibly small compared with the error of the experimental results. Therefore the recoil correction is not taken into account in the calculation of eq. (1.13).

This experiment cannot obtain the information of the differential cross sections. For that reason, the comparison between the experiment and the theoretical calculation has to be made in the total cross sections as a function of incident electron energy, namely, the excitation function.

The total cross sections for Coulomb excitation of the 357-keV level in ^{103}Rh were obtained by summation of the differential ones given by eq. (1.13) over angle θ. The excitation function thus obtained is shwon in Fig. 1.8 by the solid curve. The agreement with the experiment is good on the whole.

The product of the mass parameter B_2 and the restoring force parameter C_2 can be determined from the reduced E2 transition probability $B(E2)\uparrow$ as

$$\sqrt{B_2 C_2} = \frac{5}{2}\hbar\omega\left(\frac{3}{4\pi}Zea^2\right)^2 B(E2)\uparrow^{-1}. \qquad (1.15)$$

The $B(E2)\uparrow$ value has been obtained in the experiments using heavy-ion projectiles as $B(E2)\uparrow = 0.37 \times 10^{-48}\ e^2\ \mathrm{cm}^4$ for the 357-keV level in ^{103}Rh [ref. 27]. The total cross sections for Coulomb excitation of the 357-keV level were also obtained by substituting this value into eqs. (1.15) and (1.13). The contribution of the transverse magnetic component was neglected, because the mixing ratio $\delta(E2/M1)$ is considered to be infinitely large and therefore one may put $B(M1)\uparrow = 0$. The result is represented by the dashed line in Fig. 1.8, and found to be about half the experimental excitation function.

As shown in Fig. 1.8, an approximate formula of de Forest and Walecka can predict the cross sections for Coulomb

excitation in this lowest energy region of some tenths MeV.

The contribution of the transverse magnetic component was estimated as follows, though it can be neglected in this case. The transverse magnetic excitation can be related to the transverse electric one as

$$\frac{d\sigma_{M1}}{d\sigma_{E2}} = \frac{100}{3}(k_1^2 + k_2^2 - 2k_1k_2\cos\theta)^{-2}(\hbar c)^{-2}\frac{B(M1)\uparrow}{B(E2)\uparrow} . \tag{1.16}$$

The $B(M1)\downarrow$ value for the 295-keV level in ^{103}Rh, which constitutes the one-phonon doublet with 357-keV level, is given experimentally as $B(M1)\downarrow = 0.297\ (e\hbar/2Mc)^2$ [ref. 29]. Although the oscillating liquid drop model forbid the M1 transition between the 295-keV level and the ground state in ^{103}Rh, a non-vanishing $B(M1)$ value is due to a slight admixture of the $p_{3/2}$ single-particle configuration in the 295-keV level. The ratio $\delta(E2/M1)$ is also obtained as +0.15 in ref. 29. The ratio for the 357-keV transition is accepted to be infinitely large as mentioned above; nevertheless, one can estimate an upper limit of the reduced M1 transition probability for the 357-keV-level excitation by substituting the value for the 295-keV level as the worst case. Taking the statstical factor into account, $B(M1)\uparrow = 0.594\ (e\hbar/2Mc)^2$ was used for estimation of eq. (1.16). The ratio is obtained

as $d\sigma_{M1}/d\sigma_{E2}$ = 0.57–14.0 depending on θ. Integration of the differential cross sections yields that $\sigma_{M1} \sim \sigma_{E2}$. This contradicts the assumption made in the calculation procedure of eq. (1.13). Nevertheless, B(M1) for the 357-keV transition should be considered to be two orders of magnitude smaller than that for the 295-keV transition even in the worst case. Therefore, the contribution of the transverse magnetic excitation should be smaller by a factor of over 100 than that estimated above.

The contribution of the transverse electric excitation does not exceed 15% of that of the longitudinal electrostatic excitation as found in the calculation of eq. (1.13). Accordingly, the error resulting from neglecting the transverse magnetic contribution is smaller than 12% of the total cross sections. As a matter of fact, the 357-keV transition is almost pure E2, and therefore the calculated excitation function describes the real situation quite reasonably.

4.3. RESONANCE ABSORPTION OF PHOTONS

Resonance absorption of bremsstrahlung radiations (photons) is considered as a competitive mechanism for excitation of the 357-keV level. Bremsstrahlung radiations are produced in the target by incident electrons. Provided that photons

are produced at the surface of the target and all of them traverse the target perpendicularly, the isomer activated by this process was estimated. The number of the isomer activated per second is given, by integration of the Breit-Wigner single-level formula, as

$$N_{iso} = Nx\Phi\frac{\lambda^4}{4} g\Gamma_0 B, \qquad (1.17)$$

where Nx is the number of target nuclei per cm^2, Φ the incident rate of bremsstrahlung radiations at resonance, λ the wavelength of resonant photons, g the statistical factor, Γ_0 the partial width for the 357-keV radiative transition and B the branching ratio of the 357-keV level to the isomeric state. The energy spectra of bremsstrahlung radiations produced in the target by incident electrons of 350–800 keV were obtained from the tabulated values computed by Pratt et al.[30] The values of Φ are $\Phi = 4.376 \times 10^{-6}$–$6.116 \times 10^{-6}$ s^{-1} for incident electron energies of 425–800 keV. The observed $B(E2)\uparrow$ value leads to $\Gamma_0 = 5.7 \times 10^{-6}$ eV, and Nx is 1.813×10^{20} cm^{-2}. By substitution of these values, the numbers of isomer produced by γ-resonance absorption were estimated, in this extreme way, to be approximately two orders of magnitude smaller than the experimental results. Therefore, the contribution of resonance absorption of bremsstrahlung radiations to isomer production can be neglected.

4.4 ESTIMATE OF COULOMB EXCITATION IN ^{189}Os

The nucleus ^{189}Os in which the evidence for NEET was first obtained [refs. 2,3] is not a good example of the oscillating liquid model. The excited nuclear levels may be described by the collectively rotational model. In that model, transitions in the same band are limited to pure M1. However, this appears that the pure rotational assignment explains some properties of a few low-lying nuclear levels, and hence the second excited state of the K = 3/2 ground-state band is expected to be at about 170 keV if the rotational motion is undisturbed. Coulomb excitation experiments indicate that the collective excitations of the ground state have the energies of 70 and 219 keV, deviating strongly from those of a pure rotor. As a result, the admixture of E2 is expected for the 70-keV transition. This is established by experiments as 68% M1 + 32% E2 [ref. 27].

From reasons mentioned above, the contribution of the transverse magnetic component should be checked by eq. (1.16). The $B(\mathrm{M1})\downarrow$ value is determined to be $(4.6 \pm 0.7) \times 10^{-3}\ \mu_N{}^2$, [31] which is much smaller than that for the 295-keV transition in ^{103}Rh. It is clear, therefore, that the transverse magnetic excitation of the 70-keV level in ^{189}Os is negligibly small compared with the transverse electric excitation. Consequently, the estimate of the contribution

of Coulomb excitation in ^{189}Os in ref. 3 can be regarded to be quite reasonable. Coulomb excitation of the 70-keV level is not responsible for isomer production observed when ^{189}Os is bombarded with 70–100-keV electrons. As a result, isomers activated by electrons can be attributed to the excitation of the 70-keV level by NEET. This gives a further verification of the existence of NEET.

5. Conclusion

An approximate formula of de Forest and Walecka based on the oscillating liquid drop model for Coulomb excitation by electrons was found to be valid even in the lowest energy regions of some tenths MeV. The estimate of Coulomb excitation as a competitive mechanism in the ^{189}Os experiment using electron projectiles was reconsidered to be reasonable, and therefore NEET in ^{189}Os is concluded to conquer that alternative process for isomer production. A supplementary verification for NEET in ^{189}Os was obtained in the experiment described in this chapter.

Appendix 1.1

Estimate of η's

The bombarding current I_0 was obtained from the measured current I_{meas} by using eq. (1.1). Provided that monoenergetic electrons perpendicularly impinge on the Rh target and the Cu mount, the numerical values for η's in eq. (1.1) were estimated as the following.

A1.1. η_S

Frederickson[7] has measured backward electron yield for metals (al, Cu and Pb) bombarded with 0.4-MeV to 1.4-MeV electrons. These energies cover almost all of the range studied in this experiment. Backward electrons can be divided into two parts: energetic electrons and low-energy ones. Electrons with energies below dozens of eV are referred to as the secondary electron. Frederickson states that the low-energy component is always less than 0.5% for all of the metals and energies investigated; therefore, it is reasonable that, in this experiment, η_S is set to be 0.005 for all incident energies (0.35–0.8 MeV).

A1.2. η_B

From empirical equations for $\eta_B/\eta_B(\text{sat})$ and for $\eta_B(\text{sat})$, η_B was estimated for each incident energy E_0. Koral and cohen[8] presented an empirical expression for the ratio of the backscattering coefficients at normal incidence for a scatterer with a thickness t to the saturated value as a function of t for a given E_0 and Z. Their expression, applicable to the range from 5.0 keV to 3.0 MeV, is

$$\eta_B(t)/\eta_B(\text{sat}) = 1 - \exp[-\alpha(2t/R)^n] + a, \qquad \text{(A1.1)}$$

where α and n are the parameters, R is the range of electrons with energy E_0, and a is a small correction factor. The parameters α and n are given numerically by

$$\alpha = 0.760\ Z^{0.55} \qquad \text{(A1.2)}$$

and

$$n = 2.32 - 8.40 \times 10^{-3} Z. \qquad \text{(A1.3)}$$

In eq. (A1.1), R is given in milligrams per square centimeter by the Katz-Penfold equation:[32,33]

$$R = \frac{A}{Z}\frac{13}{27}\ 412\ E_0^{(1.265\ -\ 0.0954\ \ln E_0)}, \qquad \text{(A1.4)}$$

where E_0 is in MeV. The values used for a (0.015 for Cu and 0.005 for Rh) were based on data in ref. 8.

According to Tabata et al.,[9] $\eta_B(\mathrm{sat})$ is expressed empirically (valid for $Z > 6$ and 50 keV $< E_0 <$ 22 MeV) by

$$\eta_B(\mathrm{sat}) = a_1/[1 + a_2(E_0/m_e c^2)^{a_3}], \tag{A1.5}$$

where a_i's are constants for a given target and $m_e c^2$ is the rest mass energy of the electron ($m_e c^2$ = 511.006 keV). These a_i's are given as

$$a_1 = b_1 \exp(-b_2 Z^{-b_3}),$$

$$a_2 = b_4 + b_5 Z^{-b_6},$$

$$a_3 = b_7 - b_8/Z. \tag{A1.6}$$

Numerical values for these b_i's are given in Table A1.1.

From two empirical equations, η_B for the Rh target with thickness 31 mg/cm^2 was determined as a function of incident electron energy E_0.

A1.3. η_T

Tabata and Ito[11] has proposed an empirical equation for

Table A1.1. Numerical values of the constants b_i in eq. (A1.6) given by Tabata et al..[a)]

Constant	Numeical value
b_1	1.15 ± 0.06
b_2	8.35 ± 0.25
b_3	0.525 ± 0.020
b_4	0.0185 ± 0.0019
b_5	15.7 ± 3.1
b_6	1.59 ± 0.07
b_7	1.56 ± 0.02
b_8	4.42 ± 0.18

a) Ref. 9.

the transmission coefficient η_T as

$$\eta_T = [1 - \exp(-S_0)]/\{1 + \exp[(S_0 + 2)(t/R_{ex}) - S_0]\}, \tag{A1.7}$$

where S_0 is the parameter, t is the thickness and R_{ex} is the extrapolated range of electrons. The parameter S_0 is expressed by

$$S_0 = a_1 \exp\{-a_2/[1 + a_3(E_0/m_e c^2)^{a_4}]\}, \tag{A1.8}$$

where a_i's are constants for a given target and others are the same in eq. (A1.5). These constants a_i's are adjusted to data in the ranges of E_0 = 8 keV–30 MeV and Z = 4–82 as

$$a_1 = (0.2335 \pm 0.0091) A/Z^{(1.209 \pm 0.015)},$$

$$a_2 = [(1.78 \pm 0.36) \times 10^{-4}] Z,$$

$$a_3 = (0.9891 \pm 0.0010) - [(3.01 \pm 0.35) \times 10^{-4}] Z,$$

$$a_4 = (1.468 \pm 0.090) - [(1.180 \pm 0.097) \times 10^{-2}] Z,$$

and

$$a_5 = (1.232 \pm 0.067)/Z^{(0.109 \pm 0.017)}. \tag{A1.9}$$

From eq. (A1.7) with these adjusted constants, one can easily obtain η_T of the target for various E_0.

A1.4. η_B'

The backscattering coefficient for the Cu mount, η_B', was obtained in the same manner described in Section A4, except that E_0 was replaced by E_m, the most probable energy. The most probable energy of electrons incident on the Cu mount is $E_m = E_0 - \Delta E_m$, where ΔE_m is the most probable energy loss of transmitted electrons through the target in their forward movements. The most probable value of the energy loss is given by the expression:[10)]

$$\Delta E_m = \xi[\ell n(\xi/\varepsilon') + 0.37], \tag{A1.10}$$

where ξ and ε' are the parameters given by

$$\xi = t\frac{2\pi N_A e^4 \rho Z}{m_e c^2 \beta^2 A}, \tag{A1.11}$$

and

$$\ell n\varepsilon' = \ell n\frac{(1 - \beta^2) I^2}{2m_e c^2 \beta^2} + \beta^2. \tag{A1.12}$$

Here N_A is Avogadro's number and I is a certain ionization potential of the atom (I = 13.5 Z eV). This expression is verified to agree excellently with the experiment at 624 keV by Warshaw and Chen.[34)]

Since the Cu mount was so thick as to give the saturated

backscattering, η_B' was obtained as $\eta_B = \eta_B(\mathrm{sat})$ for E_m and $Z = 29$ by using eq. (A1.5).

Landau's theory[10] describes the energy distribution of electrons traversed a layer of matter. For reference, the distributions of the energy loss of electrons traversed the Rh target were evaluated. The distribution function is represented as functions of thickness t and energy loss Δ by

$$f(t,\Delta) = \frac{1}{\xi}\,\phi(\lambda), \tag{A1.13}$$

where

$$\phi(\lambda) = \frac{1}{2\pi i}\int_{\sigma-i\infty}^{\sigma+i\infty} \exp(u\,\ell n u + \lambda u)\,du,$$

$$\lambda = \{\Delta - \xi[\ell n(\xi/\varepsilon') + 1 - C]\}/\xi. \tag{A1.14}$$

Here $\phi(\lambda)$ is a universal function of a non-dimensional variable λ and $u = \xi p$ is an integration variable and $C = 0.5777\cdots$ is Euler's constant. The function $\phi(\lambda)$ is calculated by deriving asymptotic formulas for the large value of $|\lambda|$ and is tabulated in ref. 35. By consulting it, one can evaluate $f(t,\Delta)$ as a function of Δ. For example, the results obtained for 800 keV ($\xi = 2.453$) and 350 keV ($\xi = 3.212$) are shown in Fig. A1.1.

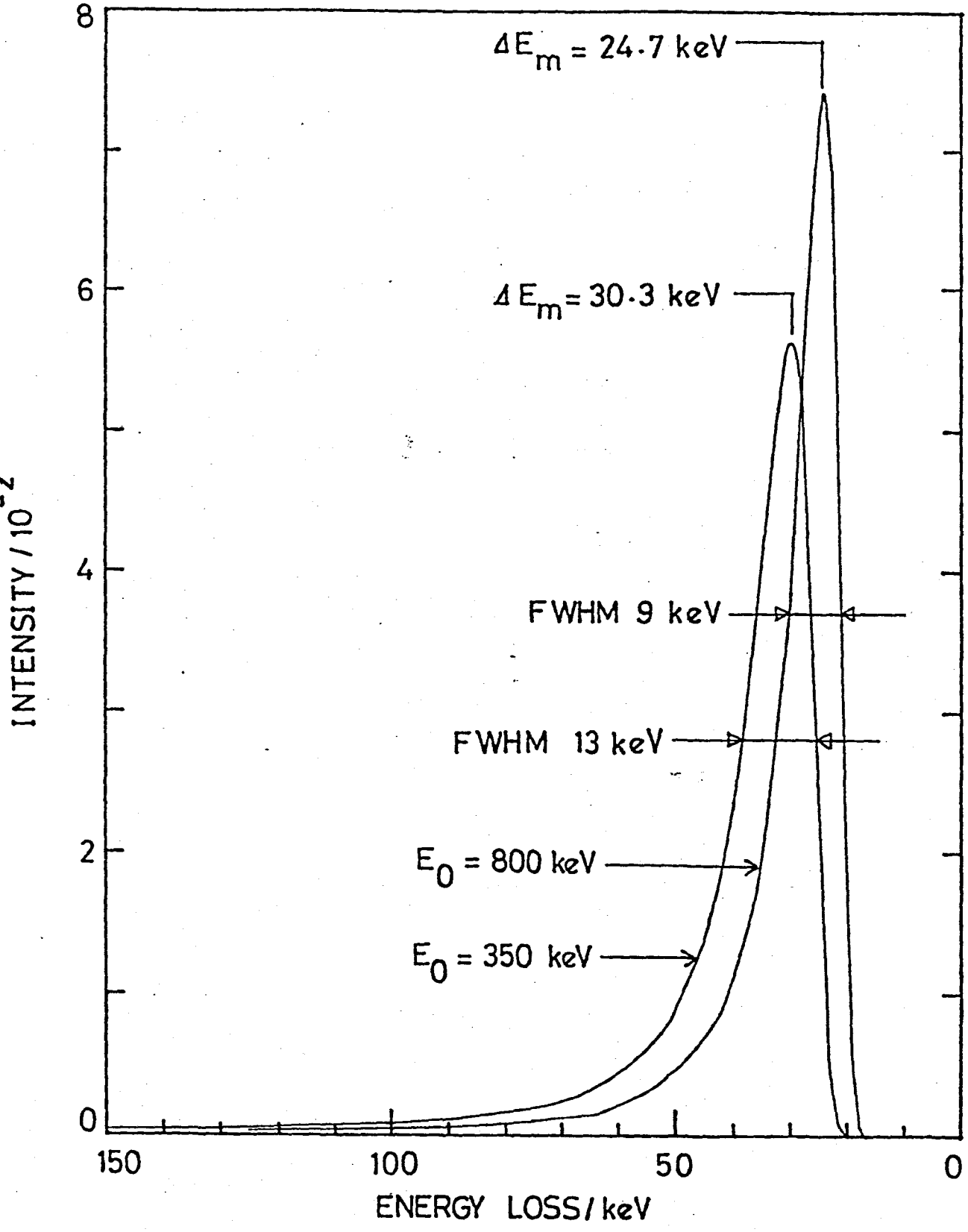

Fig. A1.1. Energy loss of the transmitted electrons in the Rh target calculated according to the Landau theory.

A1.5. η_T'

The transmission coefficient for electrons traversing the Rh target in the backward directions, η_T', was estimated in the same manner described in Section A3, except that E_0 was replaced by E_m', the most probable energy of the electrons. The most probable energy of electrons incident on the Rh target is $E_m' = E_m - \Delta E_m'$, where $\Delta E_m'$ is the most probable energy loss of backscattered electrons in the Cu mount. The value of $\Delta E_m'$ is given experimentally as[12)]

$$\Delta E_m'/E_0 = 0.31\ (E_0/m_e c^2)^{0.3140}. \qquad \text{(A1.16)}$$

Substituting E_0 by E_m, $\Delta E_m'$ was obtained readily for various E_m. The η_T' value was obtained from Eq. (A1.7) for E_m'.

The most probable energy loss of the transmitted electrons in the Rh target E_m and that of the backscattered electrons from the Cu target mount E_m' are summarized in Table A1.2.

Table A1.2. Most probable energy loss of the transmitted electrons in the Rh target, E_m, and that of the backscattered electrons from the Cu target mount, E_m'.

E_0/keV	E_m/keV[a)]	E_m'/keV[b)]
800	24.7	182.6
720	25.0	176.5
650	25.5	170.8
575	26.1	164.1
500	27.0	156.7
425	28.3	148.3
350	30.3	138.7

a) Calculated by a formula of Landau.[10] See Section A4 of the text.

b) Calculated with an empirical relation given in Ref. 12.

Appendix 1.2

Correction of radioactivity induced by backscattered electrons

This Appendix describes the correction of the amounts of ^{103m}Rh which are ascribable to activation by backscattered electrons applied in the procedure deducing the results.

The observed activity of ^{103m}Rh extrapolated at the end of bombardments with electrons of 350–800 keV are summarized in Table 2.1. The production rate of the isomer per bombarding current of 1 mA was obtained by using A and I_0, the latter is given in Table 1.1. These A/I_0 listed in Table A1.1 were used the first tentative set of data for isomer production. This set of data was fitted by a linear equation of E with weights of the inverse squares of their standard deviations, and then the first preliminary excitation function was obtained as

$$A/I_0 = 0.238\ E - 82.3. \qquad \text{(A2.1)}$$

The contribution of backscattered electrons was divided into two parts: that of electrons backscattered in the Rh target, and that of electrons scattered back from the Cu mount. The fractions of backscattered electrons having energy E were estimated in Appendix 1.1. The energy spectra

Table A2.1. Observed activity of ^{103m}Rh at the end of bombardment, A, and the first set of the production rate of the isomer per bombarding current of 1 mA, A/I_0.

E_0	A (cpm)	I_0 (mA)	E/I_0 (cpm/mA)
800	50.40 ± 1.78	0.393	128.24 ± 4.53
720	38.97 ± 1.58	0.413	94.36 ± 3.83
650	21.66 ± 0.80	0.348	62.24 ± 2.30
575	13.89 ± 1.17	0.300	46.30 ± 3.90
500	10.35 ± 0.58	0.268	38.62 ± 2.16
425	6.41 ± 0.64	0.219	29.27 ± 2.92
350	0.14 ± 0.24	0.218	0.64 ± 1.10

of backscattered electrons were assumed to be represented by the obtained experimentally by Both,[26] and further angular-independent. Backscattered electrons were treated to be efficient in activating the isomer by an extent given by eq. (A2.1) depending on their energies. The energy intervals of one thenth of full energy were used for the sake of simplicity of calculation.

The amount of activity induced by backscattered electrons were evaluated and then subtracted from the fisrt data yielding the second improved data. The second excitation function was obtained by fitting a linear equation to the second set of improved data as

$$A/I_0 = 0.210\ E - 72.4. \qquad \text{(A2.2)}$$

In this fitting procedure, only the standard deviations of the first data and those obtained in the correction of backscattered electrons were included in the weights. The residual errors obtained in the fitting were excluded, since the true excitation function was not expected to be linear on E as the prelimianry one used.

The same procedure was repeated by use of eq. (A2.3), the third excitation function was then obtained as

$$A/I_0 = 0.214\ E - 73.5. \qquad \text{(A2.3)}$$

The fourth exctiation function was obtained as

$$A/I_0 = 0.213\ E - 73.4 \qquad \text{(A2.4)}$$

The fifth set of corrected data was considered as the the final one, since the excitation function was converged as expressed by eq. (A1.4). The final set of the isomer production rate ia given in Table 1.3.

The amounts of the correction applied to backscattered electrons are shown in Fig. A2.1. All corrections are the redunction of the amounts of acitivity.

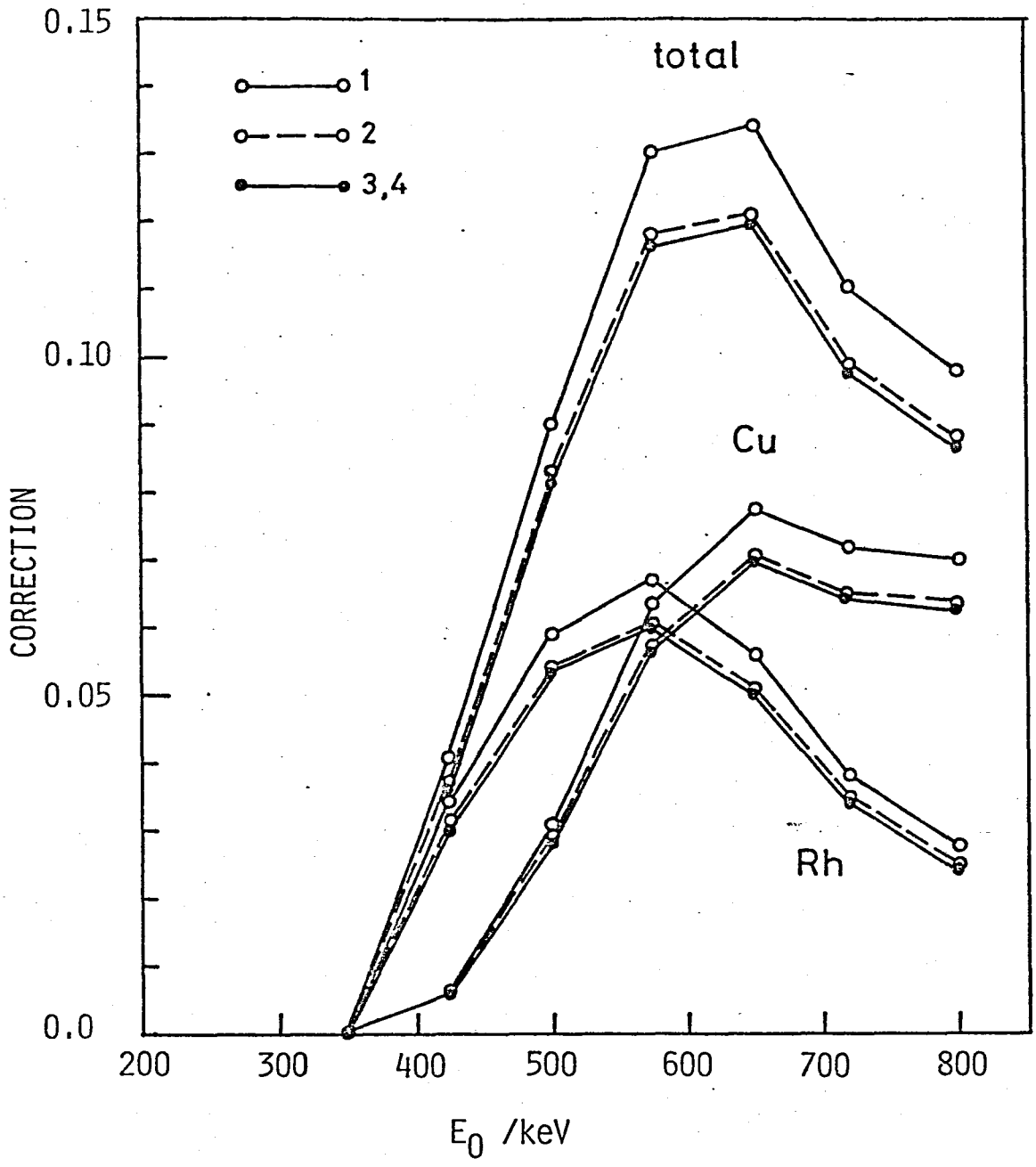

Fig. A2.1. The amounts of the correction of isomer yield for backscattered electrons from the Rh target and Cu mount, relative to the original data.

References

1) T. de Forest, Jr. and J. D. Walecka, *Adv. Phys.* 15, 1 (1966).

2) K. Otozai, R. Arakawa and M. Morita, *Prog. Theor. Phys.* 50, 1771 (1973).

3) K. Otozai, R. Arakawa and T. Saito, *Nucl. Phys.* A297, 97 (1978).

4) E. C. Booth and J. Brownson, *Nucl. Phys.* A98, 529 (1967).

5) Y. Nakai, K. Matsuda and T. Takagaki, Japan Atomic Energy Research Institute report JAERI-M 6702 (1976) p. 80.

6) Y. Nakai and S. Horikiri, *Isot. Radiat.* 2, 233 (1959).

7) A. R. Frederickson, Air Force Cambridge Research Laboratory report AFCRL-69-0144 (1969).

8) A. R. Koral and A. J. Cohen, National Aeronautics and Space Administrantion technical note NASA TN D-2909 (1965).

9) T. Tabata, R. Ito and S. Okabe, *Nucl. Instrum. Methods* 94, 509 (1971).

10) L. Landau, *J. Phys. (USSR)* 8, 201 (1944).

11) T. Tabata and R. Ito, *Nucl. Instrum. Methods* 127, 429 (1975).

12) J. Jakshik and K. P. Jüngst, *Nucl. Instrum. Methods* 79, 240 (1970).

13) K. Matsuda, private communication.

14) E. R. Günther, K. Knauf and K. F. Walz, *Int. J. Appl.*

Radiat. Isot. 24, 87 (1973).

15) J. B. Cumming, National Academy of Sciences report NAS-NS 3107 (1962) p. 25.

16) T. Tabata, R. Ito and S. Okabe, *Nucl. Instrum. Methods* 103, 85 (1972).

17) S. Baba, H. Baba and H. Okashita, Japan Atomic Energy Research Institute report JAERI 1216 (1971).

18) H. Baba, H. Okashita, S. Baba, T. Suzuki, H. Umezawa and H. Natsume, *J. Nucl. Sci. Technol.* 8, 703 (1971).

19) H. Baba, T. Sekine, S. Baba and H. Okashita, Japan Atomic Energy Research Institute report JAERI 1227 (1972).

20) H. Baba, Japan Atomic Energy Research Institute report JAERI-M 7017 (1977).

21) J. S. Hansen, J. C. McGeorge, D. Nix, W. D. Schmidt-Ott, I. Unus and R. W. Fink, *Nucl. Instrum. Methods* 106, 365 (1973).

22) L. Wielopolski, *Nucl. Instrum. Methods* 143, 577 (1977).

23) Y. Grunditz, S. Antman, H. Pettersson and M. Saraceno, *Nucl. Phys.* A133, 369 (1969).

24) J. H. Scofield, *At. Nucl. Data Tables* 14, 121 (1974).

25) W. Bambynek, B. Crasemann, R. W. Fink, H.-U. Freund, H. Mark, C. D. Swift, R. E. Price and P. V. Rao, *Rev. Mod. Phys.* 44, 716 (1972).

26) W. Bothe, *Z. Naturforsch.* 4a, 542 (1949).

27) D. C. Kocher, *Nucl. Data Sheets* 13, 337 (1974).

28) E. S. Macias, M. E. Phelps, D. G. Sarantites and R. A. Meyer, *Phys. Rev. C* 14, 639 (1976).

29) R. O. Sayer, J. K. Temperley and D. Eccleshall, *Nucl. Phys.* A179, 122 (1972).

30) R. H. Pratt, H. K. Tseng, C. M. Lee, L. Kissel, C. MacCallum and M. Riley, *Atomic Data Nucl. Data Tables* 20, 175 (1977).

31) B. Persson, H. Blumberg and M. Bent, *Phys. Rev.* 174, 1509 (1968).

32) L. Katz and A. S. Penfold, *Rev. Mod. Phys.* 24, 28 (1952).

33) L. E. Glendenin, *Nucleonics* 2(1), 12 (1948).

34) S. D. Warshaw and J. L. Chen, *Phys. Rev.* 80, 97 (1950).

35) W. Börsch-Supan, *J. Res. Nat. Bureau Stand.* 65B, 245 (1961).

CHAPTER II

NUCLEAR EXCITATION BY ELECTRON TRANSITION IN ^{189}Os FOLLOWING K-SHELL PHOTOIONIZATION

1. Introductory remarks

Nuclear excitation by electron transition was first observed in ^{189}Os by the detection of the induced activity of ^{189m}Os after the electron bombardment of naturally abundant osmium.[1] A precise experiment was also carried out by using the same technique except that the target was replaced by enriched ^{189}Os [ref. 2]. Both experiments could not exclude the contribution of Coulomb excitation of the nucleus by electron projectiles as an excitation mechanism competing with NEET. Quantitative arguments on NEET and Coulomb excitation, however, can separate the respective contributions and hence give sufficient evidence for the

existence of NEET.[2] It was further confirmed in a supplementary study on Coulomb excitation by low-energetic electrons as described in Chapter I and ref. 3.

On the other hand, NEET can be observed without the interference of Coulomb excitation by electron projectiles in those experiments in which photons are used for K-shell ionization in ^{189}Os. This situation is illustrated schematically in Fig. 2.1. As mentioned above, the observation of NEET was made by using the path (1) → (2) → (3) → (4) in the experiments of electron bombardment, where an alternative path (5) → (4) had to be taken into account as a competing mode for isomer production.[1,2] When photons are used for K-shell ionization, the path (6) → (2) → (3) → (4) should be responsible for isomer production, and Coulomb excitation, (5), cannot participate in isomer production as is evident from Fig. 2.1. The intense source of monoenergetic photons is available, e.g., in the ^{60}Co γ-irradiation facility. Nevertheless, it is probably unsuitable for this purpose, since the resonance absorption of inelastically scattered γ-rays by higher-lying nuclear levels may contribute to isomer production appreciably. The estimation of this mechanism is quite difficult from the reasons that the properties of higher-lying nuclear levels which may absorb photons are not well-established, and that the inelastic scattering of γ-rays cannot be treated by an analytical

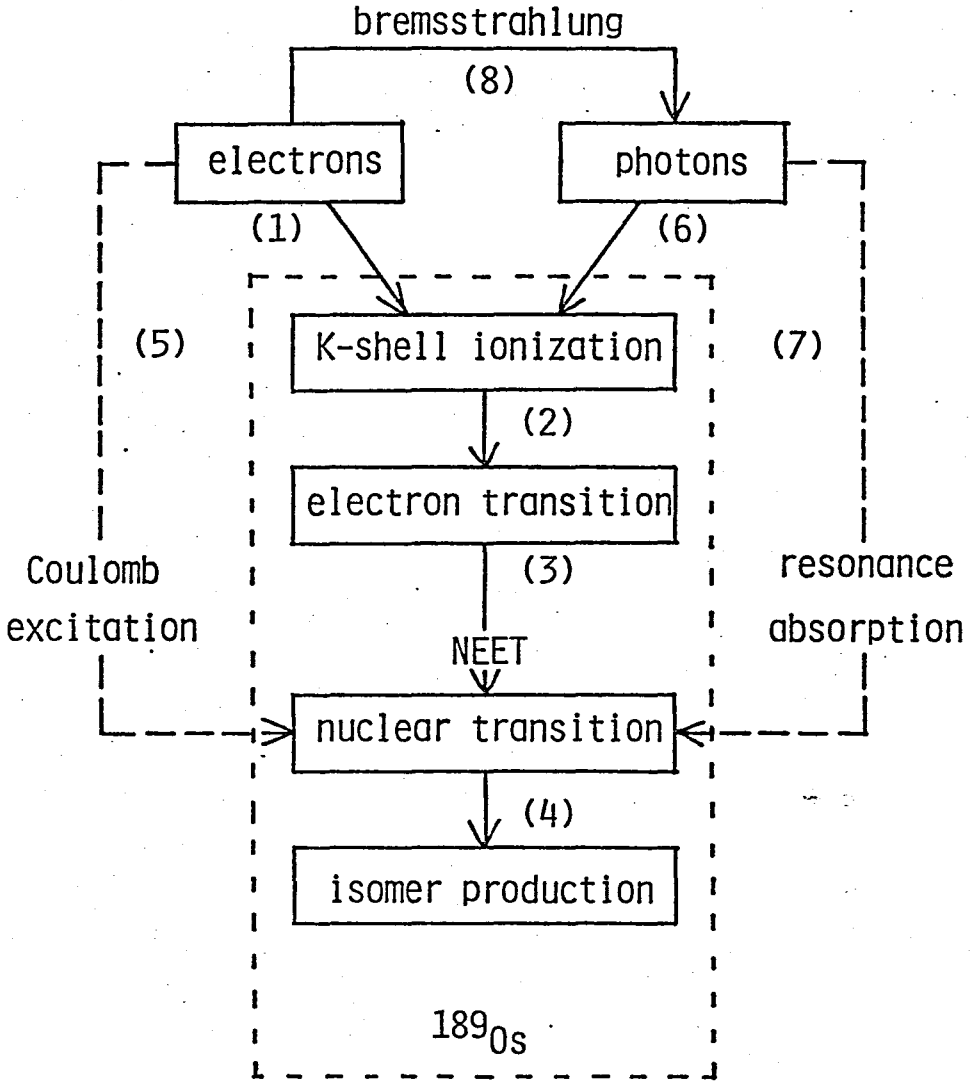

Fig. 2.1. Isomer production in ^{189}Os by NEET, Coulomb excitation and γ-resonance absorption.

form. In fact, the isomer production through this mechanism has been observed in several nuclides other than ^{189}Os.[4-7] In addition, γ-rays from ^{60}Co (1.17 and 1.33 MeV) are not so efficient in ionizing the K-shells of ^{189}Os atoms, since the cross section for photoionization decreases rapidly with the photon energy. From these reasons, bremsstrahlung radiations, produced by the deceleration of electrons in a converter, the path (8), were used for the ionization of the K-shells of ^{189}os. Primary electron beam was stopped completely in the converter, and hence the path (5) could be excluded explicitly. In this experiment aiming at the observation of NEET in ^{189}Os after K-shell photo-ionization, the path (8) → (6) → (2) → (3) → (4) is considered to participate in isomer production. The path (8) is equally a pure atomic process as (1); therefore, NEET should be observed in proportional to the ratio of (1) and (8). This may give a supplementary evidence for NEET in ^{189}Os, if the results are consistent with the expectation. In order to suppress the contribution of the resonance absorption of photons, the path (7), as much as possible, primary electrons with energy of 200 keV were used in this study. The spectral density of bremsstrahlung can be calculated and the interference of γ-resonance absorption can be evaluated reasonably. As a result, isomer production through NEET after photoionization can readily be compared with that obtained by electrons.

2. Experimental

2.1. PREPARATION OF ^{189}Os TARGET

A metallic Os layer was prepared by an electroplating technique for use as a target.[8] Metallic powder of osmium enriched to 95.66% in ^{189}Os was supplied by Oak Ridge National Laboratory (ORNL), USA. Isotopic constitution of this sample is certified to be < 0.03% (^{184}Os), < 0.05% (^{186}Os), 0.06% (^{187}Os), 0.74% (^{188}Os), 2.55% (^{190}Os) and 1.00% (^{192}Os). Although the isotopes ^{190}Os and ^{192}Os have the isomer with half-lives of 9.9 min and 6.1 s, respectively, the energies of these isomers are much higher than those of electrons and therefore the activation of these isomers can be neglected completely. Other chemical impurities are also analyzed to be Al (0.07%), Ca (0.04%), Cr (0.02%), Fe (0.08%), Mg (0.04%), Ni (0.02%), Si (0.25%) and Cu (0.02%). All nuclides of these elements have no isomers, and moreover nuclear reactions are not expected to occur on account of extremely low energy of primary electrons.

Osmium was dissolved in sodium hypochlorite solution. The solution was then added to the electrolytic bath composed of $(NH_4)_2HPO_4$ (45 g/l) and Na_2HPO_4 (240 g/l). The concentration of ^{189}Os was 4.9 g/l in this bath. In 7 cm^3 of this electrolytic bath the electroplating was carried out at 70–75 °C

with a current density of 2 mA/cm^2 for 5 h on a 26-mm diam. Pt disk placed at the bottom of the vessel by using a rotating Pt rod as the anode and stirrer. As a result, a metallic Os layer with thickness of 0.755 mg/cm^2 and diameter of 20 mm was obtained on the 0.5-mm thick Pt disk. The Os layer was satisfactorily stable in air and under vacuum, resisting electron bombardment.

2.2. IRRADIATION OF ^{189}Os WITH BREMSSTRAHLUNG

Bremsstrahlung was produced by the electrons from a Cockcroft-Walton electron accelerator at the Radiation Center of Osaka Prefecture. The target was placed at a distance of 3 mm behind from a Pt photon-producing converter which was bombarded with 200-keV electrons from the accelerator. The thickness of the converter was 106 mg/cm^2, which is thicker than the maximum range of 200-keV electrons in Pt, 89 mg/cm^2 [ref. 9]. The experimental setups for irradiation are shown in Fig. 2.2. The irradiation of ^{189}Os with bremsstrahlung was made under vacuum for 5 h with a beam current of 0.2 mA. The current incident upon the converter was measured with amperemeter connected to the mount of the converter. The loss in current due to backscattering of electrons from the converter was estimated to be 48.7% by an empirical formula

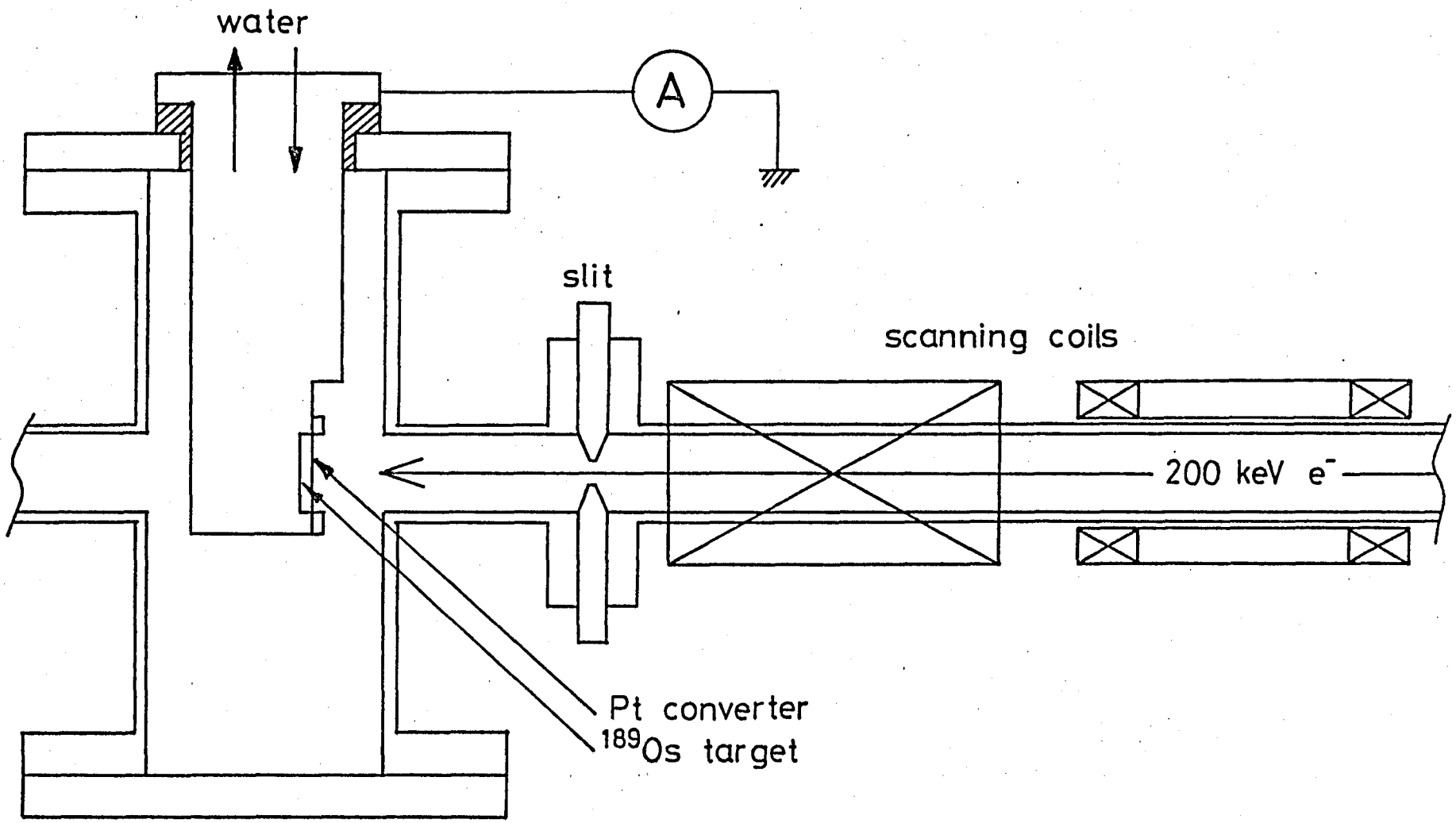

Fig. 2.2. Experimental setups for irradiation of ^{189}Os with bremsstrahlung produced by 200-keV electrons.

of Tabata et al.[10] as given in eq. (A1.5), and the corrected current was consistent with the output of the accelerator.

2.3. MEASUREMNT OF RADIOACTIVITY

The radioactivity induced in the target was measured with a 2π windowless Q-gas-flow GM counter, surrounded by peripheral GM-type anticounters, with background of below 0.02 counts/s.

The detection coefficient of this couter for ^{189m}Os was determined as described in ref. 11 for consistency with the previous study using electron projectiles.[2] The isomeric transition from ^{189m}Os proceeds for the most part by the emisssion of internal conversion electrons. The relative intensities of these conversion electrons are reported to be $L_1/L_2/L_3/M/N = 30/2/100/40/15$ [ref. 12,13]. The intensest L_3-conversion electrons (E_e-/keV = 30.80 - 10.87 = 19.93) were adopted as the representative of conversion electrons emitted from ^{189m}Os. For continuous β-rays, it is known that the transmission curve is often nearly exponential over the majority of its length. Therefore, the fraction of the total activity which is uniformly distributed throughout a thick source with a thickness of t g/cm^2 measured at the surface is represented by

$$C/C_0 = [1 - \exp(-\mu t)]/(\mu t), \qquad (2.1)$$

where μ is the mass-absorption coefficient and is nearly independent of the atomic weight of absorbing material. Empirically, μ can be related to the maximum energy of β-rays, E_m, as

$$\mu = 0.0155\, E_m^{-1.41} \qquad (2.2)$$

where E_m is in MeV and μ is in square centimeters per gram.[14] In this case, monoenergetic conversion electrons are assumed to be equal continious β-rays with the maximum enenrgy three times as much as the energy of conversion electrons, namely, E_m (β-rays) = 3 E_e-. Backscattering of conversion electrons should enhance the detection coefficient, and this was estimated as the same manner described in ref. 11. The saturated backscattering coefficients for β-rays emitted from ^{32}P, ^{204}Tl and ^{35}S were measured at the Pt backing materials.[15] Extrapolation of these data yields the correction factor of 1.20 in this case. As a result, the overall detection coefficient for ^{189m}Os was obtained to be 0.75 × 1.20/2 = 0.45. The factor 2 in the denominator corresponds to the geometric factor of this 2π counter.

The measured decay curve is shown in Fig. 2.3.

The decay curve obtained was fitted to the ^{189m}Os

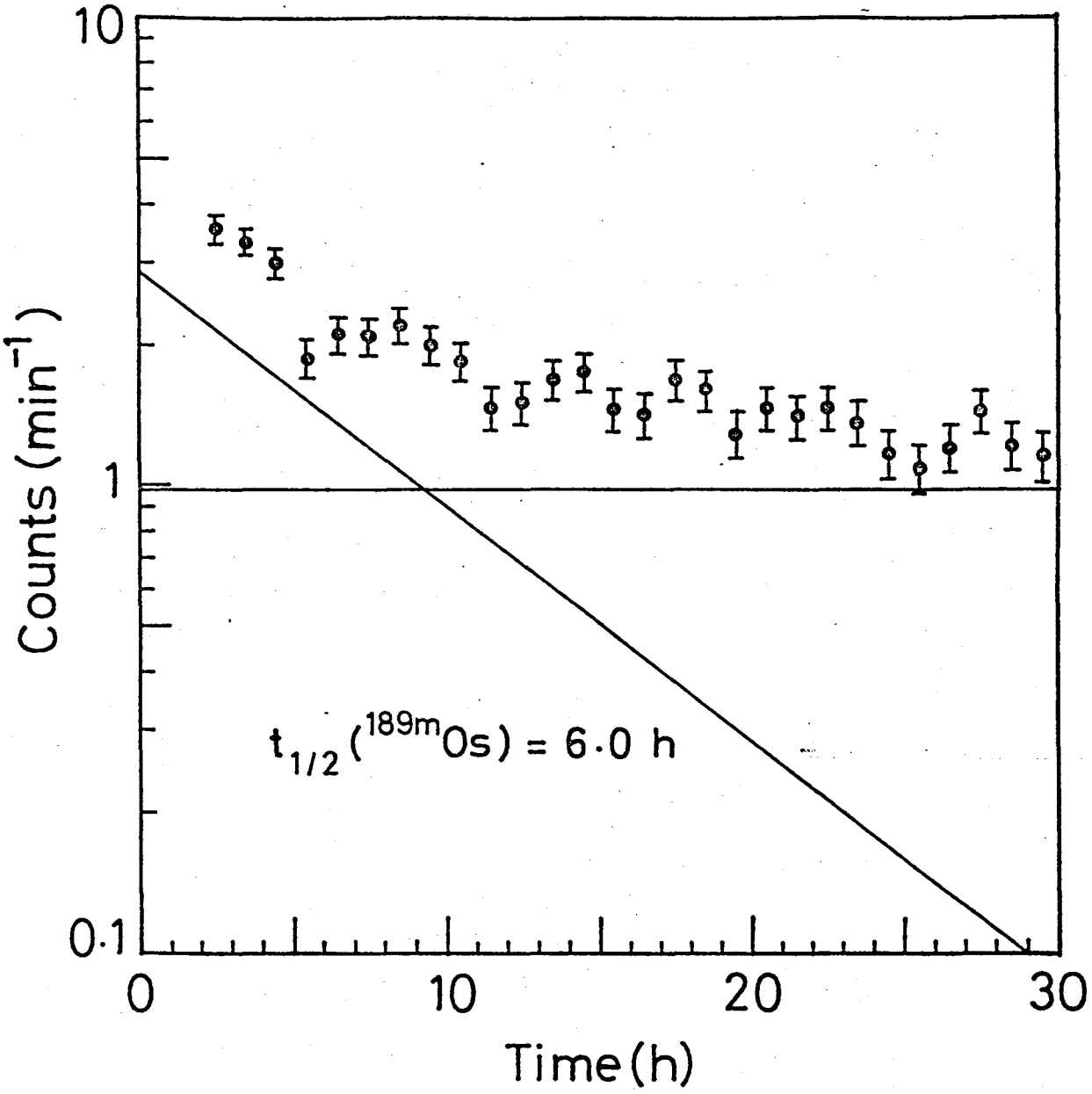

Fig. 2.3. Decay curve of the radioactivity induced in the target. The solid lines show the results of a least-squares fit.

component ($t_{1/2}$ = 6.0 h)[13] and a constant background one by a least-squares method,[16] since this experiment was free from radioactivities other than ^{189m}Os. The measurement of radioactivity was continued for the period twice as long as shown in Fig. 2.3. The solid lines in Fig. 2.3 are the results of a least-squares fit of two components.

3. Results

As shown in Fig. 2.3, the disintegration rate of ^{189m}Os induced in the target was determined as

$$A_0 = 0.107 \pm 0.005 \text{ Bq [disintegrations/s]}$$

at the end of irradiation. The quoted uncertainty includes only the one in the fitting procedure. The errors in the estimation of the detection coefficient of the counter for ^{189m}Os is not included.

4. Discussion

4.1. ESTIMATE OF THE SPECTRAL DENSITY OF BREMSSTRAHLUNG

The calculation of the spectral density of bremsstrahlung used in this experiment was executed on an ACOS computer at Osaka University by using the DIBRE-DETECTOR code developed by Nakamura et al..[17] This code gives the spectral yield of bremsstrahlung radiated from a thick converter at a given direction with respect to the primary electrons beam. In the calculation procedure, the Pt converter was treated as a stack of slabs with a thickness of 10^{-3} radiation-length units (6 mg/cm^2 in this case), and the degradation and scattering of incident electrons and the attenuation and buildup of bremsstrahlung passing through the converter were taken into account. The differential yield thus obtained was integrated over the geometric factor between the converter and the target. For the sake of simplicity of integration, the geometric factor was replaced by the solid angle that was subtended by the target at the center of the converter, euivalent to the average one subtended at the plane of the converter. The average solid angle was calculated by a Monte Carlo method,[18] provided that the converter 20 mm in diameter was uniformly impinged by the electron beam. Figure 2.4 shows the calculated

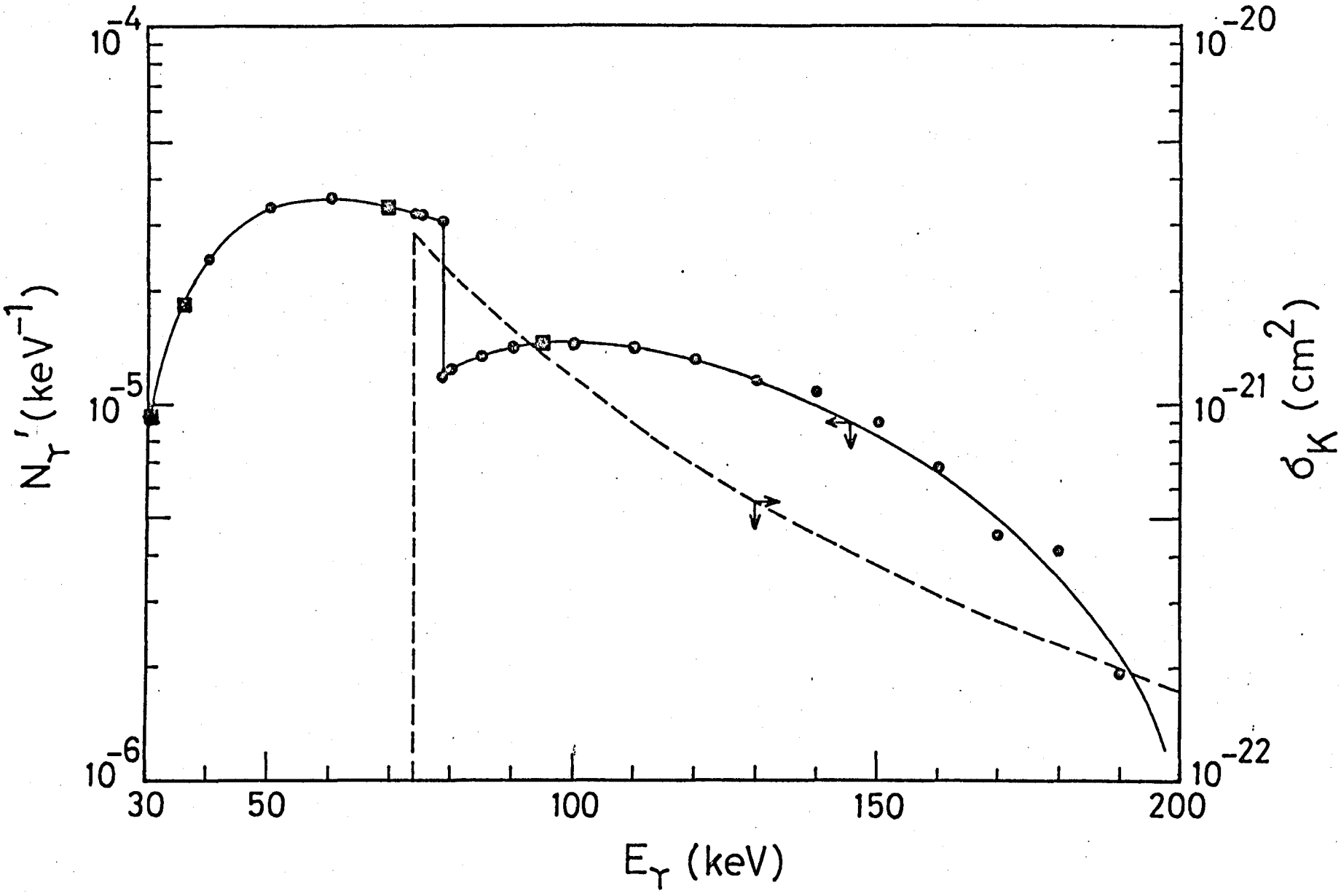

Fig. 2.4. Spectral distrubution of photons incident upon the ^{189}Os target per primary electrons, N_γ', and K-shell ionization cross sections for Os by photons, σ_K. The points show the photon yields calculated by the DIBRE-DETECTOR code.

spectrum of photons incident upon the target per primary electron, namely, the yield of photons as a function of photon energy is expressed by

$$N_\gamma(E) = N_\gamma'(E)\ N_e, \tag{2.3}$$

where $N_\gamma'(E)$ is the photon yield per primary electron and N_e is the number of primary electrons.

4.2. NEET PROBABILITY FOR ^{189}Os

The NEET probability, P, is defined in this case as the probability that the 70-keV nuclear level is excited per disappearance of a K-hole created in the ^{189}Os atom. The value of P can be calculated from the disintegration rate of ^{189m}Os at the end of irradiation, A_0, as

$$P = A_0 / [\int_{E_K}^{E_{max}} \sigma_K(E) N_\gamma(E) dE\ nB(1 - e^{-\lambda t})], \tag{2.4}$$

where $\sigma_K(E)$ is the K-shell-ionization cross section for Os by photons of energy E, $N_\gamma(E)$ is the incident rate of photons with energy E, n is the number of target atoms per unit area, B is the branching ratio of the 70-keV nuclear level to the isomeric level lying at 31 keV, λ is the decay constant of

the isomer and t is the irradiation time. The limits of integration of E are from E_K, the K-electron binding energy (73.871 keV for Os), to E_{max}, the maximum energy of incident photons corresponding to the energy of primary electrons (200 keV in this case).

The integral in the denominator in eq. (2.4) was calculated numerically as

$$\int_{E_K}^{E_{max}} \sigma_K(E) N_\gamma(E) dE = N_e \int_{73.87}^{200} \sigma_K(E) N_\gamma'(E) dE, \qquad (2.5)$$

where E is in keV and $N_\gamma'(E)$ was calculated as described in Section 4.1 and is shown in Fig. 2.4 by the solid line. The values of $\sigma_K(E)$ were taken from ref. 19, and the smoothed curve connectiong them for interpolation is depicted also in Fig. 2.4 by the dashed line. The integral was thus evaluated to be 1.35×10^{-24} N_e cm^2/s for the conditions of this experiment.

As a result, the NEET probability was obtained as $P = 4.3 \times 10^{-8}$ from eq. (2.4) with $B = 1.2 \times 10^{-3}$ as given in ref. 2. The result is smaller by a factor of four than that determined precisely in the previous experiment[2] using the electron projectiles for direct ionization of the K-shells in the ^{189}Os atoms. This disagreement is probably due to uncertainties in the irradiation procedure in this experiment. Besides, the DIBRE-DETECTOR code may overestimate the spectral

intensity of bremsstrahlung in this case of 200-keV primaries and the close configuration of converter and target, although the calculated spectra in the narrowly forward directions are declared to agree well with the experimental ones in the range 0.5–1.44 MeV.[17] Although the quantitative agreement between this experiment and the previous one[2] could not be achieved, it may be considered that the value of P obtained in this experiment agrees qualitatively with that determined in the study using electron projectiles.[2] Hereafter, a more reliable value $P = 1.7 \times 10^{-7}$ obtained in the previous experiment[2] will be used for further discussion.

4.3. RESONANCE ABSORPTION OF BREMSSTRAHLUNG

In this experiment, resonance absorption of bremsstrahlung (photons) by the nucleus remains competing with NEET for isomer production, although Coulomb excitation by electron projectiles can be excluded inherently owing to K-shell ionization by bremsstrahlung. The radioactivity of the isomer produced through this resonant process at the end of irradiation is given by integration of the Breit-Wigner single level formula as

$$A_0 = \pi^2 \lambda\!\!\!^{-2} g n \, N_\gamma(E_r) \, (1 - e^{-\lambda t}) \, \Gamma_0 \Gamma_{iso} / \Gamma \, , \qquad (2.6)$$

where $\lambda\!\!\!^{-}$ is the wavelength of photons corresponding to the resonant energy E_r divided by 2π, g is the statistical factor, Γ_0, Γ_{iso} and Γ are the radiative width to the ground state, the partial width to the isomeric level and the total width of the resonance level, respectively, and others are the same for eq. (2.4). Numerical values for the nuclear parameters required for eq. (2.6) are listed in Table 2.1 for all levels, lying at 31, 36, 70 and 95 keV, below 200 keV, the maximum energy of bremsstrahlung used in this experiment. Those were evaluated from a compilation by Lewis[13] and the tables of internal conversion coefficients by Rösel et al..[20] The value of Γ_{iso} for the 70-keV level was estimated as $\Gamma_{iso} = B\Gamma$ in ref. 2. For those levels at 36 and 95 keV, the following Weisskopf estimate were used, respectively:[21]

$$\tau_{sp}/s^{-1} = 1.1 \times 10^{-5} \, A^{8/3} \, E_\gamma{}^9 \quad \text{(for E4)} \qquad (2.7)$$

and

$$\tau_{sp}/s^{-1} = 1.1 \times 10^{1} \, A^{4/3} \, E_\gamma{}^7 \quad \text{(for M3)} \qquad (2.8)$$

where E_γ is the energy of the transition in MeV. By using the photon transition probability of a single proton, Γ_{iso} was calculated as $\Gamma_{iso} = \hbar/\tau_{sp}$. The values of Γ_{iso} listed

Table 2.1. Numerical values for the nuclear parameters required in eq. (2.6).

E_r / keV	g	Γ_0 / eV	Γ_{iso} / eV	Γ / eV
30.80	5/2	6.6×10^{-26}	$= \Gamma$	2.1×10^{-20}
36.17	1/2	3.9×10^{-8}	$\sim 10^{-20}$	8.6×10^{-7}
69.52	3/2	3.1×10^{-8}	3.4×10^{-10} a)	2.8×10^{-7}
95.23	1	6.0×10^{-8}	4.4×10^{-10}	2.0×10^{-6}

a) Estimated in ref. [2].

in Table 2.1 were obtained by multiplying the E4 enhancement factor of 100 for the 36-keV level and the M3 hindrance factor of 1/100 for the 95-keV level. However, Γ_{iso} for the latter level is replaced by the one via the 70-keV level, since the indirect feeding from the 95-keV level to the isomeric state via the 70-keV level is found to account for Γ_{iso} of the 95-keV level as compared with the direct branching as estimated above.

As is evident from eq. (2.6) and Table 2.1, isomer production by γ-resonance absorption is predominantly due to the 70- and 95-keV nuclear levels. The values of $N_\gamma(E_r)$ at each resonant energy were calculated by the DIBRE-DETECTOR code as shown in Fig. 2.4 by the solid squares [$N_\gamma(E_r) = N_e \cdot N_\gamma'(E_r)$]. The contribution of this competing mechanism is estimated to be smaller by two orders of magnitude than that observed in the experiment. The reason why 200 keV was chosen as the primary beam energy is to avoid explicitly the appreciable contribution of the 219-keV level which has much larger Γ_{iso} than these 70- and 95-keV levels, although the electrons with higher energies are much more efficient in producing and hence in activating the isomer by NEET.

Consequently the observed isomer can be wholly ascribed to the excitation of the 70-keV level by NEET following K-shell ionization by bremsstrahlung.

4.4. RECONSIDERATION OF NEET IN ^{189}Os

In ref. 2, only the KM_4 electronic transition which is of the smallest energy mismatch with the nuclear excitation of the 70-keV level has been considered to participate in the NEET process in ^{189}Os, since the NEET theory[22] was constructed on the basis of the perturbation theory of nearly degenerates two-level systems, as briefly mentioned in Section 2 of Introdution. As is evident from Fig. 2.5, the KM_5, KN_4 and KN_5 electronic transitions should partipate in the NEET process in ^{189}Os as the atomic counterparts in addition to the KM_4 transition, since these transitions and their nuclear counterpart (70-keV-level excitation) have nearly equal energies and the common multipolarity of E2. Among three electronic transitions considered newly as the atomic counterparts, the KM_5 transition should contribute comparably as the KM_4 transition, whereas other two transitions cannot be considered to contribute so much as the above. In this circumstance, the NEET theory should be based on the three-level systems even to first approximation, which demands the fundamental reconstruction of the theory. Therefore, NEET will be discussed within the original frame of the Morita theory for the sake of simplicity.

If it is permitted to neglect the mutual interference of those atomic counterparts mentioned above, the NEET

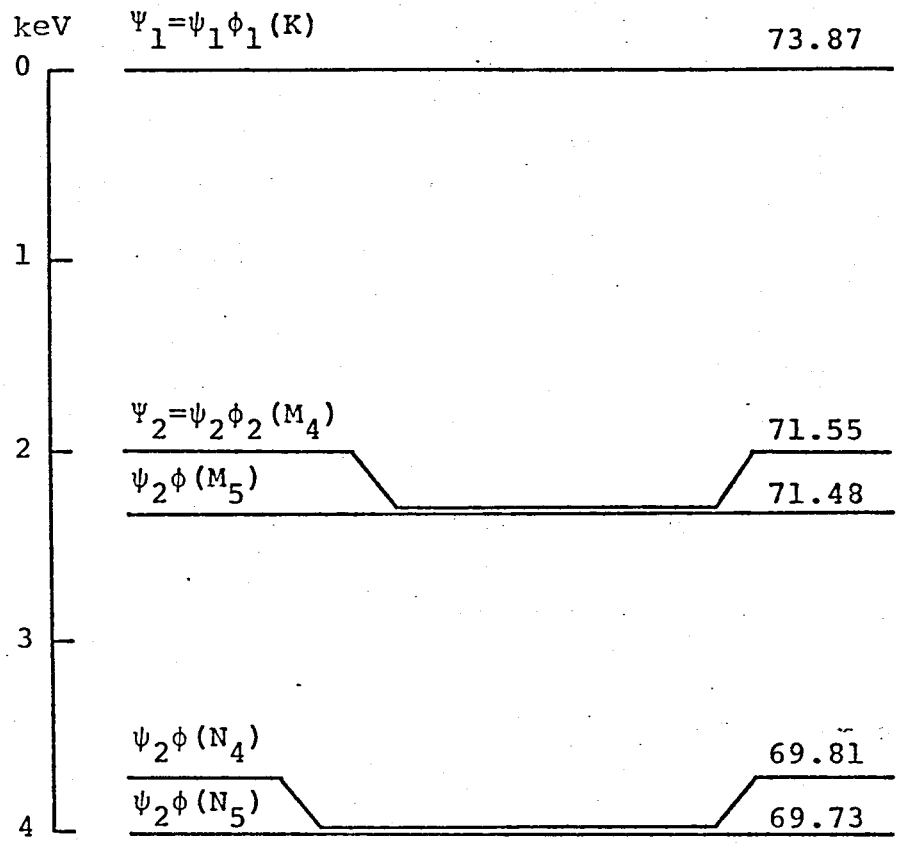

Fig. 2.5. The resultant atomic systems of nuclear levels ψ and electron-hole states ϕ participating in NEET in ^{189}Os. The coupling between Ψ_1 and other four states is of electric quadrupole interaction (E2). The energies of the resultant states are in keV.

probability for each combination can be simply related to the Coulomb interaction energy between the nucleus and orbital electron, E', as

$$P = (1 + \Gamma_2/\Gamma_1)(E'/\Delta)^2, \qquad (2.9)$$

where Γ_1 and Γ_2 are the total widths of the initial and final atomic states participating in NEET, respectively, and Δ is the energy difference between the atomic and nuclear transitions as defined by eq. (7) in Introduction. Eq. (2.9) is readily obtained by combining eq. (5) and eq. (6) in Introduction. The ratio of total decay constants of Ψ_1 and Ψ_2 is replaced by that of the level widths of ϕ_1 and ϕ_2, since the width of nuclear excited state is much narrower than those of atomic states. For Os ($Z = 76$), the value of Γ_1 was estimated by the semiempirical K-width expression of Leisi et al.[23] as

$$\Gamma_1 = \Gamma(K) = 1.73 \times 10^{-6}\ Z^{3.93}\ (eV) = 42.6\ (eV).$$

The values of Γ_2 were taken from the calculated data by McGuire[24] for the M subshells of Os, and interpolated from those calculated by McGuire[25] for N subshells of neighboring atoms. The values of E' were estimated by using eq. (10) in Introduction, with $A = 189$, $Z = 76$, $\ell = 2$, and $\bar{n} = 2$ or

2.5 according to the KM or KN electron-hole transitions. The numerical values thus obtained for the parameters in eq. (2.9) and the calculated P's are listed in Table 2.2. Evidently the total NEET probability for ^{189}Os becomes about twice as large as that estimated only for the KM_4 electronic transition.

In recent years, it has been pointed out that the magnetic interactions between the nucleus and orbital electrons should make a non-vanishing contribution to NEET in addition to the Coulomb interaction, naturally under the circumstances in which the NEET conditions are satisfied. Compared with the KM_4 transitions, a smaller Δ-value of 1.30 keV is attained by considering the KM_1 electronic transition as a substitute of the atomic counterpart. This transition had been disregarded because of its multipolarity of M1, although the 70-keV nuclear transition is an admixture of M1 and E2 as shown in Fig. 2. The M1-type interaction of such a combination should, however, be taken into consideration, since both transitions also satisfy the NEET conditions. Restricting the $ns_{1/2} \rightarrow 1s_{1/2}$ electronic transitions in atoms with the atomic number Z, Morita[26] has estimated the energy of this M1 interaction between the nucleus and orbital electron as

$$E_{M1}' = \frac{2}{3} \mu_N \mu_B (g_p/2) \, \phi_{ns_{1/2}}(0) \, \phi_{1s_{1/2}}(0)$$

Table 2.2. Numerical values for the parameters in eq. (2.9) and the calculated NEET probability P for the E2 transitions.

Transition[a]	Δ/keV	Γ_2/eV	E'/eV[b]	P[b]
KM_4	2.32	4.18	-0.60	7.35×10^{-8}
KM_5	2.39	2.35	-0.60	6.63×10^{-8}
KN_4	4.06	8.38	-0.16	1.85×10^{-9}
KN_5	4.08	8.13	-0.16	1.82×10^{-9}

a) For all transitions, E_1 = 73.871 keV, E_N = 69.52 keV, and $\Gamma_1 = \Gamma(K)$ = 42.6 eV.

b) Provided that $f = 1$ ($E' \propto f$, $P \propto f^2$).

$$= -8\ \mu_B\mu_N(Z/a_0)^3\ n^{-3/2}, \qquad (2.10)$$

where μ_B and μ_N are the Bohr and nuclear magnetons, respectively, g_p is the gyromagnetic ratio of proton, $\phi_{ns_{1/2}}(0)$ is the root of the probability for the $ns_{1/2}$ electron existing in the nucleus, and a_0 is the Bohr radius. In addition to KM_1, the KN_1, KO_1, KM_4 and KN_4 transitions (See Fig. 2.6.) can participate in NEET in ^{189}Os with the M1 interaction. The latter two transitions have already described for having the E2 contributions to NEET. In this case of M1, E' cannot be estimated so simple as other three transitions; therefore, KM_4 and KN_4 are neglected in the estimate of the contribution by M1 interaction with the nucleus. For KM_1, KN_1 and KO_1, values for E_{M1}' were estimated by eq. (2.10). For these M1 transitions, P's were also calculated by eq. (2.9), and are summarized in Table 2.3. The level width of the O_1 subshell was extrapolated from those of 5s multiplets in the rare earth region calculated by McGuire.[27] The contribution of M1 is found to amount to about 16% of that of E2. After subtraction of this M1 contribution, the correction factor appeared in eq. (10) is obtained as f = 1.0 by comparing with the experiment.

Some NEET parameters are recalculated for the resultant atomic systems including the dominant KM_4 and KM_5 electronic transitions. The mixing angles θ as defined in eq. (4)

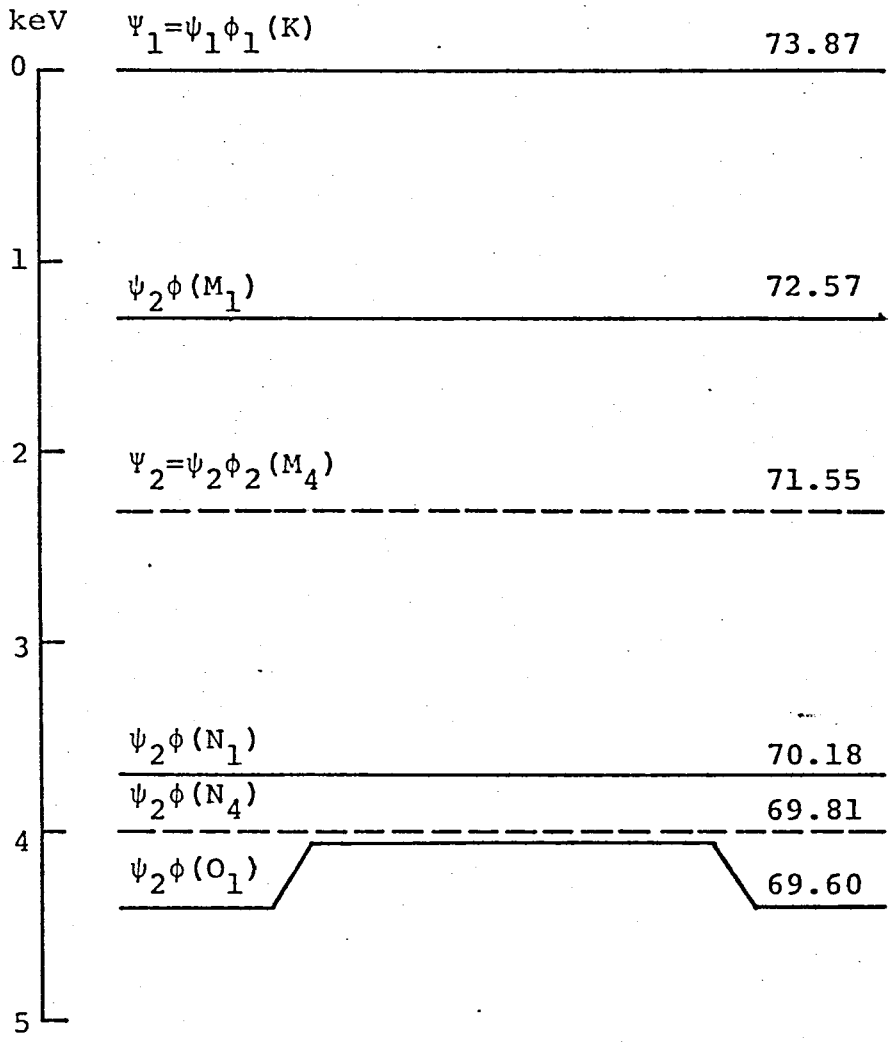

Fig. 2.6. The resultant atomic systems of nuclear levels ψ and electron-hole states ϕ participating in NEET in ^{189}Os. The coupling between Ψ_1 and other five states is of magnetic dipole interaction (M1). For those levels shown by the dashed lines, their contributions to NEET are incapable of being estimated.

Table 2.3. Numerical values for the parameters in eq. (2.9) and the calculated NEET probability P for the M1 transitions.

Transition	Δ/keV	Γ_2/eV	E'/eV	P
KM_1	1.30	20.4	-0.13	1.48×10^{-8}
KN_1	3.70	15.7	-0.09	7.57×10^{-10}
KO_1	4.27	3	-0.06	2.26×10^{-10}

were determined to be $\tan\theta = -2.6 \times 10^{-4}$ and -2.5×10^{-4} respectively for the KM_4 and KM_5 electronic transitions. The energy shifts of the resultant states δ were also obtained by using eq. (8) in Introduction as $\delta = 1.6 \times 10^{-4}$ eV and 1.5×10^{-4} eV for the KM_4 and KM_5 transitions, respectively. It is natural that these results are about a half of those obtained in ref. 2, since the interference between the participants in NEET is not taken into account. For other transitions, θ and δ are about one order of magnitude smaller than those for two dominant transitions.

5. Conclusion

In this experiment, NEET in ^{189}Os could be observed by using photons for K-shell ionization, with exclusion of Coulomb excitation by electron projectiles and with superiority over γ-resonance absorption. The results obtained may offer additional verification of NEET the first stage of which is a purely atomic process.

References

1) K. Otozai, R. Arakawa and M. Morita, *Prog. Theor. Phys.* 50, 1771 (1973).

2) K. Otozai, R. Arakawa and T. Saito, *Nucl. Phys.* A297, 97 (1978).

3) T. Saito, Y. Ohkubo, A. Shinohara, R. Arakawa and K. Otozai, *Nucl. Phys.* A330, 443 (1979).

4) A. Veres, *Int. J. Appl. Radiat. Isot.* 14, 123 (1963).

5) A. Veres and I. Pavlicsek, *J. Radioanal. Chem.* 3, 25 (1969).

6) J. Law and F. A. Iddings, *J. Radioanal. Chem.* 3, 53 (1969).

7) Y. Watanabe and T. Mukoyama, *Bull. Inst. Chem. Res., Kyoto Univ.* 57, 72 (1979).

8) R. Arakawa, T. Saito and K. Otozai, *Nucl. Instrum. Methods* 131, 369 (1975).

9) L. Pages, E. Bertel, H. Joffre and L. Sklavenitis, *At. Data* 4, 1 (1972).

10) T. Tabata, R. Ito and S. Okabe, *Nucl. Instrum. Methods* 94, 509 (1971).

11) R. Arakawa, Thesis, Osaka University (1976) (*In Japanese*).

12) J. O. Newton, *Phys. Rev.* 117, 1529 (1960).

13) M. B. Lewis, *Nucl. Data Sheets* 12, 397 (1974).

14) R. G. Baker and L. Katz, *Nucleonics* 11(2), 14 (1953).

15) J. S. Nader, G. P. Hagee and L. R. Setter, *Nucleonics* 12(6), 29 (1954).

16) J. B. Cumming, National Academy of Sciences report NAS-NS 3107 (1962) p. 25.

17) T. Nakamura, M. Takemura, H. Hirayama and T. Hyode, *J. Appl. Phys.* 43, 5189 (1972).

18) L. Wielopolski, *Nucl. Instrum. Methods* 143, 577 (1977).

19) WM. J. Veigele, *At. Data Tables* 5, 51 (1973).

20) F. Rösel, H. M. Fries, K. Alder and H. C. Pauli, *At. Data Nucl. Data Tables* 21, 291 (1978).

21) C. M. Lederer and V. S. Shirley, ed., *'Table of Isotopes'* 7th ed. (Wiley, NY, 1978).

22) M. Morita, *Prog. Theor. Phys.* 49, 1574 (1973).

23) H. J. Leisi, J. H. Brunner, C. F. Perdrisat and P. Scherrer, *Helv. Phys. Acta* 34, 161 (1961).

24) E. J. McGuire, *Phys. Rev. A* 5, 1043 (1972).

25) E. J. McGuire, *Phys. Rev. A* 9, 1840 (1974).

26) M. Morita, private communication to Prof. K. Otozai (1979).

27) E. J. McGuire, *Phys. Rev. A* 10, 13 (1974).

CHAPTER III

NUCLEAR EXCITATION BY ELECTRON TRANSITION IN ^{237}Np FOLLOWING K-SHELL PHOTOIONIZATION

1. Introductory remarks

Nuclear excitation by electron transition (NEET) was first observed in ^{189}Os by Otozai et al.[1,2] by activation of the isomer with electron bombardment. As described in Section 6 of Introduction, the nuclide ^{237}Np satisfys the NEET conditions. Unlike NEET in ^{189}Os which has a positive Δ-value and proceeds by E2 radiation, NEET in ^{237}Np has a negative Δ-value and a common multipolarity E1. The nuclear excitation of the 102.95-keV level proceeds by E1 as does the electronic transition between the K and L_3 shells with an energy of 101.072 keV. Therefore, NEET should be occur by the exchange of virtual photons between these transitions.

Since ^{237}Np has no long-lived isomer suitable for residual radioactivity measurement, a radiochemical technique cannot be applied to the observation of NEET in ^{237}Np. Some attempts to detect NEET in ^{237}Np have been made by Otozai et el.[3,4] with a ingenious technique of examining the perturbed Np X-ray spectrum exhibited in the EC decay of ^{237}Pu. As described in Introdution, no significant value for NEET probability can be deduced from the intensity ratio of the satellite X-ray pairs owing to the poorer resolution of the X-ray spectrometer used in the experiments. An upper limit of 2×10^{-3} was obtained for the NEET probability in ^{237}Np by Shinohara et al..[4] The improvement of the resolution of spectrometer is essential to obtain a significant value for the NEET probability, since other instrumental techniques such as coincidence method are incapacity for picking up the signals relating to NEET selectively.

This Chapter describes another attempt using a quite different method to observe NEET in ^{237}Np. A ^{237}Np sample was irradiated with photons to produce the K-hole in the ^{237}Np atom. Nuclear excitation of the 103-keV level can be observed by detecting one of deexcitation γ-rays emitted in the decay process of the 103-keV nuclear level. As Fig. 3.1 shows, γ-rays with energy of 60 keV are the intensest among them. Therefore, the 60-keV γ-rays are aimed at to detect in the course of irradiation of ^{237}Np by photons.

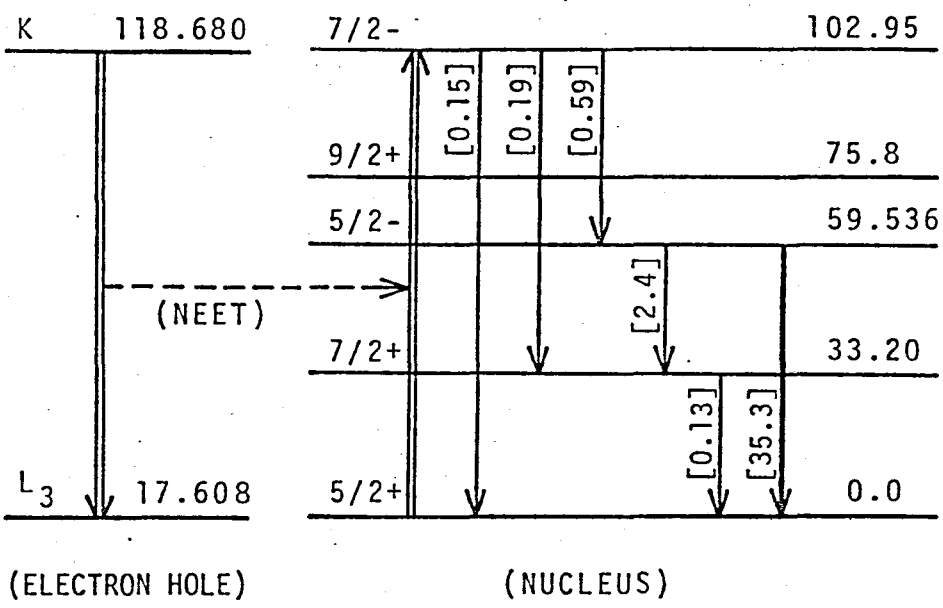

Fig. 3.1. NEET diagram for ^{237}Np. The numerical values in the brackets indicate the photon intensities per 100 disintegrations of the 103-keV level.[5] The intensest γ-ray at 60 keV was detected as an indication of NEET.

2. Experimental

2.1. PREPARATION OF ^{237}Np SAMPLE

The oxide of ^{237}Np supplied by ORNL was radiochemically impure because it contained ^{238}Pu, ^{241}Am and ^{233}Pa. These contaminants should be removed for the following reasons: ^{238}Pu ($t_{1/2}$ = 87.75 y) had its radiochemical concentration about 150 times as high as ^{237}Np, and therefore it was quite dangerous in handling the ^{237}Np sample; ^{241}Am ($t_{1/2}$ = 433 y) decays to the 60-keV level in ^{237}Np abundantly, and hence emits the 60-keV γ-rays which are the γ-ray aimed at as an indication of NEET in ^{237}Np in this experiment; and, ^{233}Pa ($t_{1/2}$ = 27.0 d), the daughter nuclide of ^{237}Np and being in radioactive equilibrium with ^{237}Np, interferes the photon spectrum since it emits various γ-rays of high intensities.

From the reasons mentioned above, the ^{237}Np sample was purified repeatedly according to the scheme of Smith[6] and Fujiwara et al..[7] About 200 mg of powder of the ^{237}Np oxide was added to the mixed solution of the same volumes of conc. HNO_3 and conc. HCl. After bromine water was added, the mixture was refluxed for 4 h to dissove the oxide of ^{237}Np completely. Neptunium was then precipitated by adding NH_4OH. The hydroxide of Np was dissolved in conc. HCl, and Np was reduced with hydroxylamine hydrochloride. Neptunium

was absorbed on the Dowex-1 anion exchange resin conditioned with HCl, and the transplutonium elements such as ^{241}Am were washed out with conc. HCl. Plutonium was eluted by conc. HCl including 10% of HI with $NH_2OH \cdot HCl$ being put on the top of the column. Neptunium was then eluted by 5N HCl, and precipitated on addition of NH_4OH. The precipitate was washed with water. As shown schematically in Fig. 3.2, this purification procedure was repeated for three times by using new column and glassware in each case. The decontamintation factor (DF) for ^{238}Pu was determined by α-spectrometry. About 1 μl of the eluate was put on a Pt disk, and the disk was assayed to α-spectrometry after it was flamed. In the second run, the eluate was electrodeposited on a stainless steel disk. Alpha-spectrum was taken with a Si surface barrier type spectrometer connected with a 400-channel analyser through standard electronics. The spectrum obtained is shown in Fig. 3.3. The pulse-height was biased at 2 MeV. Relative amounts for ^{238}Pu and ^{237}Np can be evaluated from the peak areas appeared in the spectrum. The final DF value for ^{238}Pu was obtained to be 1300. This method is inapplicable to the decision of DF for ^{241}Am, since α-rays from ^{241}Am (E_α = 5.486 and 5.234 MeV) are indistinguishable from those of ^{238}Pu (E_α = 5.499 and 5.457 MeV) in the spectrum taken by this system. Therefore, DF for ^{241}Am was determined by another method as will be described later.

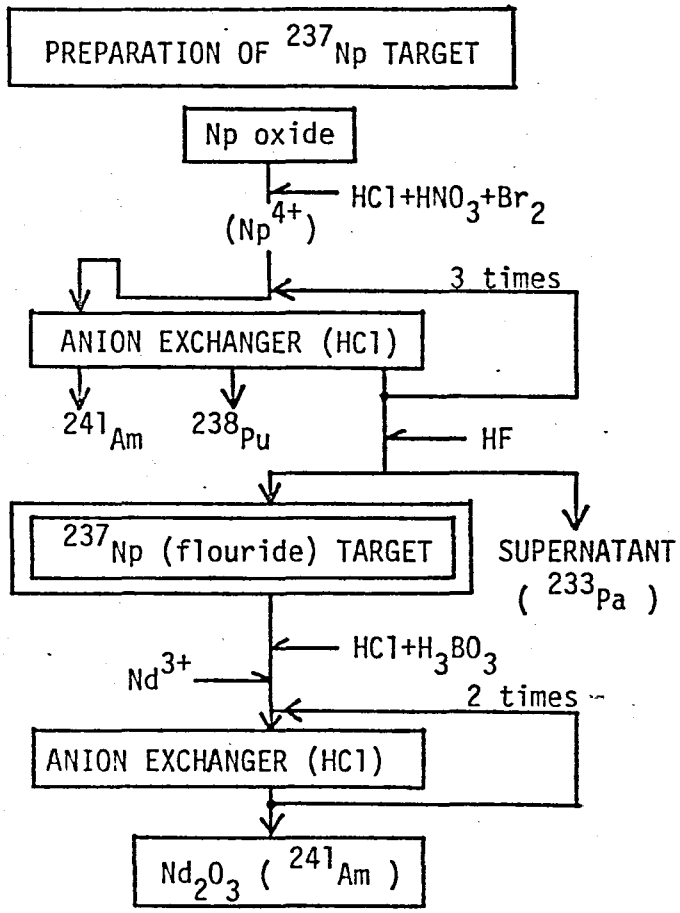

Fig. 3.2. Flow diagram for the preparation of the ^{237}Np target. Chemical procedure for determining the ^{241}Am content is also shown.

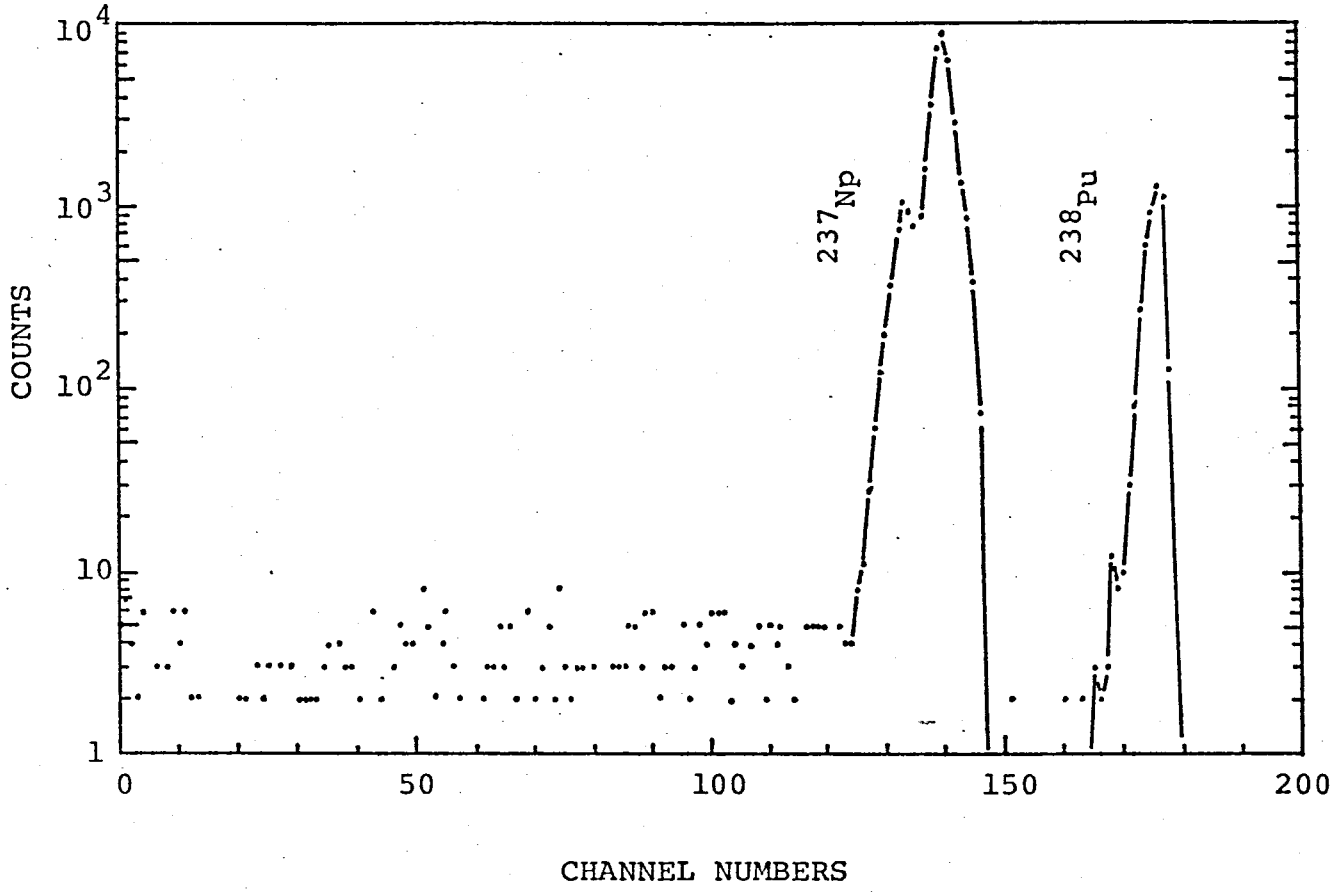

Fig. 3.3. Alpha-spectrum of the eluate after the second purification measured with a Si(Au) detector and a 400-ch MCA (biased at 2 MeV).

After purification, the hydroxide of Np was dissolved in conc. HCl. The fluoride of ^{237}Np was precipitated by addition of hydrofluoric acid, whereas the daughter atom ^{233}Pa was left in the supernatant. The precipitate was collected on a 7.4-mg/cm^2 thick Teflon filter, leaving ^{233}Pa in the filtrate. The ^{237}Np fluoride, 2 cm^2 in area, together with the filter, was placed between two 0.9-mg/cm^2 thick Mylar films, and sealed with epoxy-resin adhesive. This assembly containing 266 mg of $^{237}NpF_4$ was used as a target. This weight of $^{237}NpF_4$ agrees with the radioactivity of ^{237}Np obtained by γ-spectrometry (0.14 mCi = 5.18 MBq). By γ-spectrometry using a Ge(Li) γ-ray spectrometer and a 4000-channels multi-channel analyser (MCA), DF for ^{233}Pa was determined to be 1.7×10^4.

For comparison purpose, a similar assembly containing the same amount of $^{238}UF_4$ as $^{237}NpF_4$ was prepared in the same manner. In ^{238}U, NEET is not expected to occur, whereas the scattering of γ-rays are quite analogous for these two assemblies.

After the measurement of NEET in ^{237}Np had been done, the ^{241}Am content in the ^{237}Np target was measured by the chemical isolation of ^{241}Am and γ-spectrometry of the isolated sample. The ^{237}Np target (fluoride) was dissolved in the mixed solution of the same volumes of saturated boric acid solution and conc. hydrochloric acid. Neptunium was

precipitated with NH_4OH, and then dissolved in conc. HCl. After 9.2 mg of the Nd carrier was added to the solution, Np was absorbed on the Dowex-1 anion exchange resin column. The solution passed through the column was purified by the precipitation of the Nd hydroxide including ^{241}Am, and then dissolved in conc. HCl. Neptunium was removed once more by the Dowex-1 resin column. Ammonium oxalate was added to the eluate, and then the Nd oxalate was precipitated by adjustment of the solution to pH 2 with NH_4OH. The precipitate was collected on a cellulose acetate filter, and reduced to the oxide in a porcelain crucible by heating. The oxide of Nd was collected on a filter and assayed to γ-spectrometry. Chemical yield of the Nd carrier was 79.5%. The 60-keV γ-ray from ^{241}Am was measured with a low-energy photon spectrometer, as described in Section 2.3 of Chapter I. Intensity for the γ-ray was obtained to be 0.0618 ± 0.0009 counts/s with the spectrometer in the closest configuration. The efficiency of this spectrometer for the 60-keV γ-ray was obtained from a curve as shown in Fig. 1.6. The disintegration rate of ^{241}Am was determined to be 93 ± 1 pCi.

2.2. MEASUREMENT OF PHOTON SPECTRA OF ^{237}Np AND ^{238}U

The ^{237}Np (fluoride) target was measured with a low-

energy photon spectrometer system as shown in Fig. 1.6. The spectrometer consists of a 16-mm diam. × 7-mm sensivive depth hyperpure Ge crystal and a preamplifier cooled at the liquid N_2 temperature. The entrance window is made of 0.13-mm thick Be and the front contact is evaporated light metal; thererore, the interfering photons cannot be produced in this front end of the spectrometer. The MCA was replaced by a NAIG 4000-channel MCA. The resolution of this system was typically 390 eV for photons with energy of 60 keV at count rate below 1500 counts/s.

The arrangement of the target, the spectrometer and a ^{57}Co source is schematically shown in Fig. 3.4. The 4.7-mCi ^{57}Co photon source for Mössbauer spectroscopy was placed at a distance of 2 cm from the target. The detector was placed at a distance of 15 cm from the ^{237}Np target perpendicularly to the source-target axis. The Pb shield was carefully placed not to enhance the inelastic scattering of photons. Some parts of the surface of the Pb shields were lined with brass plate in order to reduce the scattering of photons. The measurements were made for three-types of the combination of target and source:

i) ^{237}Np target irradiated with the ^{57}Co γ-rays,

ii) ^{237}Np target without the ^{57}Co source,

and

iii) ^{238}U target irradiated with the ^{57}Co γ-rays.

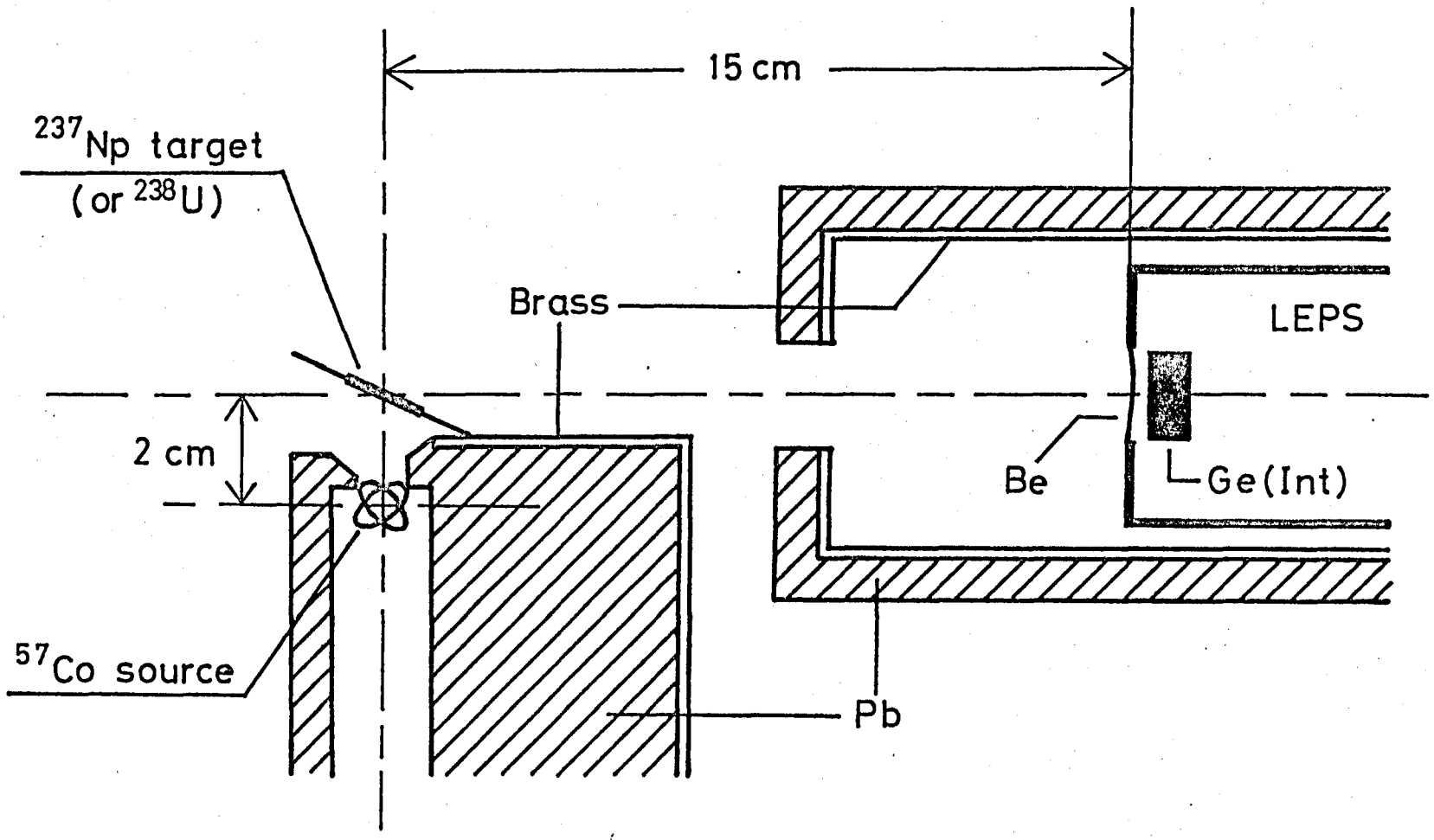

Fig. 3.4. Schematic view of the experimental setups for observation of NEET in ^{237}Np. Photon spectra were taken for (i) ^{237}Np + ^{57}Co, (ii) ^{237}Np, and (iii) ^{238}U + ^{57}Co.

The purposes of the combinations of (ii) and (iii) are to check the appearance of 60-keV peaks from the ^{237}Np target (mainly due to ^{241}Am) without photon irradiation and from the inelastic scattering of the ^{57}Co γ-rays, respectively. The photon spectra taken with the spectrometer are shown in Figs. 3.5–3.7. The reason why the ^{57}Co photon source was used in this experiment for NEET in ^{237}Np is that the γ-rays emitted from ^{57}Co are probably most suitable for ionization of the K-shells of the ^{237}Np atoms, since they have energies of 122 and 136 keV which are slightly higher than the K-binding energy of Np (119 keV). In addition, rather intense ^{57}Co sources are available as those for Mössbauer spectroscopy.

In this experiment, the self-absorption of photons in the ^{237}Np target is not insignificant since the target was not so thin. This self-absorption was corrected including the geometrical factor by the measurement of γ-rays and X-rays from ^{237}Np. Those used for correction were the 29.373-, 46.53-, 57.15-, 86.503-, 106.12-, 131.043-, 143.208-, 151.37-, 169.17-, 195.096-, 212.415-, and 238.04-keV γ-rays from ^{237}Np, the Pa $K_{\alpha 1}$ and $K_{\alpha 2}$ X-rays, and the 75.28-keV γ-rays from ^{233}Pa. The peak areas were calculated with the aid of the BOB75 γ-spectra analyzing code[8–11], and compared with the literature.[5,12] The relative efficiency curve for photons emitted from the ^{237}Np target was then constructed as shown

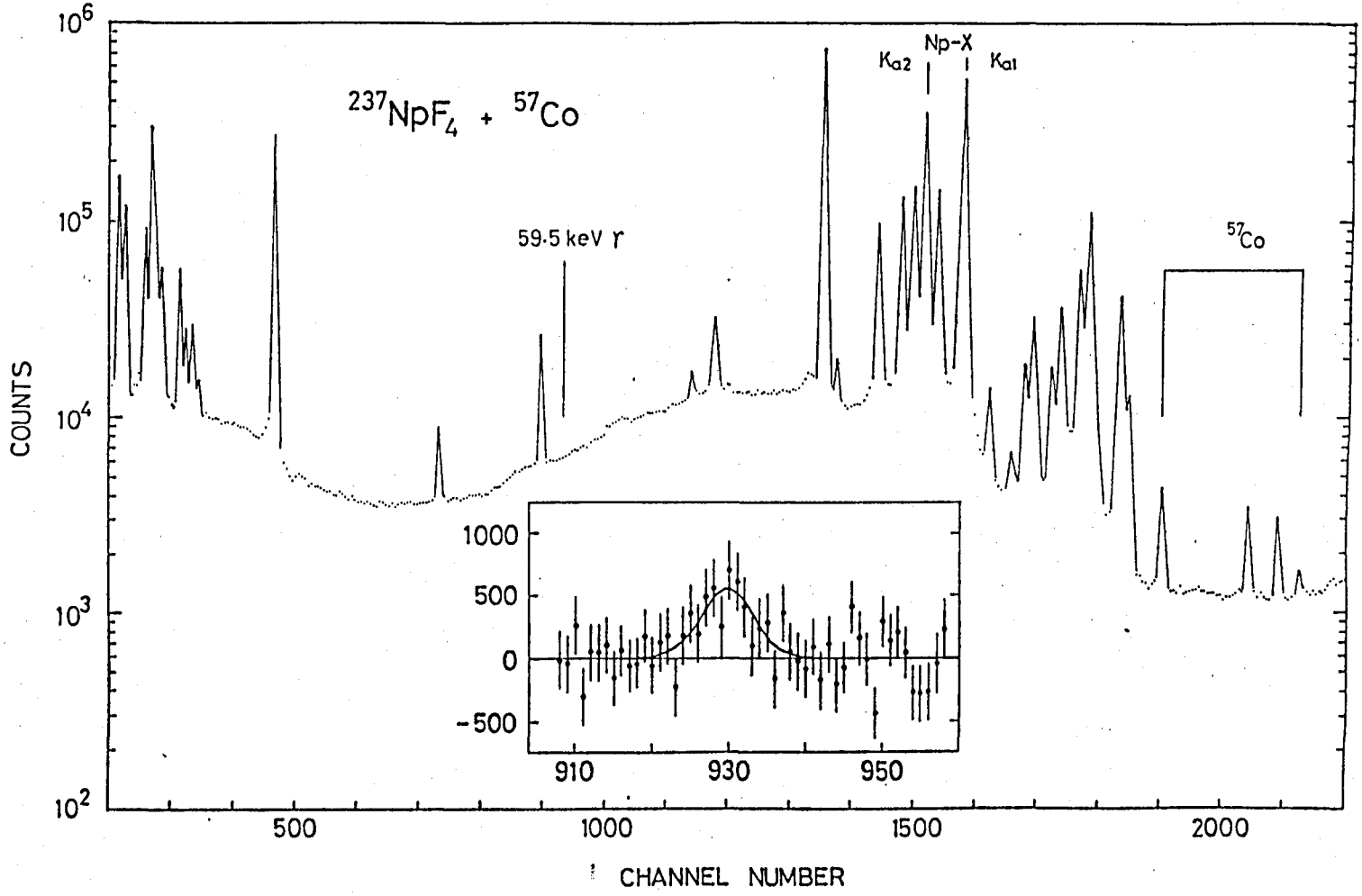

Fig. 3.5. The photon spectrum of ^{237}Np irradiated with the ^{57}Co gamma-rays with an accumulation time of 3×10^4 s. After that time, counts in the peak regions overflowed the memory capacities of MCA. The results of analysis for the region near 59.5 keV is also shown.

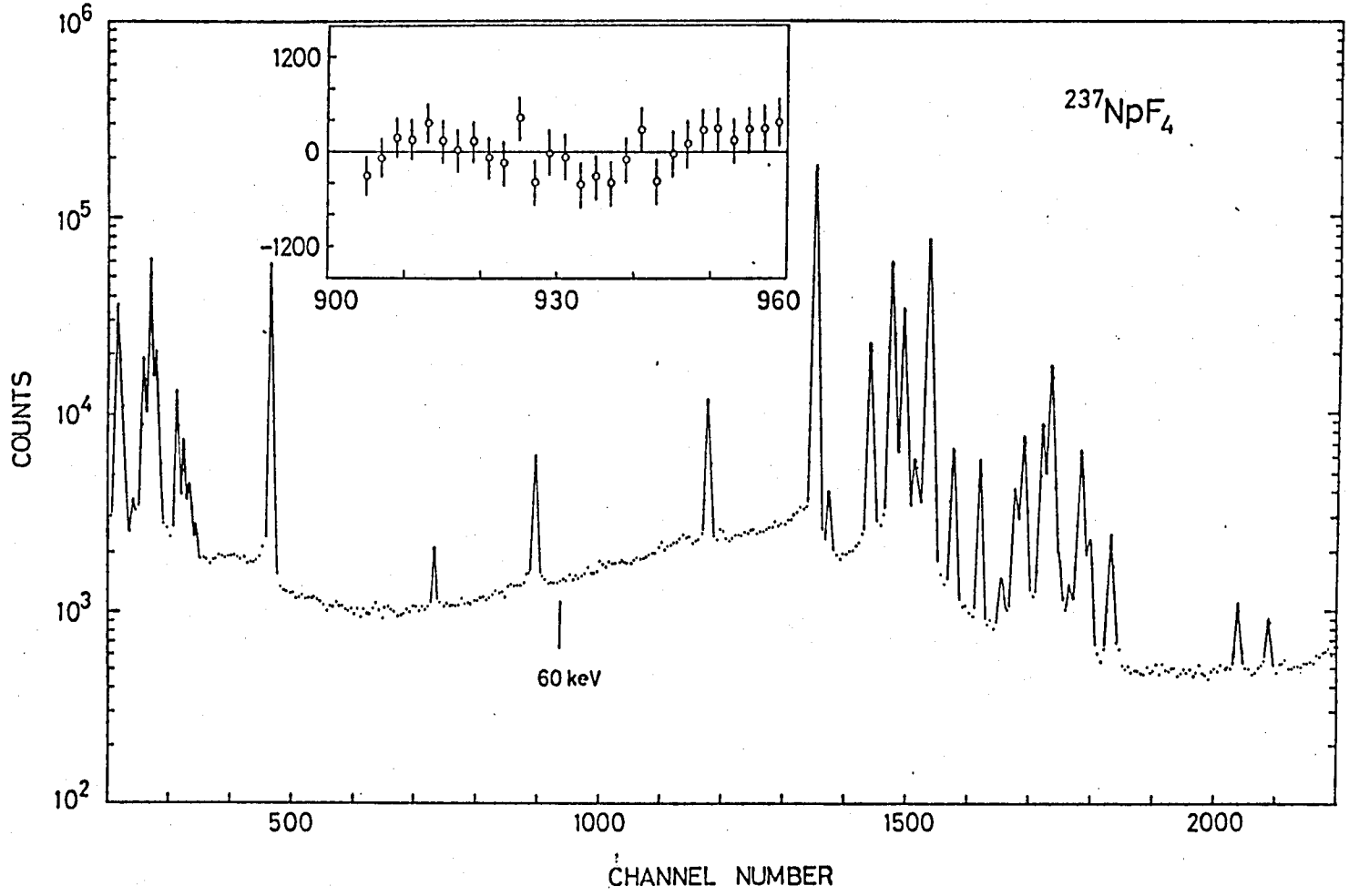

Fig. 3.6. The photon spectrum of ^{237}Np without the ^{57}Co photon source. The results of analysis for the region near 59.5 keV is also shown.

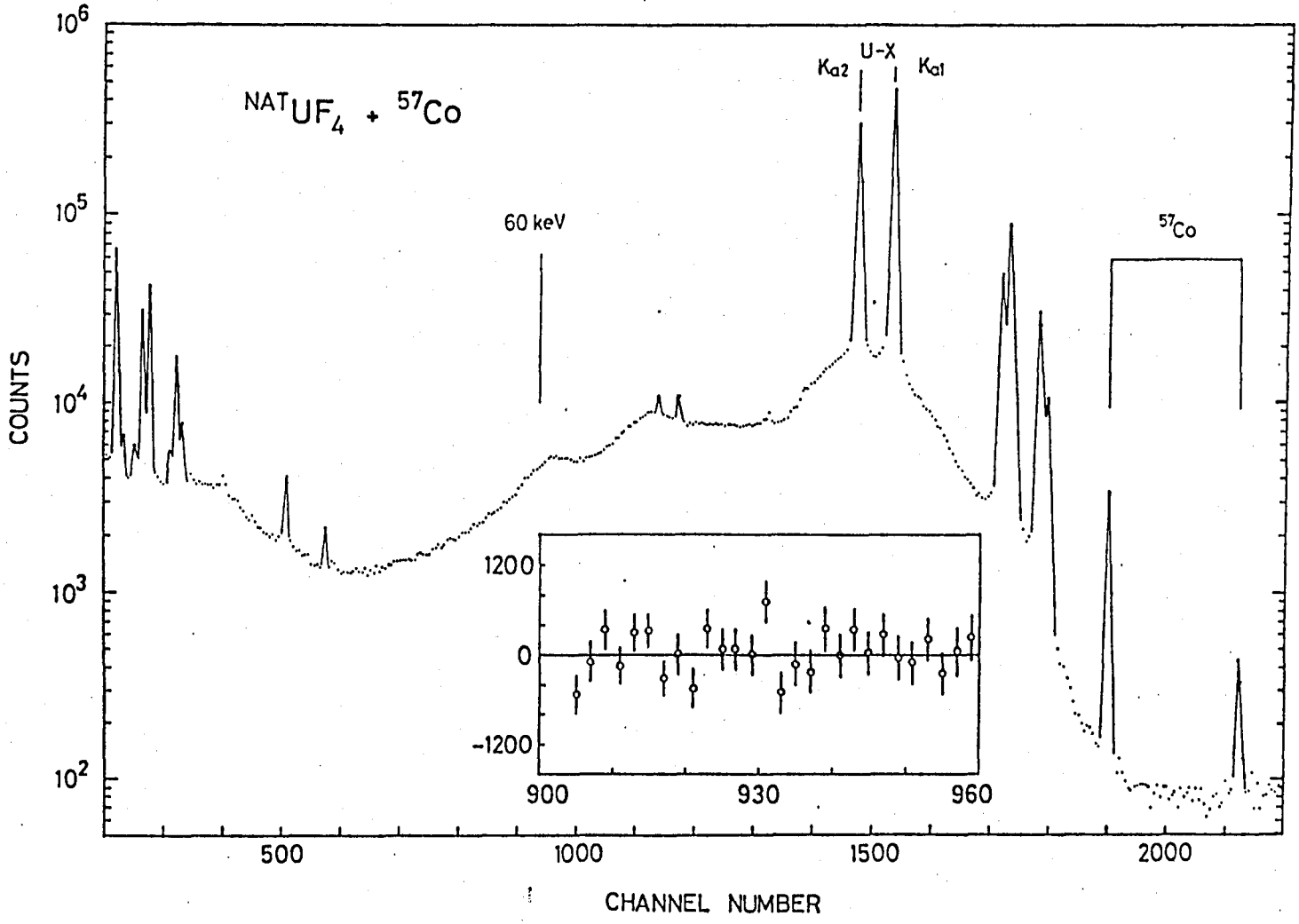

Fig. 3.7. The photon spectrum of ^{238}U irradiated with the ^{57}Co gamma-rays. The results of analysis for the region near 59.5 keV is also shown.

in Fig. 3.8. The lower energy part (< 106.12 keV) and the higher energy part (> 106.12 keV) were fitted separately by a biquadratic equation and a cubic equation as shown in Fig. 3.8 by a solid line. The relative efficiencies for photons with energies of 60 and 101 keV were calculated by using the fitted equation as $\varepsilon_{101} = 0.90 \pm 0.06$ and ε_{60} 0.76 ± 0.06 relative to ε_{86}, where ε_E is the efficiency for E-keV photons emitted in the target. Therefore, one obtains $\varepsilon_{101}/\varepsilon_{60} = 1.2 \pm 0.1$. The quoted error includes those of the emission probability of γ-rays and X-rays and of the analysis of the measured peak areas.

2.3. ANALYSIS OF THE 60-keV PEAK

As is described in Section 1, NEET in ^{237}Np can be observed by the detection of the 59.5-keV γ-ray emitted in the decay of the 103-keV level which is excited by NEET. In the region near 60 keV of the photon spectrum of ^{237}Np irradiated with the ^{57}Co γ-rays, no peaks were recognized by the automatic peak-search routine of the BOB75 γ-spectra analyzing code.[8–11] Consequently, that region was analyzed separately in the following manner. The first and second derivatives of the data points were obtained with the aid of the smoothing routine of the BOB75 code. The second

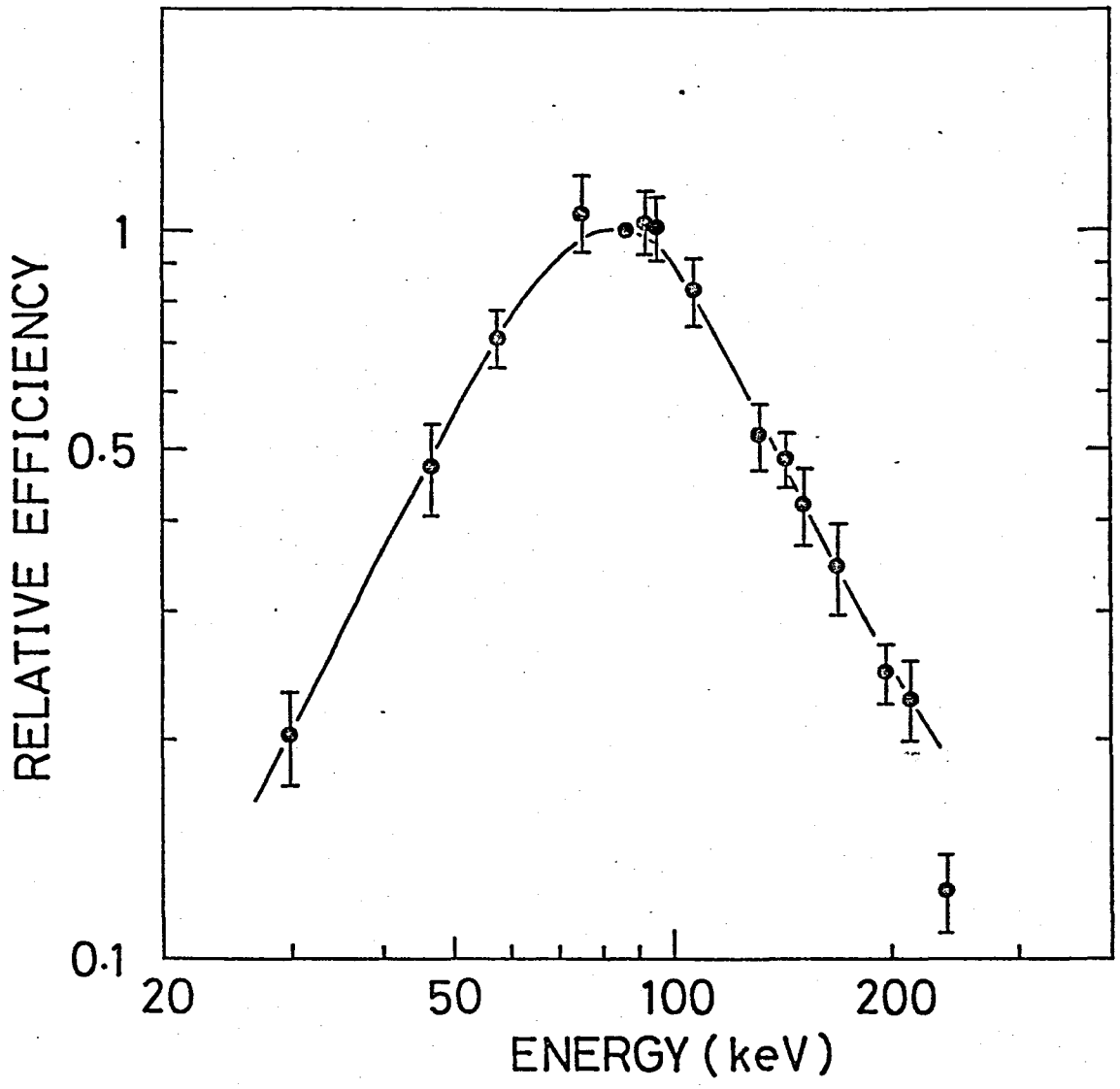

Fig. 3.8. Relative efficiency of the spectrometer for photons emitted in the ^{237}Np target, including the self-absorption in the target ($\varepsilon_{86} = 1$).

derivative clearly indicates the presence of a peak at 59.5 keV with a width close to that expected for singles photopeak, as shown in Fig. 3.9. The baseline counts in the peak region were interpolated by a cubic expression fitted to the data points (908–920, 940–960 channels) outside the full width at one tenth of the presumed maximum of the peak at 59.5 keV, where the width at one tenth maximum was assumed to be equal to half of that at half maximum. The reduced χ^2-value in this fit is 0.83 for 30 degrees of freedom, and the obtained cubic equation ($c_1 = -0.36996 \times 10^8$, $c_2 = 0.1226 \times 10^6$, $c_3 = -0.13560 \times 10^3$, and $c_4 = 0.50014 \times 10^{-1}$) has inflection points outside the fitted and peak regions. The remaining counts form a symmetric distribution centered at 59.50 keV, which is extremely close to that of the γ-ray of ^{237}Np to be detected, 59.536 keV. The results are shown in Figs. 3.5 and 3.10. Its full width at half maximum (FWHM) is 7.94 channels, which is consistent with those of the nearest neighbors (7.25 channels at 57.15 keV, and 7.98 channels at 86.50 keV) within a difference of 10%. From these facts, it may be judged that the 60-keV γ-ray of ^{237}Np was observed in the photon spectrum of ^{237}Np being irradiated with the ^{57}Co γ-rays.

The peak area was obtained by summention of remained counts in each channels in the 60-keV peak region after subtraction of baseline counts. The result was 4701.1 ±

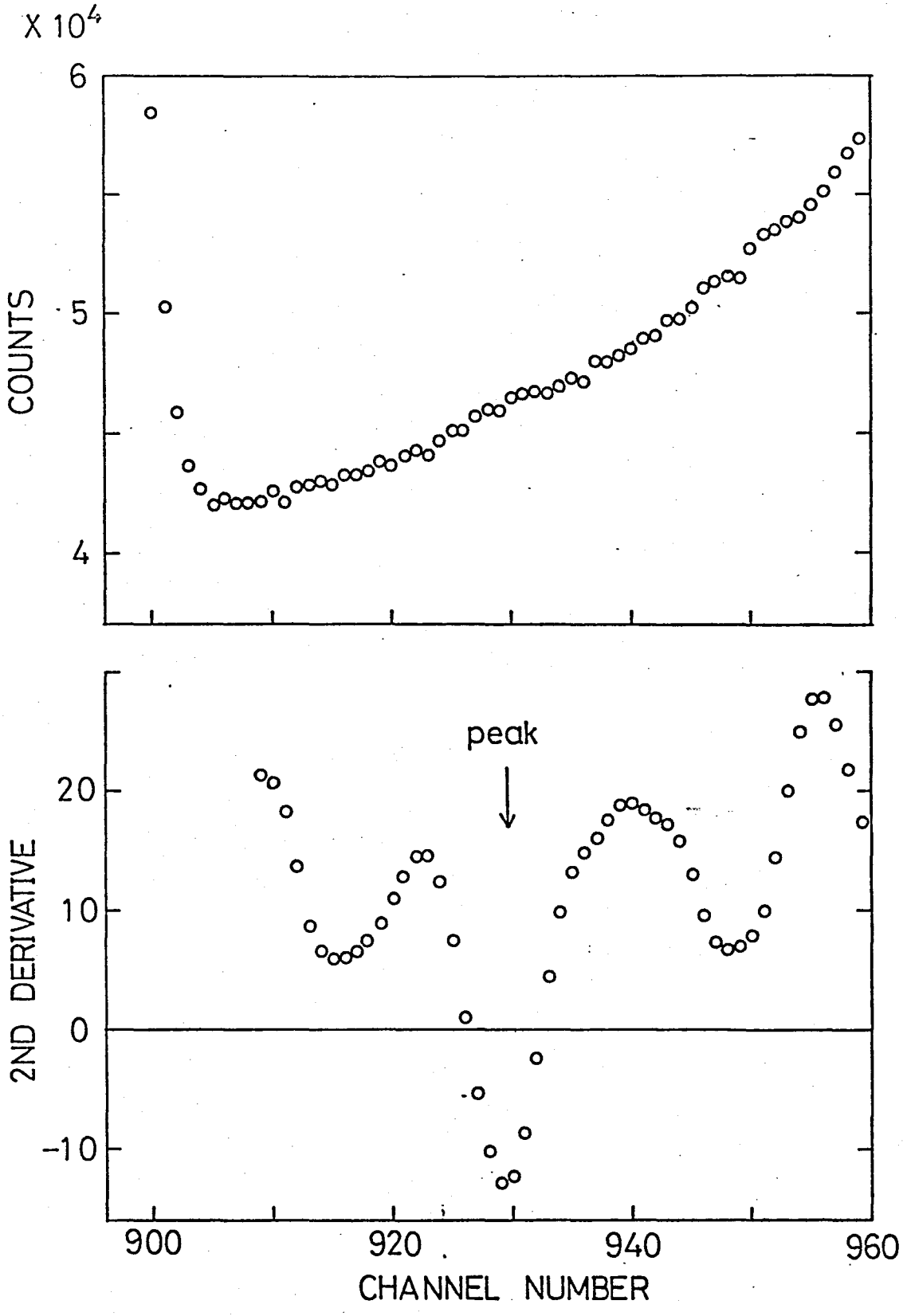

Fig. 3.9. The observed photon spectrum of ^{237}Np with ^{57}Co near 60 keV (upper) and the second derivative of the data points (lower).

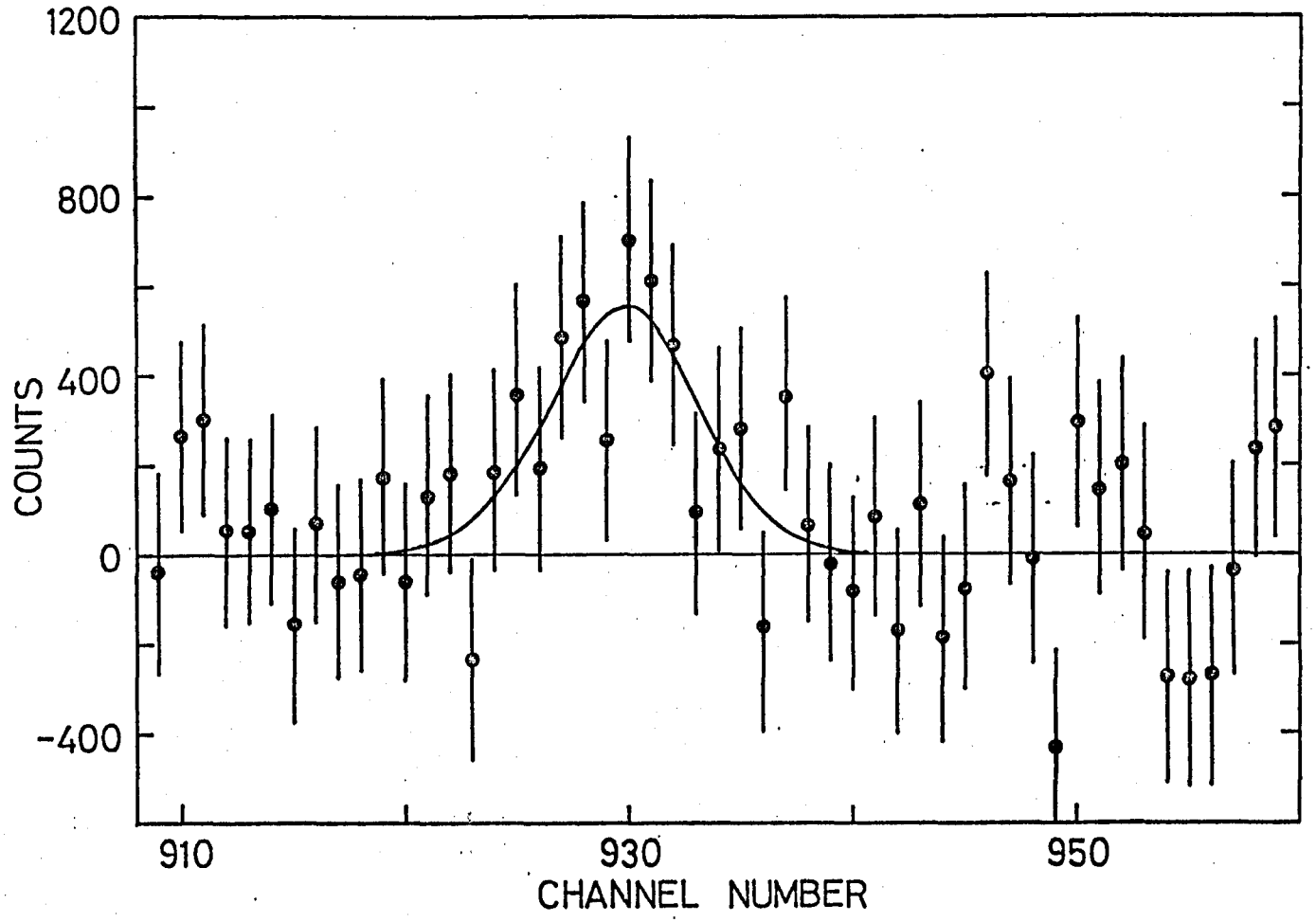

Fig. 3.10. The remained counts of the photon spectrum of ^{237}Np with ^{57}Co after subtraction of the baseline counts interpolated from the neighboring region.

1002.1 counts for an accumulation time of 2.1×10^5 s, and hence 0.0224 ± 0.0048 counts/s.

The same procedure was applied to the analysis of the photon spectra of ^{237}Np and ^{238}U irradiated with the ^{57}Co γ-rays. As shown in Figs. 3.6 and 3.7, no peaks could be extracted in the vicinity of 60 keV for both cases.

2.4. INTERFERING COMPONENTS OF THE 60-keV PEAK

Interfering components of the 60-keV peak are considered to arise from the following origins:

i) 59.5-keV γ-rays emitted from the ^{241}Am impurity present in the ^{237}Np target,

ii) sum-coincidence peaks appearing in the vicinity of 60 keV, by summation of lower-energy photons,

iii) pulse pile-ups in the circuits of the spectrometer system, and

iv) 59.5-keV γ-rays following γ-resonance absorption of the 103- and 60-keV nuclear levels in ^{237}Np.

The alternative origin of the 60-keV γ-ray is most probably ^{241}Am that may have remained in the ^{237}Np target owing to insufficient removal of that element. The ^{241}Am content was assayed efficiently by γ-spectrometry after the chemical isolation of ^{241}Am with the Nd carrier from the

target, as already described in Section 2.1.

In the decay of ^{237}Np, sum peaks may appear at 59.82 and 59.65 keV if the 46.43-keV γ-ray is added to the Pa $L\alpha_1$ and $L\alpha_2$ X-rays emitted in a cascade transition, respectively. The intensity ratio of the sum peaks to the original γ-ray peaks could be determined by examining the photon spectrum of ^{237}Np without the ^{57}Co source. Although this interfering component was found to be negligible from the experiment, a more acculate estimate was made from the nuclear data given in ref. 5. The ratio was obtained to be less than 1×10^{-4}.

There is a possibility that pulse pile-up generates broad pseudopeaks at positions near 60 keV. Pulse pile-up is considered to be proportional to the product of the count rates of independent pulses. The count rate of pile-up is given by

$$N = f \cdot N_1 \cdot N_2 \qquad (3.1)$$

where N_1 and N_2 are the count rates of independent pulses and f is a proportionality constant corresponding to the resolving time of the spectrometer. The value of f was determined from the experiment using the 122- and 136-keV γ-rays from ^{57}Co and the 60-keV γ-ray from ^{241}Am for the spectrometer used in this study. By use of $f = 10^{-5-6}$, an upper limit of 1×10^{-5} counts/s was obtained for this

interfering component.

The 60-keV γ-rays may be emitted as a result of γ-resonance absorption by the 60- and 103-keV levels in ^{237}Np. There is a quite small possibility that the inelastically scattered photons are in resonance with these nuclear levels. In the estimate of this interfering component, an extreme case was considered such that all photons emitted from the ^{57}Co source distrubute in one-keV interval around the resonant energy. The emission rate of the 60-keV γ-rays following γ-resonance absorption is expressed by

$$I = N_{\gamma}(E_r) \cdot n \cdot \int \sigma(E)\,dE \cdot B \cdot G \cdot \varepsilon_{60} \ , \tag{3.2}$$

where $N_{\gamma}(E_r)$ is the incident rate of photons with energy at resonance, n is the number of ^{237}Np atoms, B is the factor including the branching ratio to the 60-keV level and the emission probability in the decay of the 60-keV level for the 60-keV γ-rays, G is the geometric factor and ε_{60} is the efficiency of the spectrometer for the 60-keV γ-rays. The integral of σ over E is given by

$$\int \sigma(E)\,dE = (\lambda^4/4)\, g \Gamma_0 , \tag{3.3}$$

where Γ_0 is the radiative width of the resonant nuclear level and $\lambda = hc/E_r$. This is included in eqs. (1.17) and (2.6).

By using the nuclear data of the 60- and 103-keV levels in ^{237}Np [ref.5], $G = 6.67 \times 10^{-4}$ (at a distance of 15 cm in this case), $n = 2.52 \times 10^{20}$ cm^{-2} and $N_\gamma(60) = N_\gamma(103) = 1.6 \times 10^{7}$ keV$^{-1}\cdot$s^{-1}, one obtains $I = 1.4 \times 10^{-6}$ counts/s for the 60-keV-level excitation and 2.2×10^{-6} counts/s for the 103-keV-level excitation. As a result, one can consider this interfering component contributes much less than 4×10^{-6} counts/s.

2.5. EVALUATION OF THE FLUORESCENCE Np $K\alpha_1$ X-RAY INTENSITY

The formation rate of the K-hole in the ^{237}Np atom is obtained from the measurement of the fluorescence Np K X-rays emitted in the cource of the irradiation of the ^{237}Np target with the ^{57}Co source. Among the Np K X-rays, the $K\alpha_1$ peak was selected to be analyzed, since the $K\alpha_2$ X-ray lies between the U and Pa $K\alpha_1$ X-rays emitted respectively in the decays of ^{233}Pa and ^{237}Np. The peak area of the Np $K\alpha_1$ X-ray was calculated by the BOB75 code[8-11] from the photon spectum of ^{237}Np with ^{57}Co taken simultaneously with the 60-keV γ-ray. The conditions of the peak fitting were: skewness factor = 0.94, tail-to-peak ratio = 0.005, tail-to-peak separation = 10.3589 channels and FWHM = 9.7458 channels. The degree of fitting was 0.17027×10^{-4}, and the peak area obtained was

4912771 ± 2584 counts for an accumulation time of 3×10^4 s, and hence the count rate of the Np $K\alpha_1$ X-ray was evaluated to be 163.76 ± 0.09 counts/s.

3. Results

The estimated intensities for interfering components of various origins, as described in Section 2.4, and the observed intensity for the 60-keV peak in the spectrum of ^{237}Np with ^{57}Co are summarized in Table 3.1. As is evident from the table, the 60-keV peak cannot be explained except by NEET in ^{237}Np following K-shell photoionization. The observed 60-keV peak can be ascribed fully to the nuclear excitation of the 103-keV level in ^{237}Np by NEET following K-shell ionization by the ^{57}Co γ-rays.

The count rate for the 60-keV γ-ray following NEET is expressed by

$$C_\gamma = n \cdot \sigma_K \cdot N_\gamma \cdot P \cdot B \cdot \varepsilon_{60} \qquad (3.4)$$

where n is the number of ^{237}Np atoms, σ_K is the K-shell ionization cross section for Np by incident photons, N_γ is the incident rate of photons, P is the NEET probability for excitation of the 103-keV level per K-hole created in the ^{237}Np atom, B is the branching ratio of the 103-keV level to the 60-keV level times the emission probability for the 60-keV γ-ray per disintegration of the 60-keV level, and ε_{60} is the counting efficiency of the spectrometer for the 60-keV photons. In a quite similar way, the count rate for

Table 3.1. Comparison of the estimated intensities for interfering components of various origin and the observed intensity for the 60-keV peak in the spectrum obtained with a combination of ^{237}Np and ^{57}Co.

Origin	Count rate (s^{-1})
Gamma-rays from ^{241}Am	$(4.2 \pm 0.5) \times 10^{-4}$
Sum coincidence	1.3×10^{-4}
Pulse pile-up	$<1 \times 10^{-5}$
Gamma-rays following γ-resonance absorption	$<4 \times 10^{-6}$
Observed	$(2.2 \pm 0.5) \times 10^{-2}$

the Np $K\alpha_1$ X-ray is expressed by

$$C_{K\alpha 1} = n \cdot \sigma_K \cdot N_\gamma \cdot \omega_K [\Gamma_R(KL_3)/\Gamma_R(K)] \varepsilon_{101}, \qquad (3.5)$$

where σ_K is the fluorescence yield for the Np K-shell, $\Gamma_R(KL_3)$ is the radiative width of the KL_3 electronic transition in Np, and $\Gamma_R(K)$ is the total radiative width of the K shell in Np. By combining eq. (3.4) and (3.5), one can obtain the following relation for P:

$$P = \frac{C_\gamma \ \varepsilon_{101} \ \omega_K \ \Gamma_R(K\alpha_1)}{C_{K\alpha 1} \ \varepsilon_{60} \ B \ \Gamma_R(K)}, \qquad (3.6)$$

where $\Gamma_R(K\alpha_1)$ is the natural width of the Np $K\alpha_1$ line and equal to $\Gamma_R(KL_3)$. Therefore, P can be determined from a singles photon spectrum of ^{237}Np irradiated with the ^{57}Co γ-rays independent of the number of the ^{237}Np atoms, the incident rate of ionizing photons and the K-shell-ionization cross-section data. The ratio $\varepsilon_{101}/\varepsilon_{60}$ was determined experimentally as 1.2 ± 0.1, as described in Section 2.2. Therefore, $(C_\gamma/C_{K\alpha 1})(\varepsilon_{101}/\varepsilon_{60})$ was obtained to be $(1.6 \pm 0.4) \times 10^{-4}$. The other values were taken from the literature as $\omega_K = 0.971 \pm 0.003$ [ref. 13], $B = 0.35 \pm 0.02$ [ref. 5], and $\Gamma_R(K\alpha_1)/\Gamma_R(K) = 0.476$ [ref. 14]. The lastest value is the result of the theoretical calculation

and is stated that the uncertainty is about 10%; therefore, the error was assumed to be 10% of the quoted value. The NEET probability was then obtained as

$$P = (2.1 \pm 0.6) \times 10^{-4}.$$

This is consistent with an upper limit of 4×10^{-3} obtained by Shinohara et al. from the measurement of the $K\alpha_1$ satellite pairs emitted in the decay of ^{237}Pu.[4)]

4. Discussion

The result obtained for the 60-keV peak area was considered statistically by Shinohara[15] according to the definitions proposed by Currie.[16] Three specific levels: (1) a decision limit, (2) a detection limit, and (3) a determinataion limit were introduced by Currie for the statistical statements of the experimental results in analytical and nuclear chemistry.[16] It was found that the peak area obtained from the spectrum could satisfy the conditions for level (2).[15] Therefore, the result can be stated to be detected qualitatively, although it is insufficiently precise to yield a satisfactory quantitative estimate.

If it is permitted to consider that the result is quantitatively significant, some NEET parameters can be deduced readily from P obtained in this experiment.

The Coulomb interaction energy between the nucleus and orbital electron, E', is approximately related to P in this case as

$$E' = - |\Delta| \sqrt{P/[1 + \Gamma(L_3)/\Gamma(K)]} \qquad (3.7)$$

where $\Gamma(L_3)$ and $\Gamma(K)$ are the total widths of the L_3 subshell and K shell, respectively. The ratio $\Gamma(L_3)/\Gamma(K)$ can be

evaluated as

$$\Gamma(L_3)/\Gamma(K) = [\Gamma_R(L_3)/\Gamma_R(K)] \cdot (\omega_K/\omega_3), \qquad (3.8)$$

where $\Gamma_R(L_3)$ and ω_3 are the total radiative width and the fluorescence yield of the L_3 subshell, respectively. The value of $\Gamma_R(L_3)/\Gamma_R(K)$ is calculated to be 3.93×10^{-2} by Scofield,[14] and that of ω_3 is presented to be 0.484 by Fink and Rao.[17] The value of E' was then determined experimentally as $E' = -26 \pm 4$ eV.

A theoretical estimate for E' is given by eq. (10). With $\ell = 1$, $A = 237$, $Z = 93$ and $\bar{n} = 1.5$, E' was evaluated to be $-2.54\ f$ keV. By comparing it with the experimental value, one obtains $f \approx 10^{-2}$ as a reasonable value.

The mixing angle θ defined in eq. (4) was calculated by eq. (6) as

$$\cos\theta\sin\theta \simeq \tan\theta = E'/\Delta = -26/(-1.88 \times 10^3) = 1.4 \times 10^{-2}.$$

The energy shift of the levels was evaluated by eq.(8) as

$$\delta = E'^2/\Delta = 0.36 \text{ eV}.$$

These results for ^{237}Np are compared with those for

^{189}Os reevaluated in Chapter II in Table 3.2. The reason why NEET in ^{189}Os could be observed more precisely in spite of the smaller P value is due to the experimental technique used on ^{189}Os. Indirect measurement using the residual radioactivity can achieve the excellent signal-to-noise ratio as compared with direct one.

The small f-value obtained as above is qualitatively understandable by the fact that the rates of the low-lying E1 transitions in odd-A nuclei of the actinide region are retarded by a factor of 10^{4-5} with respect to those calculated by the Weisskopf single-proton formula.[18] The NEET probability is proportional to the square of f , and hence should be retarded by four orders of magnitude from that obtained when $f = 1$. This is expected from eq. (9), since the term $< r_N^{\ell} >$ in eq. (9) describes the off-diagonal matrix elements for the nucleus and therefore the square $|< r_N^{\ell} >|^2$ is proportional to the probability of nuclear transition. The retardation of nuclear transition of low-energy E1 in the actinide elements is due to the violation of the conservation law of the asymptotic quantum numbers.[18] These quantum numbers are not quite good ones, and hence retard the transition probability instead of inhibiting the transition. Therefore, the NEET probability obtained for ^{237}Np can be considered to reflect the character of the nuclear transition involved quite faithfully.

Table 3.2. Comparison of the NEET parameters for ^{189}Os and ^{237}Np

	^{189}Os			^{237}Np
Electron-hole transition (A)	$K \rightarrow M_4$	$K \rightarrow M_5$	$K \rightarrow M_1$	$K \rightarrow L_3$
Nuclear transition (N)		$3/2- \rightarrow 5/2-$		$\frac{5}{2}+ \rightarrow \frac{7}{2}-$
E_A/keV	71.840	71.911	70.822	101.072
E_N/keV		69.52		102.95
Δ/keV	+2.32	+2.39	+1.30	-1.88
Common multipolarity	E2 (M1)	E2	M1	E1
P	7.4×10^{-8}	6.6×10^{-8}	1.5×10^{-8}	2.1×10^{-4}
$\tan\theta$	-2.6×10^{-4}	-2.5×10^{-4}	-1.0×10^{-4}	1.4×10^{-2}
E'/eV	-0.60	-0.60	-0.13	-26
δ/eV	1.6×10^{-4}	1.5×10^{-4}	1.3×10^{-5}	0.36

5. Conclusion

Nuclear excitation by electron transition in ^{237}Np, subsequent to ^{189}Os, was successfully observed in the singles photon spectrum of ^{237}Np irradiated with the ^{57}Co γ-rays. The value of P obtained for ^{237}Np is much larger than that for ^{189}Os as expected from the fact that NEET proceeds by E1 in ^{237}Np and by E2 (and M1) in ^{189}Os. The result is consistent with the upper limit obtained in the ^{237}Pu experiment. The small f-value is understandable by the well-established character of the nuclear transition involved in NEET.

References

1) K. Otozai, R. Arakawa and M. Morita, *Prog. Theor. Phys.* 50, 1771 (1973).

2) K. Otozai, R. Arakawa and T. Saito, *Nucl. Phys.* A297, 97 (1978).

3) K. Otozai, R. Arakawa, M. Morita, H. Baba, K. Hata and T. Suzuki, unpublished work.

4) A. Shinohara, T. Saito, R. Arakawa, K. Otozai, H. Baba, K. Hata and T. Suzuki, to be published.

5) Y. A. Ellis, *Nucl. Data Sheets* 23, 71 (1978); *ibid.* 23, 123 (1978); *ibid.* B6, 539 (1971); *ibid.* B6, 621 (1971).

6) D. C. Hoffman, Los Alamos Scientific Laboratory of Univ. California report LA-1721, 3rd ed. (1967) p. 91.

7) I. Fujiwara, N. Imanishi and T. Nishi, to be published.

8) S. Baba, H. Baba and H. Okashita, Japan Atomic Energy Research Institute report JAERI 1216 (1971).

9) H. Baba, H. Okashita, S. Baba, T. Suzuki, H. Umezawa and H. Natsume, *J. Nucl. Sci. Technol.* 8, 703 (1971).

10) H. Baba, T. Sekine, S. Baba and H. Okashita, Japan Atomic Energy Research Institute report JAERI 1227 (1972).

11) H. Baba, Japan Atomic Energy Research Institute report JAERI-M 7017 (1977).

12) Y. A. Ellis, *Nucl. Data Sheets* 24, 289 (1978); *ibid.* B6, 257 (1971).

13) I. Ahmad, *Z. Phys.* A290, 1 (1979).

14) J. H. Scofield, *At. Data Nucl. Data Tables* 14, 121 (1974).

15) A. Shinohara, Master thesis, Osaka University (1980).

16) L. A. Currie, *Anal. Chem.* 40, 586 (1968).

17) R. W. Fink and P. V. Rao, in *'Handbook of Spectroscopy'*, ed. J. W. Robinson, Vol. 1 (CRC press, Cleveland, 1974) p. 219.

19) E. K. Hyde, I. Perlman and G. T. Seaborg, *'The Nuclear Properties of the Heavy Elements'*, Vol. 1 (Prentice-Hall, Englewood Cliffs, NJ, 1964) p. 187.

CONCLUDING REMARKS

Nuclear excitation by electron transition was first considered to occur as a result of the accidentally near degeneracy of a nuclear and an electron-hole states by Morita.[1] Experimental evidence for the existence of NEET was first obtained by Otozai et al.[2] on ^{189}Os and the quantitative study was repeated by the same authors.[3] Complementary studies on NEET in ^{189}Os were made to check a competing mechanism, Coulomb excitation by electron, appeared in the experiment using the electron projectiles,[3] and to verify that NEET in ^{189}Os can be achieved by photo-ionization of the K-shells. These studies are described in Chapter I [ref. 4] and Chapter II. NEET was also observed in ^{237}Np as described in Chapter III [ref. 5]. It was found that NEET is a extremely minor deexcitation mode as compared with the emissions of X-rays and Auger electrons. Other candidates which satisfy the NEET conditions can be found by comparing the transition energies of the nucleus and electron system and their multipolarity. This is illustrated in Fig. C1. Excited levels of stable and long-lived β-stable nuclei are shown together with the binding energies of

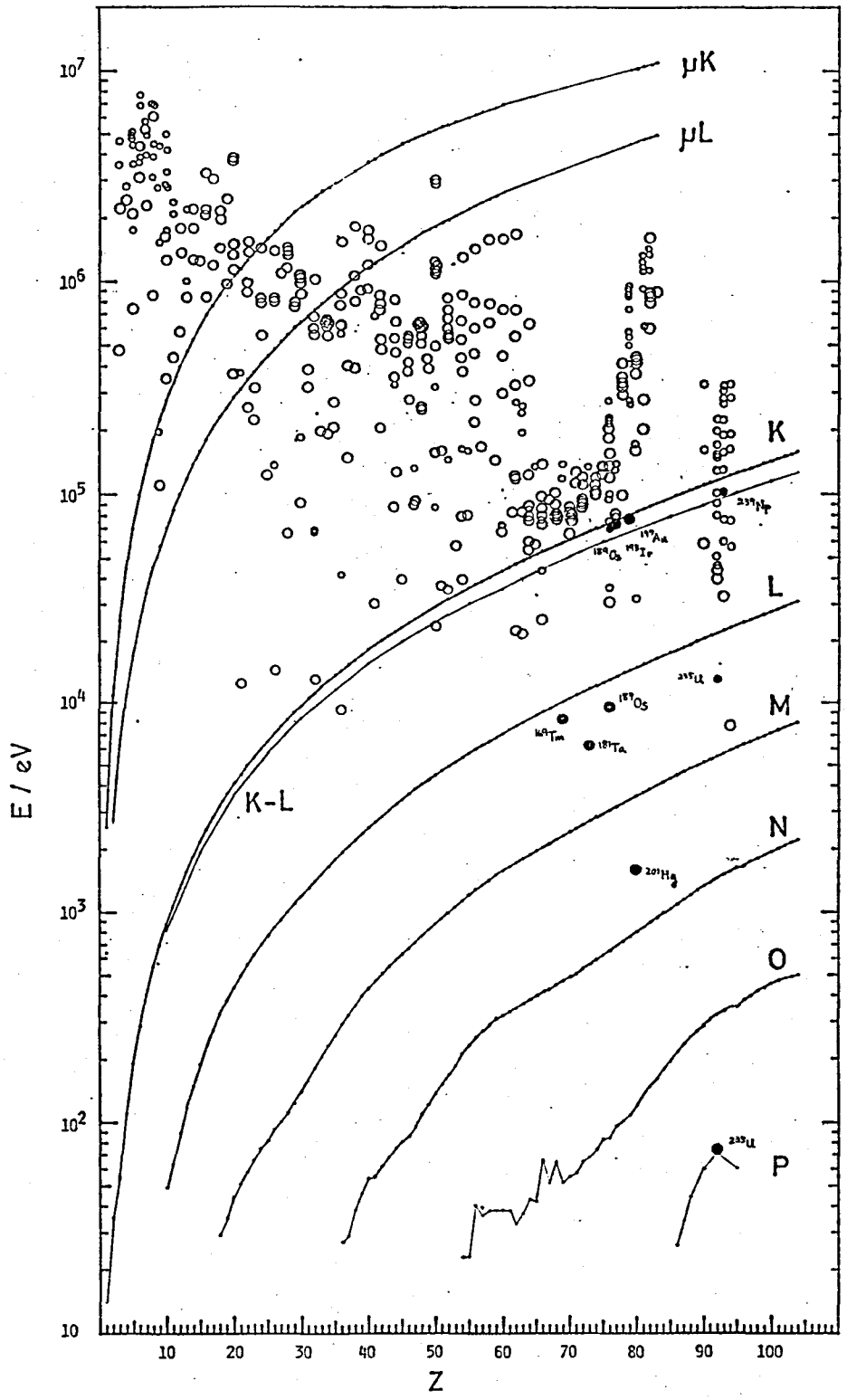

Fig. C1. Excited levels of stable and long-lived β-stable nuclei and the binding energies of electron and muon. The NEET levels are shown by the solid circles.

electron and muon. Nuclear levels which can be excited by NEET are shown by the solid circles. As is evident from Fig. C1, there exist a quite small number of candidates for NEET. The isomer production in ^{235}U by the TEA CO_2 laser beams was interpreted in terms of NEET in ^{235}U;[6] nevertheless, the values for the NEET parameters could not be deduced. Therefore, further extensive studies on NEET are expected including ^{235}U. There is a possibility that the nuclear transitions in unstable nuclei may coincide nearly with those of the electronic transitions. In such circumstances, NEET should play more important role in the decaying modes of atoms and nuclei than those observed in ^{189}Os and ^{237}Np. This may be realized in the heavy element region.

References

1) M. Morita, *Prog. Theor. Phys.* 49, 1574 (1973).

2) K. Otozai, R. Arakawa and M. Morita, *Prog. Theor. Phys.* 50, 1771 (1973).

3) K. Otozai, R. Arakawa and T. Saito, *Nucl. Phys.* A297, 97 (1978).

4) T. Saito, Y. Ohkubo, A. Shinohara, R. Arakawa and K. Otozai, *Nucl. Phys.* A330, 443 (1979).

5) T. Saito, A. Shinohara and K. Otozai, *Phys. Lett.* 92B, 293 (1980).

6) Y. Izawa and C. Yamanaka, *Phys. Lett.* 88B, 59 (1979).